ALMA MATER STUDIORUM
UNIVERSITÀ DI BOLOGNA

DOTTORATO DI RICERCA IN

ONCOLOGIA, EMATOLOGIA E PATOLOGIA

Ciclo 37

Settore Concorsuale: 05/H2 - ISTOLOGIA

Settore Scientifico Disciplinare: BIO/17 - ISTOLOGIA

DEVELOPMENT OF PERINATAL CELL SPHEROIDS WITH DUAL POTENTIAL FOR TYPE 1 DIABETES THERAPY: INSULIN PRODUCTION AND IMMUNE MODULATION.

Presentata da: Francesca Paris

Coordinatore Dottorato

Manuela Ferracin

Supervisore

Francesco Alviano

Co-supervisore

Laura Bonsi

Esame finale anno 2025

Abstract

Type 1 diabetes mellitus (T1DM) is an autoimmune disorder characterized by the immune system's destruction of pancreatic beta-cells, leading to insulin deficiency. Conventional treatments focus on insulin replacement, which does not address the underlying immune attack against beta-cells. Therefore, considerable research has been directed towards stem cell therapy, specifically taking advantage of three-dimensional (3D) cell cultures for enhancing the immunomodulatory and differentiative capacities of stem cells. The final goal of the study is to develop a cellular therapy for T1DM by using perinatal cells to create spheroids that can release insulin and mitigate autoimmune responses.

The aim of this study is to create a reliable cellular model for regenerative medicine applications in T1DM. Specifically, it aims to develop 3D co-culture spheroids of amniotic epithelial cells (AECs) and Wharton's jelly mesenchymal stromal cells (WJ-MSCs) to restore insulin production and protect insulin producing cells from autoimmune destruction.

We created co-culture spheroids of AECs and WJ-MSCs in a 1:1 ratio. These spheroids were analyzed for viability, extracellular matrix production, and hypoxic state. The immunomodulatory ability was evaluated by co-culturing with activated PBMCs and T cells. AECs were differentiated into insulin-producing cells, confirmed by immunofluorescence for specific markers, and combined with undifferentiated WJ-MSCs, which have strong immunomodulatory properties.

The undifferentiated co-culture spheroids remained stable and viable in long-term culture with consistent extracellular matrix production. Moreover, the perinatal spheroids showed significant immunomodulatory properties, reducing pro-inflammatory cell activation and promoting anti-inflammatory responses. Spheroids with differentiated cells combined with undifferentiated WJ-MSCs successfully formed cohesive structures and showed potential for insulin production.

Perinatal spheroids represent a promising dual approach for developing new T1DM treatment. Their ability to modulate the immune system and differentiate into insulin-producing cells may address both the symptoms and underlying causes of T1DM, offering a comprehensive cellular therapy beyond traditional insulin replacement.

Abbreviations

2D	Two-dimensional
3D	Three-dimensional
AEC	Amniotic Epithelial Cell
ANOVA	Analysis of Variance
APC	Allophycocyanin
ASCs	Adult Stem Cells
BSA	Bovine Serum Albumin
CD	Cluster of Differentiation
CFSE	Carboxyfluorescein succinimidyl ester
CGM	Continuous Glucose Monitoring
CSII	Continuous Subcutaneous Insulin Infusion
CTR	Control
CiPSCs	Chemically Induced Pluripotent Stem Cells
DAPI	4',6-diamidino-2-phenylindole
DC	Dendritic Cell
DKA	Diabetic Ketoacidosis
DMEM	Dulbecco's Modified Eagle Medium
ECM	Extracellular Matrix
EDTA	Ethylenediaminetetraacetic Acid
EGF	Epidermal Growth Factor
FACS	Fluorescence-Activated Cell Sorting
FBS	Fetal Bovine Serum
FoxP3	Forkhead box P3
GAD65	Glutamic Acid Decarboxylase
GDM	Gestational Diabetes Mellitus
GrzB	Granzyme B
H&E	Hematoxylin and Eosin
HLA	Human Leukocyte Antigen
HbA1c	Hemoglobin A1c
IA-2	Islet Antigen-2

ICM	Inner Cell Mass
ICs	Pancreatic Islet Cells
IDO	Indoleamine 2,3-dioxygenase
IF	Immunofluorescence
IL	Interleukin
INS	Insulin
MHC	Major Histocompatibility Complex
MSC	Mesenchymal Stromal Cell
NF-κB	Nuclear Factor Kappa B
NGN3	Neurogenin3
NK	Natural Killer
NOD	Non-obese Diabetic
PBMC	Peripheral Blood Mononuclear Cell
PBS	Phosphate-buffered Saline
PDX-1	Pancreatic and Duodenal Homeobox 1
PFA	Paraformaldehyde
PHA	Phytohaemagglutinin
Pan-Ck	Pan Cytokeratin
RPMI	Roswell Park Memorial Institute medium
SOX17	SRY-Box Transcription Factor 17
SSEA4	Stage-Specific Embryonic Antigen-4
T1DM	Type 1 Diabetes Mellitus
T2DM	Type 2 Diabetes Mellitus
Treg	Regulatory T Cell
ULA	Ultra-Low Attachment
WJ-MSC	Wharton's Jelly Mesenchymal Stromal Cell
WJ	Wharton's Jelly
hCG	Human Chorionic Gonadotropin
hESCs	Human Embryonic Stem Cells
hPSCs	Human Pluripotent Stem Cells
rAAV	Recombinant Adeno-associated Viruses

Content

Abstract ... 1
Abbreviations ... 2
Content ... 4
List of Figures ... 7
List of Table ... 9
Introduction ... 10
1. Diabetes Mellitus ... 10
1.1 Type 1 Diabetes ... 11
1.2 Pathogenesis and Stages of Type 1 Diabetes Mellitus ... 12
1.3 Immunological mechanisms in type T1DM ... 14
1.4 Therapies for Type 1 Diabetes ... 20
1.4.1 Insulin Therapy for Type 1 Diabetes ... 20
1.4.2 Pancreatic and Islet Transplantation in Type 1 Diabetes Mellitus ... 21
1.4.3 Alternative Therapies Type 1 Diabetes Mellitus ... 22
1.5 Placenta ... 25
1.6 Perinatal Cells ... 28
1.7 Amniotic Epithelial Cells (AECs) ... 30
1.8 Wharton's Jelly Mesenchymal Stem/Stromal Cells (WJ-MSCs) ... 33
1.9 Three-Dimensional (3D) Culture Systems: A Superior Approach to Mimic In Vivo Conditions ... 36
Aim of the Thesis ... 38
Materials and Methods ... 39
2.1 Ethics Statement ... 39
2.2. Isolation of Human Amniotic Epithelial Cells (AECs) ... 39
2.3. Isolation of Wharton's Jelly Mesenchymal Stromal Cells (WJ-MSCs) ... 40
2.4. Immunophenotype of AECs and WJ-MSCs ... 40
2.5. Scaffold-free 3D perinatal cell culture ... 41
2.6. Time-lapse imaging of Spheroid Formation ... 41
2.7. Prestoblue® Assay for Spheroid Viability ... 41
2.8. Live and Dead Staining ... 42
2.9. Slide Preparation and Histology ... 42
2.10. Hematoxylin and Eosin Staining ... 43

2.11. Biophysical Properties Analysis of Perinatal Spheroids (W8 Analysis) 43
2.12. Immunofluorescence Analysis 43
2.13. Hypoxia Staining 45
2.14. Isolation of PBMCs 45
2.15. Coculture of PBMCs and spheroids 46
2.16. Flow cytometry and labelling 46
2.17. Annexin/7-AAD labelling 47
2.18. CFSE Proliferation Assay 47
2.19. Differentiation of co-culture spheroids into insulin producing islet-like spheroids 48
2.20. Differentiation of Amniotic Epithelial Cells into insulin producing cells 48
2.21. Formation of Pseudo-Islet Spheroids from Differentiated AECs and WJ-MSCs 49
2.22. Statistical Analysis 49
Results 50
3.1. Immunophenotypic Characterization of Isolated AECs and WJ-MSCs 50
3.2. Spheroid Formation 51
3.3. Evaluation of Spheroid Viability 53
3.4. Histological Analysis 54
3.5. Characterization of the Physical Properties of Mono- and Co-Culture Spheroids 55
3.6. Expression of Pan-Cadherins in Mono- and Co-Culture Spheroids 56
3.7. Pan-Cytokeratins and Vimentin Expression in Mono- and Co-Cultures 57
3.8. Extracellular Matrix Formation 58
3.9. Evaluation of Hypoxia 60
3.10 Co-culture of Perinatal spheroids and PBMCs 60
3.11 Analysis of apoptosis and proliferation rate of PBMCs 61
3.12. Analysis of proliferation rate of $CD4^+$ and $CD8^+$ T cells 62
3.13. Analysis of immune activation of $CD4^+$ and $CD8^+$ T cells 63
3.14. Immunophenotypic analysis of regulatory T cells and GrzB-secreting T cells ($CD8^+$) 64
3.15. Differentiation of co-culture spheroids into insulin producing islet-like spheroids 65
3.16 Differentiation of AEC into insulin producing cells 66
3.17 Formation of Pseudo-Islet Spheroids from Differentiated AECs and WJ-MSCs 69

3.18 Pan-Cytokeratin and Vimentin Expression in Pseudo-Islet Spheroids 70
3.19 Pancreatic differentiation marker in Pseudo-Islet Spheroids 71
Discussion 75
Conclusions 81
Bibliography 82

List of Figures

Figure 1 Graph shows functional beta-cell mass through the stages of T1D.

Figure 2 Immune mechanism in Type 1 Diabetes Mellitus.

Figure 3 Mechanism of the suppressive action of Treg lymphocytes in type 1 diabetes mellitus.

Figure 4 Pathways and opportunities to intervene in type 1 diabetes.

Figure 5 Schematic representation of a term placenta.

Figure 6 Schematic illustration of the contribution of cells, biomolecules and extracellular matrix to the bioactivity of perinatal tissues and derived biomaterials.

Figure 7 Schematic representation of the main differences between 2D and 3D cell cultures.

Figure 8 Immunophenotype of isolated AECs and WJ-MSCs.

Figure 9 Representative images showing mono-culture spheroids of AECs and WJ-MSCs and co-culture spheroid formation at different ratios.

Figure 10 Viability of mono-culture WJ-MSC (black) spheroids and co-culture (white) spheroids.

Figure 11 Hematoxylin and eosin staining on WJ-MSC mono-culture and co-culture spheroid sections after 4 and 14 days of culture.

Figure 12 Measurement of mass density and diameter of mono-culture WJ-MSCs spheroids (red dots) and co-culture (WJ-MSCs + AECs) spheroids (blue dots).

Figure 13 Representative images of WJ-MSC mono-culture and co-culture spheroids at early (4 days) and late (14 days) time points stained with Pan-Cadherin (red) and DAPI for nuclei staining (blue).

Figure 14 Representative images of WJ-MSC mono-culture and co-culture spheroids at early (4 days) and late (14 days) time points stained with Pan-Ck (green), vimentin (red), and DAPI for nuclei staining (blue).

Figure 15 Representative images of WJ-MSC mono-culture and co-culture spheroids at early (4 days) and late (14 days) time points stained to evaluate the presence of ECM proteins with laminin, fibronectin, and collagen I (red) and DAPI for nuclei staining (blue).

Figure 16 Hypoxia levels in mono-culture WJ-MSC spheroids and co-culture spheroids.

Figure 17 Immunomodulation Assay: Co-culture of perinatal spheroids and PBMCs.

Figure 18 Apoptosis and proliferation rates of PBMCs under various experimental conditions.

Figure 19 Proliferation rates of $CD4^+$ and $CD8^+$ T cells in the various experimental conditions.

Figure 20 Flow cytometry analysis of CD69 expression in $CD4^+$ and $CD8^+$ T cells under the three experimental conditions.

Figure 21 Immunophenotypic analysis of $CD4^+$ Treg, $CD8^+$ Treg and $CD8^+$ T cells producing granzyme B (GrB).

Figure 22 Immunofluorescence analysis of WJ-AEC co-culture spheroids after 14 days of differentiation towards the beta-pancreatic lineage.

Figure 23 Immunofluorescence staining for DAPI (blue, nucleus), Sox17 (Sox17, green), and Vimentin (red) in AEC cells. (Top) Pre-differentiation condition shows low detectable Sox17 and Vimentin expression.

Figure 24 Immunofluorescence staining for DAPI (blue, nucleus), Neurog3 (Neun3, green), and PDX-1 (red) in AEC cells.

Figure 25 Immunofluorescence of AEC cells stained for DAPI (blue, nucleus), insulin (INS, green), and C-peptide (C-PEP, red).

Figure 26 Comparison of the physical parameters diameter (μm), density (fg/μm3), and mass (ng) of spheroids composed of non-differentiated AEC and WJ cells (blue) and spheroids assembled with AEC cells differentiated in 2D and WJ cells (green). No statistically significant differences were observed between the two conditions (ns).

Figure 27 Representative images of co-culture spheroids and pseudo-islet spheroids stained with Pan-Ck (green), vimentin (red), and DAPI for nuclei staining (blue).

Figure 28 Immunofluorescence analysis of SOX17 expression in spheroids composed of non-differentiated AEC and WJ-MSC (control condition) and spheroids assembled with 2D-differentiated AEC and WJ-MSC (pseudo-islet spheroids).

Figure 29 Immunofluorescence analysis of Neurogenin3 (Neurog3) and PDX-1 expression in control and pseudo-islet spheroids.

Figure 30 Immunofluorescence analysis of insulin (INS) and C-peptide (C-PEP) expression in control and pseudo-islet spheroids.

List of Table

Table 1 List of primary antibodies, dilution and Specification for immunofluorescence staining.

Table 2 Summary of Differentiation Stages Using the STEMdiff™ Pancreatic Progenitor Kit.

Introduction

1. Diabetes Mellitus

Diabetes Mellitus (DM) is a multifaceted metabolic disorder primarily defined by chronic hyperglycemia, which can arise from defects in insulin production, insulin action, or both. Insulin, a hormone produced by the beta-cells of the pancreas, plays a critical role in glucose homeostasis by facilitating glucose uptake into peripheral tissues such as skeletal muscle, adipose tissue, and the liver. When this finely regulated system is disrupted, glucose accumulates in the bloodstream, leading to the hallmark condition of hyperglycemia [1,2].

Diabetes is broadly categorized into three main types, though the spectrum of the disease is highly heterogeneous. Type 1 Diabetes Mellitus (T1DM) is an autoimmune disorder characterized by the destruction of insulin-producing beta-cells, resulting in absolute insulin deficiency. Type 2 Diabetes Mellitus (T2DM) is the most common form of diabetes, often associated with obesity, metabolic syndrome, and older age. It is characterized by peripheral insulin resistance, where tissues become less responsive to insulin, and a relative insulin deficiency as the disease progresses. In T2DM, the pancreas initially compensates by producing more insulin, but over time, this response becomes inadequate, leading to hyperglycemia. While insulin resistance plays a central role, factors such as chronic low-grade inflammation and lipotoxicity further complicate the metabolic disturbances in T2DM [1].

Gestational Diabetes Mellitus (GDM) occurs during pregnancy and is defined as glucose intolerance that is first identified or develops during gestation. While the exact pathophysiology of GDM is not fully understood, it is believed to involve a combination of insulin resistance induced by pregnancy-related hormonal changes and an inability of the pancreas to adequately compensate. GDM poses risks not only to the mother, including a higher likelihood of developing T2DM later in life, but also to the fetus, [3]increasing the risk of macrosomia, neonatal hypoglycemia, and other complications [4].

Given the rising global incidence of both T1DM and T2DM, as well as the growing awareness of GDM's long-term consequences, diabetes has emerged as a major public health concern. Understanding its pathogenesis, and the molecular mechanisms underlying its various forms, remains a critical focus of medical research.

1.1 Type 1 Diabetes

T1DM is a chronic autoimmune condition in which the immune system mistakenly attacks and destroys the insulin-producing beta-cells in the pancreas. As a result, the body is unable to produce insulin, leading to uncontrolled blood glucose levels, or hyperglycemia. T1DM represents about 5-10% of all diabetes cases and is most often diagnosed during childhood or adolescence, although it can develop at any age [5,6].

The development of T1DM is complex, involving a combination of genetic, environmental, and immunological factors. Genetically, individuals with specific human leukocyte antigen (HLA) alleles, particularly HLA-DR and HLA-DQ, have a higher risk of developing the disease. However, genetics alone does not explain the onset, as environmental triggers, such as viral infections (e.g., enteroviruses), may initiate or accelerate the autoimmune response in genetically predisposed individuals [7,8].

Immunologically, T1DM is marked by the presence of autoantibodies against beta-cell antigens, including insulin, glutamic acid decarboxylase (GAD65), and islet antigen-2 (IA-2). These autoantibodies can be detected long before the appearance of clinical symptoms, indicating a prolonged subclinical phase. However, the actual destruction of beta-cells is driven by autoreactive T cells, primarily $CD8^+$ cytotoxic T cells, which directly attack and eliminate the beta-cells. The loss of these cells leads to a complete dependence on exogenous insulin for survival [9,10].

Without treatment, T1DM can lead to life-threatening complications like diabetic ketoacidosis (DKA). Long-term, poorly managed T1DM significantly increases the risk of complications, including cardiovascular disease, nephropathy, neuropathy, and retinopathy. Although there is no cure, advancements in insulin therapy and glucose monitoring have improved patient outcomes and quality of life, highlighting the importance of early diagnosis and tight glycemic control [5].

1.2 Pathogenesis and Stages of Type 1 Diabetes Mellitus

The underlying pathogenesis of T1DM involves a complex interplay of genetic predisposition, environmental triggers, and immune-mediated mechanisms. The progression of the disease can be understood through a well-established three-stage model that highlights the transition from genetic susceptibility to clinical diabetes (see Figure 1).

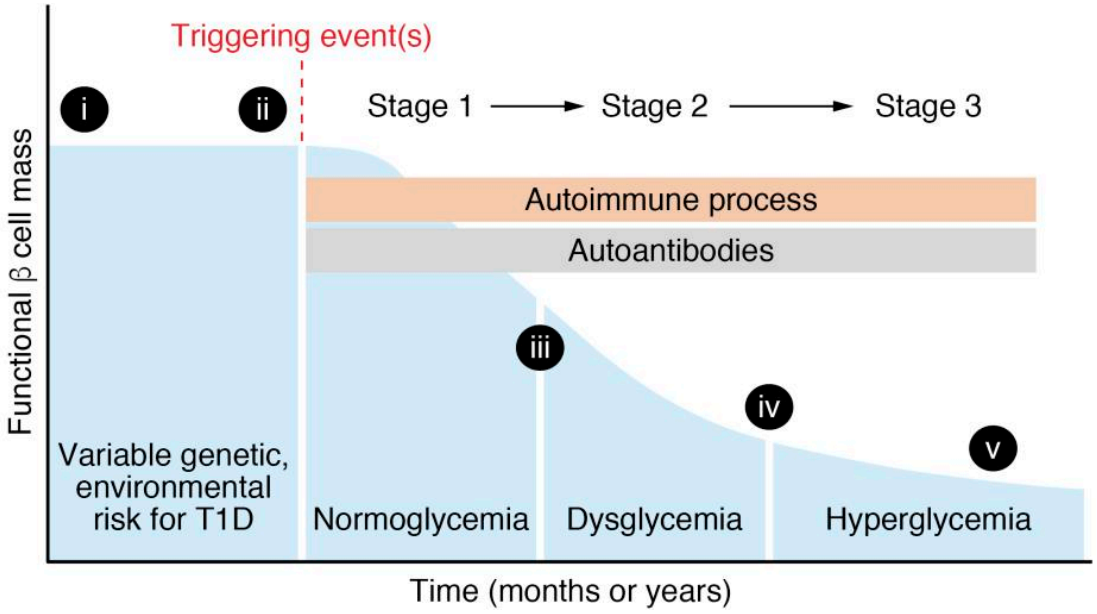

Figure 1 Graph shows functional beta-cell mass through the stages of T1D. The blue shaded area shows number or insulin secretory capacity of beta-cells, with time on the x axis reflecting a broad range (could be months or years of T1D development). See text for definition of T1D stages [11].

Genetic Susceptibility

The most significant genetic risk factors for T1DM lie within the human HLA region, specifically the HLA class II molecules. Individuals carrying certain haplotypes, such as HLA-DR3/DR4-DQ8, are at a significantly higher risk of developing T1DM. These HLA molecules present beta-cell antigens to T cells, and some alleles are more efficient at promoting autoreactive T cell activation, thus contributing to disease onset [79].

Non-HLA genes, including polymorphisms in the insulin gene (INS), which affect central tolerance to insulin, and other loci like PTPN22, CTLA4, and IL2RA, further contribute to T1DM susceptibility by influencing immune regulation and tolerance. However,

genetic predisposition alone is not sufficient for disease development, as environmental triggers also play a crucial role in initiating the autoimmune attack [8].

Environmental Triggers

While the exact environmental triggers remain uncertain, certain factors are believed to initiate or accelerate the autoimmune response in genetically susceptible individuals. Viral infections, especially enteroviruses such as Coxsackievirus B, have been implicated in triggering the autoimmune destruction of beta- cells through a mechanism known as "molecular mimicry." Other potential triggers include early exposure to dietary proteins (e.g., cow's milk), vitamin D deficiency, and changes in gut microbiota, all of which may disrupt immune tolerance mechanisms and contribute to the onset of autoimmunity [12,13].

T1DM develops in a predictable sequence, moving from a preclinical stage of autoimmunity to overt diabetes, and finally to complete beta-cell destruction. This process can be divided into three key stages:

Stage 1: Preclinical Autoimmunity

The first stage of T1DM is characterized by the emergence of autoimmunity. Autoantibodies targeting beta-cell antigens, such as IAA, GAD65, and IA-2, begin to appear, often years before any clinical symptoms. At this stage, there is no evidence of glucose dysregulation, and the individual remains asymptomatic. However, the detection of multiple autoantibodies strongly predicts the eventual development of T1DM [7].

Stage 2: Progressive Loss of Beta-Cell Function

During stage 2, the autoimmune destruction of beta-cells continues, leading to a progressive decline in insulin production. Although blood glucose levels remain within the normal range due to compensatory mechanisms, impaired glucose tolerance can be detected through oral glucose tolerance tests or rising levels of hemoglobin A1c (HbA1c). While individuals are still asymptomatic at this stage, the metabolic abnormalities indicate ongoing beta-cell damage [3].

Stage 3: Clinical Onset of Diabetes

In the final stage, clinical diabetes manifests when 80-90% of the beta-cell mass has been destroyed. At this point, insulin production is no longer sufficient to regulate blood glucose levels, resulting in symptomatic hyperglycemia. Patients typically present with classic symptoms such as polyuria, polydipsia, polyphagia, and unintended weight loss. Many individuals are diagnosed during an episode of DKA, a life-threatening complication of T1DM caused by severe insulin deficiency.

Following clinical onset, the autoimmune process continues until the majority of beta-cells are destroyed. Patients become entirely dependent on exogenous insulin to regulate blood glucose levels. Long-term management focuses on preventing both acute complications (e.g., DKA) and chronic complications, such as retinopathy, nephropathy, and cardiovascular disease, which are associated with prolonged hyperglycemia.

1.3 Immunological mechanisms in type T1DM

The immune system, particularly autoreactive T cells, plays a central role in initiating and perpetuating this process. This chapter reviews the immune players involved in the destruction of beta-cells and how the breakdown of immune regulation contributes to T1DM development. Recent findings on environmental influences, such as viral infections and microbiota, further elucidate the complex nature of this disease (see Figure 2).

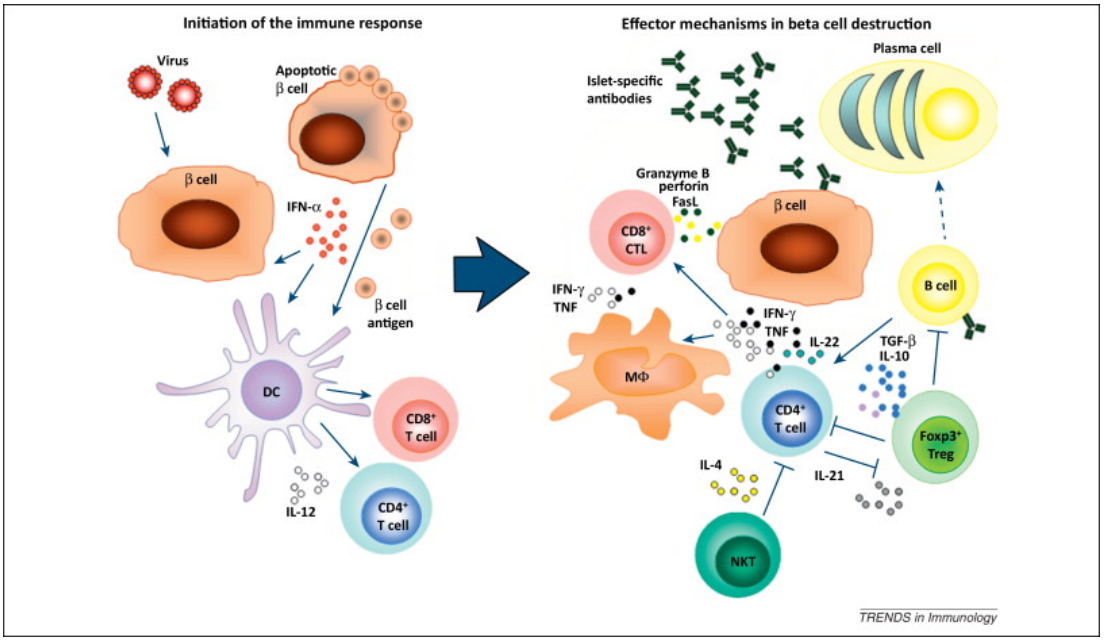

Figure 2 Immune mechanisms driving beta-cell destruction involve both physiological and infection-induced processes. Dendritic cells (DCs) in the islets capture beta-cell antigens and, when activated by type I interferons (IFNs), present these antigens to T cells. $CD4^+$ T cells can then promote macrophage-mediated beta-cell death via cytokines and reactive oxygen species, while also activating B cells to produce antibodies that mediate complement and Fc receptor-dependent killing. $CD8^+$ T cells, primed by cross-presentation, release cytotoxic granules to directly kill beta-cells. Regulatory cells like NKT and Treg cells temper these responses, but their function can be impaired by cytokines like IL-21, weakening immune regulation.

Activation and Role of Autoreactive T Cells

The onset of T1DM is initiated by the activation of autoreactive T cells that recognize beta-cell antigens. The breakdown of immune tolerance enables these T cells to evade deletion in the thymus. Beta-cell antigens, such as insulin and IA-2, are presented by dendritic cells and macrophages via MHC class II molecules, leading to the activation of $CD4^+$ T helper cells. $CD8^+$ T cells, once activated, recognize beta-cell antigens presented by MHC class I and directly mediate cytotoxicity through perforin and granzyme release [10,14,15]. Dendritic cells (DCs) are pivotal in initiating the autoimmune response in T1DM. These antigen-presenting cells capture beta-cell antigens and activate both $CD4^+$ and $CD8^+$ T cells. In patients with T1DM, DCs in the pancreas are more readily activated due to aberrant NF-ϰB signaling, leading to an exaggerated production of proinflammatory cytokines, such as IL-12. Macrophages, while crucial for antigen presentation, also contribute to inflammation and beta-cell destruction through the production of TNF-α and other cytokines [16–18].

Additionally, findings show that beta-cells may contribute to their own destruction. beta-cells exposed to inflammatory cytokines upregulate the expression of chemokines such as IL-8, attracting immune cells that amplify the local immune response. Moreover, more than 50% of genes associated with T1DM risk are expressed in beta-cells themselves, indicating a significant cross-talk between beta-cells and the immune system [10]

T Cells as Key Players in Beta-Cell Destruction

Both $CD4^+$ and $CD8^+$ T cells are crucial for the progression of T1DM. $CD8^+$ T cells (cytotoxic T lymphocytes, CTLs) directly kill beta-cells through recognition of antigenic peptides presented on MHC class I molecules. These T cells release cytotoxic granules containing perforin and granzymes, which induce apoptosis in beta-cells. Importantly, $CD8^+$ T cells isolated from individuals with T1DM have been shown to target specific beta-cell antigens such as preproinsulin. These findings highlight the antigen-specific nature of the cytotoxic response, where CTLs cause beta-cell lysis [19].

$CD4^+$ T helper cells (Th1 subtype) play an auxiliary role by activating macrophages and dendritic cells. These antigen-presenting cells (APCs) then further amplify the immune response by secreting pro-inflammatory cytokines, such as IFN-γ and TNF-α [20,21]. These cytokines not only activate macrophages to release reactive oxygen species and nitric oxide, but also facilitate the recruitment and activation of additional immune cells into the pancreatic islets. In mouse models, depletion of $CD4^+$ T cells can delay or prevent diabetes onset, underscoring their critical role in beta-cell destruction [22].

B Cells and Autoantibodies: Supporting Beta-Cell Destruction

Although T cells are considered the primary mediators of beta-cell destruction, B cells and their associated autoantibodies also play an important role. B cells act as APCs and produce autoantibodies that target beta-cell antigens, such as insulin and GAD65 [23,24]. These autoantibodies are commonly detected in the serum of patients before the clinical onset of T1DM, serving as biomarkers of disease risk.

Despite their presence, autoantibodies are not sufficient to induce beta-cell death on their own. Instead, B cells contribute to the disease primarily by presenting beta-cell antigens to T cells, thereby enhancing T cell activation. In non-obese diabetic (NOD) mice, B cell

depletion via monoclonal antibodies against CD20 has been shown to prevent or reverse diabetes, indicating that B cells play a non-redundant role in disease progression [25–27].

Role of Regulatory T Cells (Treg)

In the immunological landscape of T1DM, where immune tolerance is breached, regulatory T cells (Tregs) play a critical role in maintaining immune homeostasis. Tregs are a specialized subset of $CD4^+$ T cells defined by the expression of CD25 and the transcription factor FoxP3, which is pivotal for their development and function. The hallmark of Treg activity is their ability to suppress autoreactive immune responses and maintain self-tolerance, preventing the immune system from attacking the body's own tissues, such as the insulin-producing beta-cells in the pancreas [28,29].

Tregs utilize a variety of mechanisms to modulate immune responses and ensure peripheral tolerance (see Figure 3). One key approach is the secretion of inhibitory cytokines such as IL-10 and TGF-β, which suppress the activation and proliferation of effector T cells and other immune cells involved in inflammation [30–32]. These cytokines act in an autocrine and paracrine manner, creating an anti-inflammatory milieu that dampens immune activation. In addition to cytokine-mediated suppression, Tregs can induce cytolysis of target cells through the release of granzyme and perforin, leading to apoptosis of effector T cells and other pro-inflammatory cells. This cytotoxic capability underscores the potent regulatory capacity of Tregs in controlling aberrant immune responses. Another essential mechanism is metabolic disruption. Tregs compete with effector T cells for IL-2, a critical cytokine for T cell growth and survival. By consuming IL-2, Tregs effectively limit the resources available to effector T cells, thus curbing their expansion and inflammatory potential [33]. Tregs also exert their influence on APCs, such as dendritic cells, through direct modulation. By inhibiting the maturation and co-stimulatory capacity of APCs, Tregs reduce their ability to prime and activate effector T cells, contributing to an overall decrease in autoimmune activity [34,35].

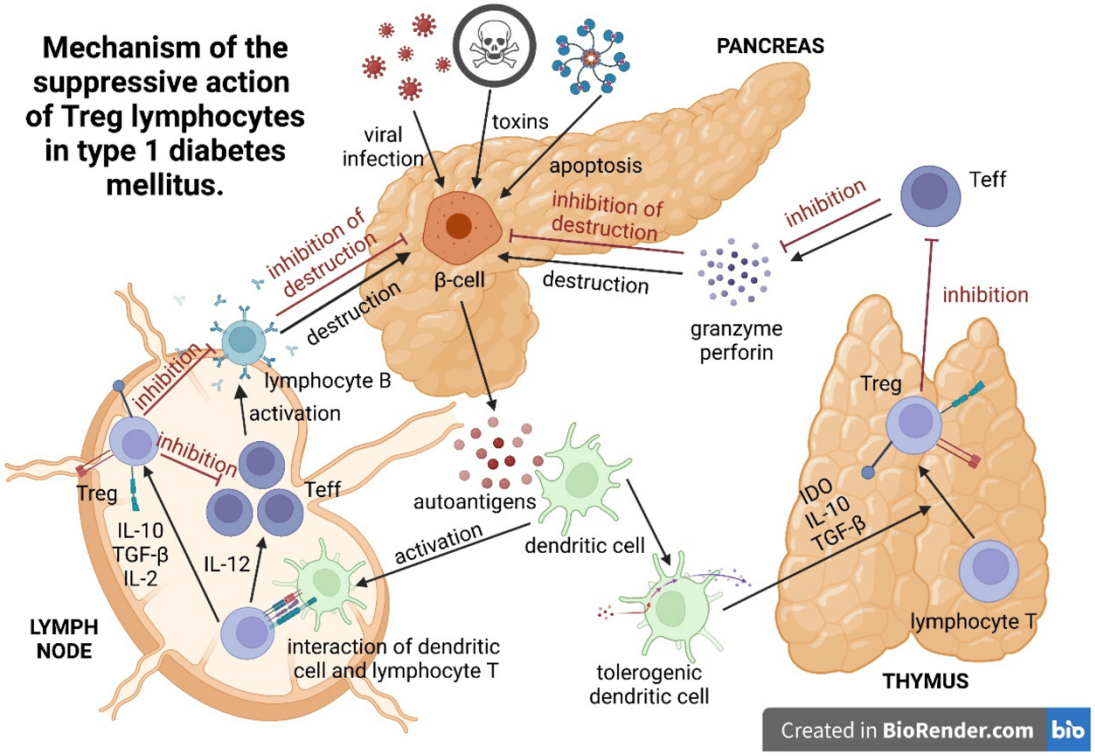

Figure 3 Mechanism of the suppressive action of Treg lymphocytes in type 1 diabetes mellitus [35].

In the context of T1DM, however, Tregs are often dysfunctional. Both quantitative and qualitative defects in Tregs have been reported in individuals with T1DM. Some studies have shown a reduction in the number of circulating Tregs, while others have documented impaired suppressive function despite normal Treg frequencies [36]. The inability of Tregs to effectively suppress autoreactive T cells is a major contributor to the immune-mediated destruction of pancreatic beta-cells. Several factors have been implicated in the dysfunction of Tregs in T1DM. Genetic predispositions play a significant role, with mutations or polymorphisms in the FoxP3 gene leading to defects in Treg development and stability. FoxP3 is essential for the transcriptional programming of Tregs, and any disruption in its expression can result in profound immune dysregulation. The inflammatory milieu in individuals with T1DM is another critical factor. Elevated levels of pro-inflammatory cytokines, such as IL-6 and TNF-α, have been shown to inhibit Treg function. These cytokines not only promote effector T cell activity but also reduce the suppressive capacity of Tregs, tipping the balance toward autoimmunity. Metabolic stress, particularly in the form of hyperglycemia and other metabolic disturbances, can also impair Treg function. High glucose levels are associated with decreased Treg stability and

an altered immune response, further exacerbating the autoimmune attack on beta-cells [36] [37].

Given their central role in maintaining immune tolerance, strategies to restore or enhance Treg function hold great promise as therapeutic approaches for T1DM. Several potential interventions are under investigation.

Low-Dose IL-2 Therapy: IL-2 is a cytokine essential for Treg survival and proliferation. Low-dose IL-2 therapy has been explored as a means to selectively expand the Treg population without activating effector T cells. Clinical trials have shown that low-dose IL-2 can increase Treg numbers and improve their functional capacity, providing a promising approach for modulating the immune system in T1DM [38].

Adoptive Transfer of Tregs Adoptive Treg transfer is another innovative strategy. This approach involves isolating Tregs from the patient, expanding them *ex vivo*, and reintroducing them into the patient to boost the Treg population. Preliminary clinical trials have demonstrated the safety of this method and suggest that it may prolong the survival of transplanted pancreatic islets by enhancing immune regulation [39].

Immune Environment Modulation Another potential therapeutic avenue is the modulation of the immune environment to support Treg function. Agents such as methotrexate and rapamycin, which possess anti-inflammatory properties, have been investigated for their ability to enhance Treg activity and create a more favorable immune environment. These immunomodulatory therapies aim to shift the cytokine balance towards an anti-inflammatory state, thus promoting Treg stability and function [10,40].

Despite the potential of Treg-based therapies, several challenges remain. One of the primary concerns is maintaining Treg stability. Expanded Tregs may lose their regulatory phenotype over time or even differentiate into pro-inflammatory cells under certain conditions, posing a significant risk. Ensuring that Tregs retain their suppressive function is crucial for the long-term success of these therapies. Long-term outcomes are still uncertain. Although early results from clinical trials are encouraging, more research is needed to determine the durability of Treg-based therapies and their impact on disease progression in the long term [38]

1.4 Therapies for Type 1 Diabetes

The treatment landscape for T1DM has evolved significantly over the past decades. Despite the advances, the central aim of all therapeutic strategies remains the same: to control blood glucose levels and prevent the complications associated with chronic hyperglycemia. The gold standard of T1DM management is insulin therapy, which is indispensable for replacing the insulin that the body can no longer produce. However, in recent years, a growing focus has been placed on alternative treatments, such as beta-cell replacement, stem cell therapies, immunomodulatory approaches, and gene therapy, as potential routes to curing T1DM or mitigating its impact [41].

1.4.1 Insulin Therapy for Type 1 Diabetes

Insulin therapy remains the most widely used and effective treatment for managing T1DM. Due to the autoimmune destruction of pancreatic beta-cells, patients with T1DM rely on exogenous insulin to regulate blood glucose levels and prevent life-threatening complications such as diabetic ketoacidosis. The main goal of insulin therapy is to replicate physiological insulin secretion, maintaining blood glucose levels within a target range.

Technological advances, including continuous subcutaneous insulin infusion (CSII) pumps and closed-loop insulin delivery systems (artificial pancreas), have enhanced glycemic control and improved quality of life for patients. These systems integrate continuous glucose monitoring (CGM) with automated insulin delivery, dynamically adjusting insulin doses in response to blood glucose fluctuations [42].

One of the primary challenges of insulin therapy is maintaining tight glycemic control. Even with modern delivery technologies, it is difficult to perfectly mimic the natural secretion of insulin by the pancreas. This limitation results in frequent episodes of hypoglycemia or hyperglycemia, contributing to glycemic variability. Additionally, long-term use of insulin does not prevent the onset of diabetes-related comorbidities such as cardiovascular disease, retinopathy, and nephropathy, which continue to reduce life expectancy in patients with T1DM. Studies show that, even with optimal insulin therapy, life expectancy in individuals with T1DM remains significantly lower than in the general population. Moreover, the burden of daily insulin management including frequent blood

glucose monitoring, injections, and dietary restrictions affects the quality of life and imposes a considerable physical and psychological toll on patients [43].

1.4.2 Pancreatic and Islet Transplantation in Type 1 Diabetes Mellitus

Pancreatic islet transplantation has emerged as a viable alternative for beta-cell replacement therapy in patients with T1DM, aiming to restore endogenous insulin production. Islet transplantation involves the infusion of islets from a cadaver donor pancreas into the liver via the portal vein. Once engrafted, the islets can produce insulin and help maintain normoglycemia without the need for exogenous insulin.

One of the most successful protocols is the Edmonton protocol, which involves the transplantation of islets from multiple donors combined with immunosuppressive therapy to prevent graft rejection. This method has shown significant improvements in glycemic control and even insulin independence in a subset of patients [44,45]. However, the long-term success of islet transplantation is limited by several factors:

1. **Scarcity of Donor Organs**: The availability of suitable donor pancreases is a major limitation, and many patients with T1DM are not eligible for transplantation due to this scarcity.
2. **Immunosuppression**: Recipients must undergo lifelong immunosuppression to prevent rejection, which increases the risk of infections and malignancies.
3. **Variable Graft Survival**: Over time, transplanted islets may lose function due to immunologic attack or poor engraftment, requiring patients to revert to insulin therapy.

In recent years, alternative transplantation strategies are being explored to overcome these challenges. Researchers are investigating encapsulation techniques, where islets are encapsulated in biocompatible materials to protect them from immune attack while eliminating the need for systemic immunosuppression. Furthermore, alternative sites for islet transplantation, such as the omentum and subcutaneous tissue, are being explored to improve islet engraftment and survival.

Another promising approach is the use of stem-cell-derived islets as an alternative to cadaveric donor islets. Advances in stem cell research have enabled the generation of insulin-producing beta-cells from human pluripotent stem cells (hPSCs), providing a potentially unlimited source of islets for transplantation [41].

1.4.3 Alternative Therapies Type 1 Diabetes Mellitus

The request for more effective therapies for T1DM has led to the exploration of alternative approaches, including regenerative medicine, immunomodulatory therapies, and gene therapy.

Immunomodulatory Therapies

Given the autoimmune nature of T1DM, immunotherapy strategies that modulate the immune system are also being explored. Therapies targeting specific immune cells, such as Tregs, aim to restore immune tolerance and prevent further beta-cell destruction (see Figure 4). Clinical trials using Treg therapy have shown encouraging results in terms of safety and the ability to preserve residual beta-cell function [35,38,46]. Additionally, anti-CD3 monoclonal antibodies and other immune-modulating agents are being tested in clinical trials to prevent the onset or progression of T1DM by dampening the autoimmune response [47,4849].

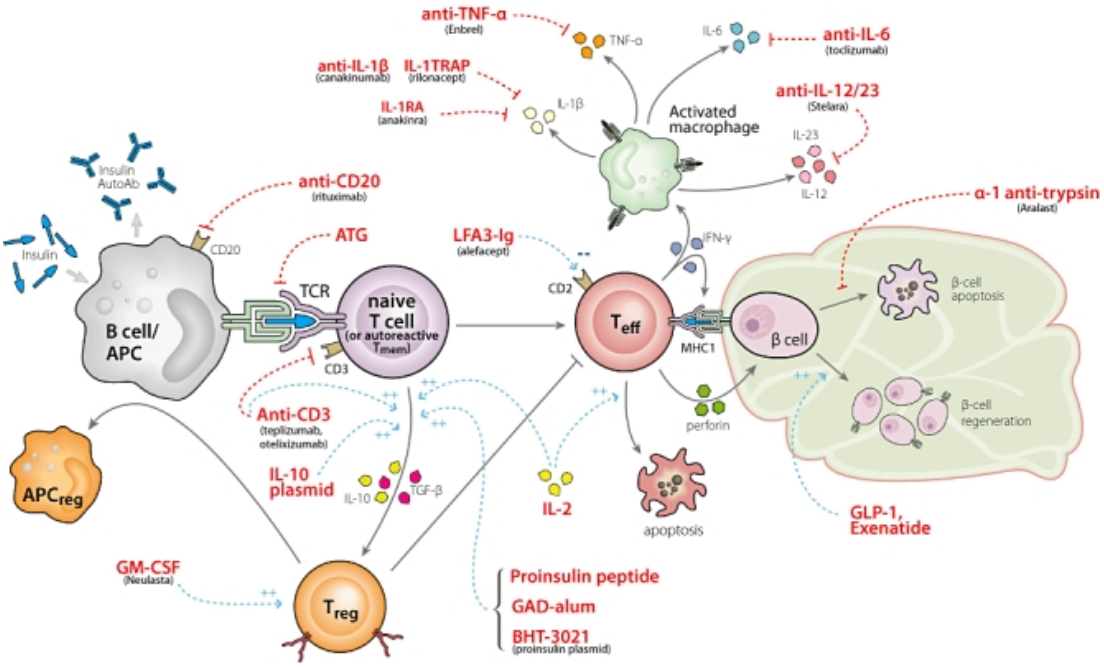

Figure 4 Pathways and opportunities to intervene in type 1 diabetes. This figure shows crucial pathways known to contribute to the pathogenesis of type 1 diabetes and relevant drugs for intervention. A key juncture is the antigen-presenting cell–T cell interaction, where activation of effector T cells can be prevented and generation of regulatory T cells (T_{regs}) can be enhanced. Another pivotal cell is the beta-cell itself. Augmentation of beta-cell mass or function along with prevention of apoptosis may be achievable goals. Most probably a combination of agents dampening inflammation, preventing effector cell activation, enhancing T_{regs} and augmenting beta-cell mass will be the ultimate solution for curing type 1 diabetes [49].

Gene Therapy

Gene therapy is emerging as a highly promising strategy for the treatment of T1DM. The goal is to correct genetic factors that contribute to beta-cell destruction or introduce genes that protect beta cells from autoimmune attacks. Various approaches are being investigated, such as using viral vectors like recombinant adeno-associated viruses (rAAV) to deliver therapeutic genes to pancreatic beta cells.

For instance, research has demonstrated that gene therapy can potentially modulate the immune response, reducing inflammation and preserving beta-cell function. Techniques like the delivery of protective cytokines or immune-modulatory genes are being tested in preclinical models with encouraging results. These approaches have shown promise in preventing or delaying the progression of T1DM by enhancing beta-cell survival and promoting immune tolerance [50–52].

Although most studies are still in the preclinical phase, gene therapy holds great potential to transform T1DM management by providing long-lasting protection to beta cells or even promoting their regeneration.

Stem Cell Therapy

Stem cell therapy holds considerable promise for the treatment of T1DM, with the potential to generate new insulin-producing beta-cells. One of the most exciting developments in this field is the use of human pluripotent stem cells (hPSCs) to create insulin-secreting cells that can be transplanted into T1DM patients. Clinical trials, such as those led by Vertex Pharmaceuticals with VX-880, have demonstrated encouraging results, with patients showing restored insulin production and improved glycemic control. Recent advancements include the use of chemically induced pluripotent stem cells (CiPSCs), which offer a novel approach to generating patient-specific beta cells. A clinical trial involving the transplantation of CiPSC-derived islets under the abdominal anterior rectus sheath of a T1DM patient showed promising outcomes, with the patient achieving insulin independence after 75 days and maintaining stable glycemic control for over a year. This method is particularly advantageous due to the non-genomic integration of CiPSCs, which reduces the risk of tumorigenicity and offers an autologous solution to immune rejection [53,54]

However, while stem cell-derived islets offer a potential solution to the limitations of donor islet transplantation, several challenges remain. These include ensuring long-term survival of the transplanted cells, preventing immune-mediated destruction, and achieving efficient engraftment. Moreover, many stem cell sources, such as human embryonic stem cells (hESCs), raise ethical concerns and can be difficult to access [55].

To overcome these challenges, researchers are exploring alternative, less conventional sources of stem cells, such as perinatal stem cells. Derived from the placenta and umbilical cord, these cells have shown remarkable immunomodulatory properties and the ability to differentiate into insulin-producing cells. Perinatal stem cells offer several advantages over traditional sources, including higher availability, reduced ethical concerns, and better immune tolerance [40]. Before discussing these cells in greater detail, it is important to first explore the placenta, their origin, to better understand its unique properties and functions. This overview will provide the necessary background for comprehending the full therapeutic potential of perinatal stem cells [40,56,57].

1.5 Placenta

Embryonic Development

The development of the human placenta commences approximately 6-7 days post-fertilization, following the implantation of the blastocyst into the uterine wall. At this critical juncture, the blastocyst segregates into two distinct lineages: the inner cell mass (ICM) and the trophoblast. The ICM, a compact group of cells located on one side of the blastocyst, is responsible for generating all embryonic tissues, the umbilical cord, and the epithelial layer of the amniotic membrane. In contrast, the trophoblast, a single-layered epithelial cover, evolves into the fetal portion of the placenta, known as the chorion [58,59].

As implantation proceeds, the trophoblast in direct contact with the endometrial epithelium undergoes rapid proliferation and differentiates into two distinct layers: an inner cytotrophoblastic layer and an outer syncytiotrophoblastic mass. The syncytiotrophoblast invades the endometrial epithelium, establishing early contact between the maternal and fetal systems. By the 8th day post-conception, lacunae (fluid-filled spaces) start to form within the syncytial mass. These lacunae expand, merging to form larger structures, and as the syncytiotrophoblast erodes maternal capillaries, they fill with maternal blood, initiating the primitive uteroplacental circulation [58].

Around day 13, the cytotrophoblast further proliferates and extends into the syncytiotrophoblast, forming primary villi. These villi subsequently undergo further development; fetal mesenchyme grows into the cytotrophoblast, leading to the formation of secondary villi. By the third week of gestation, fetal capillaries develop within the villous mesenchyme, transforming the villi into tertiary structures that facilitate the vital exchange of nutrients and gases between the maternal and fetal circulatory systems. As gestation advances, some cytotrophoblast cells penetrate the maternal decidua, where they undergo epithelial-mesenchymal transition and form extravillous trophoblasts. These extravillous trophoblasts invade maternal blood vessels, remodeling and dilating them to ensure an adequate maternal blood supply to the placenta [60].

By the end of the first trimester, the chorionic villi, initially covering the entire chorion, undergo differentiation. The villous tissue at the abembryonic pole regresses and becomes smooth, forming the chorion laeve, while the chorion frondosum, the villous tissue at the

embryonic pole, continues to develop into the chorionic plate. During this period, the basic placental structures necessary to support fetal development and ensure a sufficient nutrient supply are fully established [59].

Term Structure

At term, the human placenta is a disc-shaped organ, typically measuring 15-20 cm in diameter and 2-3 cm in thickness. Its main components include the umbilical cord, the placental disc, and the fetal membranes[61]. The umbilical cord, serving as a critical conduit between the developing fetus and the maternal circulatory system, contains two umbilical arteries and one umbilical vein. The arteries transport deoxygenated blood from the fetus, while the vein carries oxygenated blood back to the fetus. These vessels are embedded in Wharton's jelly, a protective mucoid connective tissue rich in collagen and glycosaminoglycans, primarily hyaluronic acid [62].

The placental disc is composed of two sides: the fetal side (chorionic plate) and the maternal side (basal plate). The chorionic plate contains the fetal blood vessels that branch from the umbilical cord, while the basal plate anchors the placenta to the maternal endometrium. Between these two plates lies the intervillous space, which contains the villous trees responsible for nutrient and gas exchange between maternal and fetal blood[60,62]. The terminal villi, the final branches of these trees, are highly vascularized by fetal capillaries and covered by a thin syncytiotrophoblast layer, ensuring efficient diffusion of oxygen, nutrients, and waste products. Maternal blood enters the intervillous space through spiral arteries and bathes the villi, facilitating the exchange of gases and nutrients before being drained back by endometrial veins [59,63].

The fetal membranes, composed of the amniotic and chorionic membranes, form the protective amniotic sac that encloses the amniotic fluid and the developing fetus. The amniotic membrane, the innermost layer, is an avascular structure consisting of a single layer of epithelial cells and a collagen-rich mesoderm. The chorionic membrane, the outermost layer, is separated from the amniotic membrane by a spongy layer of connective tissue and contains vascularized stroma and cytotrophoblasts in contact with the maternal decidua (see Figure 5) [60].

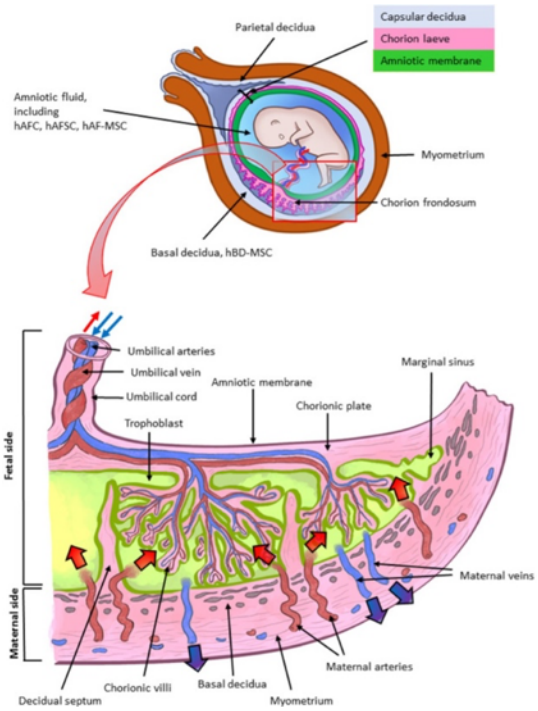

Figure 5 Term placenta, the fetus bathes in the amniotic fluid and is connected to the mother through the umbilical cord. The fetus and the amniotic fluid are surrounded by the amniotic membrane and the chorion. The chorion can be divided into chorion leave and chorion frondosum at the level of the placental disc. The placental disc is composed of a fetal side, the chorionic plate, and a maternal side, the basal plate. In the middle, there is the intervillous space where exchanges between maternal and fetal circulation occur [64].

Functions

The placenta performs a multitude of essential functions during gestation, including nutrient transport, waste removal, gas exchange, hormone production, and immunological protection [65,66]. In the early stages of pregnancy, the trophoblast mediates histotrophic nutrition, phagocytosing maternal secretions from the endometrial glands. After 10-12 weeks of gestation, maternal blood makes direct contact with the terminal villi, allowing the efficient transfer of respiratory gases, nutrients, and waste products across the placental membrane [61]. Fetal hemoglobin's higher affinity for oxygen, combined with the placenta's unique structural adaptations, facilitates optimal oxygen transfer from the mother to the fetus, while carbon dioxide and other waste products are transferred back to the maternal circulation [66].

In addition to its role in fetal nourishment, the placenta also provides immunological protection. Despite the fetus being a semi-allogeneic graft due to the presence of paternal antigens, the placenta prevents maternal immune rejection by employing various

immunomodulatory strategies. Trophoblast cells express non-classical MHC class I molecules (HLA-G) that inhibit the activation of maternal natural killer (NK) cells and $CD8^+$ T cells. Additionally, trophoblasts express immune checkpoint molecules such as PD-L1, which suppress T cell activation, and enzymes like indoleamine 2,3-dioxygenase (IDO), which deplete tryptophan, limiting T cell proliferation and promoting the differentiation of regulatory T cells (Tregs) [67,68].

Moreover, the placenta serves important endocrine functions throughout pregnancy. Hormones such as estrogen, progesterone, human chorionic gonadotropin (hCG), and placental lactogen are produced by the syncytiotrophoblast and play key roles in maintaining pregnancy, regulating fetal development, and preparing the maternal body for labor [69].

Finally, the placenta acts as a selective barrier, protecting the fetus from harmful substances in the maternal circulation. While it effectively blocks the passage of many pathogens and toxins, some substances, including alcohol, certain medications, and specific infectious agents like HIV, can cross the placental barrier and cause developmental complications [70].

1.6 Perinatal Cells

Perinatal tissues, particularly those derived from the placenta and umbilical cord, are increasingly recognized for their vast potential as sources of human stem cells, extracellular matrix proteins, and growth factors. These tissues are naturally programmed to support fetal development and thus exhibit unique biological properties, including angiogenic, anti-inflammatory, anti-fibrotic, anti-microbial, and immunomodulatory capabilities (see Figure 6). Moreover, as the placenta is a temporary organ typically discarded as medical waste after birth, it represents an easily accessible and cost-effective biological materials for medical and biotechnological applications [71]. The temporary nature of the placenta, along with its role in mediating between the mother and fetus, gives it unique characteristics. Notably, it hosts two independent circulatory systems one fetal and one maternal which allows it to support the development of an allogeneic fetus without triggering immune rejection. These biological properties are reflected in the cells derived from this organ, making perinatal cells ideal candidates for a wide range of

applications in regenerative medicine [72,73]. These cells are positioned between embryonic stem cells (ESCs) and adult stem cells (ASCs), offering unique advantages: they are easier to isolate than ESCs, do not present the same risks of tumorigenicity, and are free from the ethical concerns associated with ESC use. Additionally, compared to ASCs, they exhibit a broader differentiation potential and can be expanded *in vitro* for multiple passages without losing their regenerative capabilities[74]. One of the key advantages of using perinatal stem cells is their ethical accessibility. Unlike embryonic stem cells, which require the destruction of embryos to be obtained, perinatal tissues such as the placenta and umbilical cord are considered medical waste after birth. This eliminates the ethical concerns that often limit the use of ESCs and provides an abundant source of stem cells without controversy. Moreover, since these tissues are readily available and abundant, they can be used on a large scale for therapeutic purposes. Another practical advantage of perinatal stem cell is their high *in vitro* expandability. Compared to adult stem cells, which often show limited proliferation and differentiation potential, perinatal stem cells can be cultured over numerous passages without losing their regenerative properties, making them a feasible option for therapies that require large quantities of cells.[57] One of the most remarkable characteristics of perinatal stem cells is their immunomodulatory capacity. MSCs derived from Wharton's jelly have been shown to inhibit the production of pro-inflammatory cytokines, such as TNF-α, and promote the expansion of Tregs, which are essential for regulating immune responses. This ability to positively modulate the immune system is particularly useful for treating autoimmune diseases like T1DM, where the autoimmune destruction of pancreatic beta cells requires both cell regeneration and immune protection to prevent further damage [75].

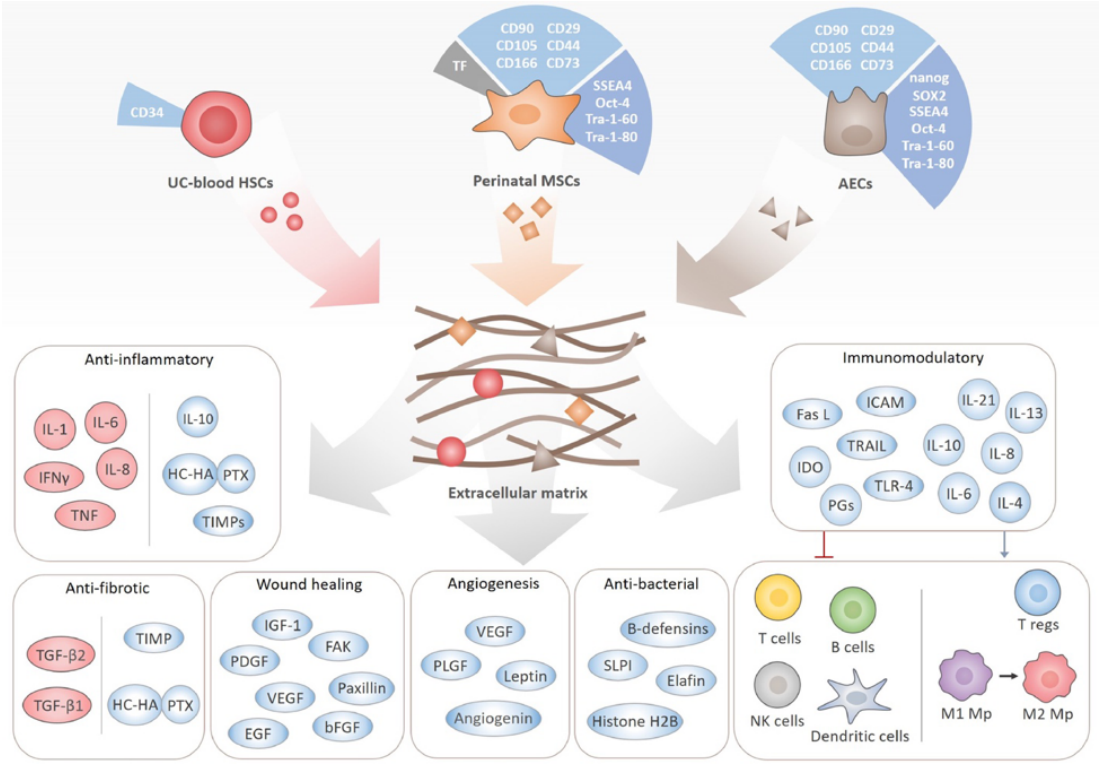

Figure 6 Schematic illustration of the contribution of cells, biomolecules and extracellular matrix to the bioactivity of perinatal tissues and derived biomaterials. Stem cells produce and secrete a range of bioactive factors into the extracellular environment that are responsible for their therapeutic properties through paracrine signaling: anti-inflammatory, anti-fibrotic, pro-regenerative, angiogenic, anti-bacterial and immunomodulatory [71].

1.7 Amniotic Epithelial Cells (AECs)

The amniotic membrane, a vital structure derived from the inner cell mass of blastocysts, is a thin, avascular tissue comprising five distinct layers: the epithelial cell layer, basement membrane, compact layer, fibroblast layer, and spongy layer. Amniotic epithelial cells (AECs), which arise from the pluripotent epiblast around eight days after fertilization, are found within the epithelial layer [76,77]. Notably, a subset of these cells retains pluripotency and plasticity similar to ESCs, though this capacity decreases over time. In contrast, mesenchymal stem cells from the amniotic membrane are derived from the embryonic mesoderm and reside in the fibroblast layer [78].

AECs, characterized by their cuboidal morphology, form a monolayer on the inner surface of the amniotic membrane. These cells are easily accessible and can be isolated with high viability and yield [79,80].One commonly used method for isolating AECs involves

digesting the amniotic membrane with trypsin/ethylenediaminetetraacetic acid (EDTA), which facilitates the dissociation of the epithelial layer from the underlying tissue [81]. Once isolated, AECs are cultured in a medium supplemented with epithelial growth factor (EGF) and can be expanded for up to five passages [82,83]. Importantly, these cells express pluripotency markers, such as NANOG, OCT-4, SSEA-3, and TRA1-60, although their expression diminishes with gestational age [84,85]. AECs also express typical mesenchymal markers, such as CD44, CD73, CD90, and CD105, while hematopoietic markers like CD31, CD34, and CD45 are minimally expressed [74,86].

Differentiation Potential of AECs

Due to their early developmental origins, AECs maintain significant plasticity and have demonstrated the ability to differentiate into all three germ layers under specific culture conditions[87]. For instance, Marongiu et al. successfully induced AEC differentiation into functional hepatocytes, both *in vitro* and *in vivo* [88]. AECs have also been directed toward neuronal and corneal epithelial-like cells [89,90]. Importantly, there has been growing interest in the differentiation of AECs into pancreatic lineages, particularly IPCs. While early studies used agents like nicotinamide to induce differentiation, these approaches often fell short in fully recapitulating beta-cell development. More recent protocols, which closely mimic pancreatic development from the definitive endoderm to mature pancreatic endocrine cells, have improved the efficiency of *in vitro* differentiation. However, challenges remain, particularly in generating IPCs that function comparably to native beta-cells *in vivo* [91–93].

Recent advances have incorporated three-dimensional (3D) culture systems, which more closely resemble the *in vivo* cellular environment. AECs cultured in 3D spheroids have shown enhanced differentiation potential, improved viability, and increased insulin secretion in response to glucose [94]. Our research group has successfully differentiated AECs into IPCs using a stepwise differentiation protocol in 3D spheroids, achieving glucose-dependent insulin secretion and c-peptide release [95].

Immunomodulatory Capacity of AECs

Perinatal cell populations deriving from placenta are involved in the achievement of feto-maternal tolerance, which naturally avoids the immune mediated rejection of the embryo

during pregnancy [96]. The modulation of the immune response is achieved both by cell–cell contact and by the release of soluble signals [96]. AECs play a crucial role in mediating immune tolerance during pregnancy by preventing immune-mediated rejection of the fetus. These cells exhibit an immune-privileged phenotype, characterized by low expression of HLA class Ia molecules and an absence of HLA class II and co-stimulatory molecules. However, AECs express non-canonical HLA class Ib molecules, particularly HLA-G, which is highly expressed and plays a pivotal role in maintaining feto-maternal tolerance. HLA-G is preserved during *in vitro* expansion and even after cryopreservation, supporting the immunosuppressive properties of AECs [97–99].

AECs have been shown to inhibit the cytotoxic activity of natural killer (NK) cells, suppress dendritic cell (DC) activation, and promote the induction of regulatory T cells (Tregs), while inhibiting Th1 and Th17 subsets [100–102]. These immunomodulatory properties are further enhanced by the release of soluble factors such as interleukin-10 (IL-10) and prostaglandin E2 (PGE2), which counteract pro-inflammatory cytokines, including tumor necrosis factor-alpha (TNF-α) and interleukin-6 (IL-6) [103,104]. Moreover, the paracrine features of AECs increase their phagocytic activity and promote the anti-inflammatory phenotype (M2) of the macrophage population. As for the pro-angiogenic potential of this cell population, it has already been previously demonstrated [105,106].
All in all, the immune-privileged and immune-suppressive phenotype of AECs along with their anti-inflammatory properties supports their use in several immune-based and inflammatory disorders as well as in regenerative medicine strategies.
In the context of T1DM pancreatic islet transplantation is a well-established therapy for beta cell replacement. However, the procedure faces significant limitations due to the scarcity of donor islets and the risks of immune rejection. To address these challenges and reduce the need for immunosuppressive therapies, stem cells have been explored for their potential to modulate the pancreatic microenvironment, thereby minimizing immune rejection and local inflammation [107].
Among various approaches, the co-culture of pancreatic islet cells (ICs) with AECs has shown particular promise. AECs, compared to mesenchymal stem cells (MSCs), form more stable hybrid spheroids with ICs, effectively mitigating immune response and transplant rejection [105,108]. Studies have demonstrated that these AEC/IC cultures exert a strong anti-proliferative effect on phytohaemagglutinin (PHA)-stimulated peripheral

blood lymphocytes (PBLs), and PBLs cultured in AEC-conditioned media also show reduced proliferation [109].

Zafar et al. reported that AECs co-cultured with porcine islets reduced $CD4^+$ T-cell proliferation *in vitro* and delayed islet rejection in immunocompetent mice [110]. Additionally, AEC-islet constructs improved insulin secretion in response to glucose and protected islet cells from hypoxic damage, maintaining their viability and functionality.

In diabetic SCID mice, transplantation of AEC/islet constructs significantly improved islet engraftment, increased beta cell mass, and normalized blood glucose levels[105]. Furthermore, AECs promote angiogenesis and re-vascularization of transplanted islets, enhancing their survival and function [105,111]. Lebreton et al. further demonstrated that culturing AECs with inflammatory cytokines such as IFN-γ, TNF-α, and IL-1β boosted their anti-inflammatory and cytoprotective effects on pancreatic islets [105].

1.8 Wharton's Jelly Mesenchymal Stem/Stromal Cells (WJ-MSCs)

Wharton's jelly, the gelatinous substance surrounding the umbilical vessels, is an important source of perinatal stem cells. Structurally, it consists of two arteries and one vein, embedded in an extracellular matrix (ECM) rich in mucopolysaccharides such as hyaluronic acid, along with abundant collagen fibers [112]. Mesenchymal stem/stromal cells derived from Wharton's jelly (WJ-MSCs) were first identified in 1991 [112], and since then, they have garnered significant attention due to their express some pluripotency markers such as NANOG, OCT-4, and SSEA-4 [113] and their ability to differentiate into various cell types. These include osteoblasts, chondrocytes, adipocytes, and even pancreatic endocrine cells, highlighting their potential utility in regenerative medicine [114].

In the context of Type 1 Diabetes Mellitus (T1DM), WJ-MSCs are particularly promising not only for their ability to differentiate into insulin-producing cells (IPCs) [115,116117] but also for their robust immunomodulatory properties [118,119]. These cells could serve a dual purpose: restoring insulin production while simultaneously modulating the immune system, which is crucial in autoimmune diseases like T1DM.

Differentiation Potential of WJ-MSCs

One of the defining characteristics of WJ-MSCs is their high differentiation potential. Numerous studies have demonstrated that these cells can be directed towards a variety of cell fates using specific differentiation protocols [115,116]. In the treatment of T1DM, this differentiation capacity is particularly relevant, as WJ-MSCs can be induced to form IPCs. This process typically involves stepwise protocols that rely on key differentiation factors such as retinoic acid and nicotinamide, which guide the cells through stages of pancreatic lineage commitment.

Immunomodulatory Capacity of WJ-MSCs

The immunomodulatory potential of WJ-MSCs is perhaps one of their most exciting attributes, particularly in the context of autoimmune diseases like T1DM, where aberrant immune responses target insulin-producing β-cells. The immune system in T1DM is characterized by an imbalance between pro-inflammatory and anti-inflammatory signals, with an excessive activation of autoreactive T cells and a concomitant reduction in regulatory mechanisms [10]. WJ-MSCs can intervene in this process by influencing multiple arms of the immune response [119]. A key mechanism through which WJ-MSCs exert their immunomodulatory effects is via the secretion of anti-inflammatory cytokines and growth factors. Among the most well-characterized are TGF-β1, IL-10, and prostaglandin E2 (PGE-2), which collectively promote immune tolerance and suppress the activity of pro-inflammatory cells such as Th1 and Th17 cells. TGF-β1 plays a central role in converting naïve T cells into regulatory T cells (Tregs), which are crucial for maintaining immune homeostasis and preventing autoimmune reactions [120]. IL-10, on the other hand, inhibits the activation of antigen-presenting cells (APCs), including dendritic cells and macrophages, thus reducing their ability to prime autoreactive T cells [121].

Moreover, WJ-MSCs can induce a phenotypic switch in macrophages, promoting the polarization of these cells toward the M2 anti-inflammatory phenotype. M2 macrophages contribute to tissue repair and resolution of inflammation by secreting anti-inflammatory mediators and reducing the recruitment of pro-inflammatory immune cells to the site of injury or inflammation [10,122]. This ability to modulate macrophage activity is particularly

relevant in T1DM, where the inflammatory environment within the pancreas plays a key role in β-cell destruction [10].

Preconditioning WJ-MSCs with pro-inflammatory stimuli such as interferon-γ (IFN-γ) or tumor necrosis factor-α (TNF-α) has been shown to enhance their immunomodulatory properties. This preconditioning "primes" the cells, increasing the expression of immunosuppressive molecules and improving their therapeutic efficacy [120]. Additionally, studies have demonstrated that when cultured in 3D environments, WJ-MSCs exhibit a more potent immunomodulatory profile compared to traditional 2D cultures. This is due to the enhanced secretion of key molecules like PGE-2 and TGF-β1 in 3D, which better simulates the *in vivo* conditions and amplifies their immunosuppressive capabilities [123].

In addition to their differentiation and immunomodulatory properties, WJ-MSCs are notable for their ability to secrete a rich and complex ECM. The ECM is a dynamic structure composed of various proteins such as collagen, fibronectin, and laminin, along with glycosaminoglycans like hyaluronic acid. This matrix not only provides structural support but also plays a critical role in cellular signaling and tissue organization. The ability of WJ-MSCs to produce ECM is particularly advantageous in 3D culture systems, where cell-matrix interactions are essential for the formation of functional spheroids [124]. These spheroids, which mimic the architecture of pancreatic islets, rely on the presence of a robust ECM to maintain their structure, enable cell-cell communication, and support differentiation [125]. The ECM produced by WJ-MSCs enhances the formation of cohesive spheroids that are more resistant to mechanical stress and exhibit improved functional properties, such as insulin secretion in response to glucose stimulation [126]. Furthermore, the ECM provides biochemical cues that influence the behavior of both WJ-MSCs and other cells within the spheroid, promoting cell survival and maturation. The synthesis of ECM components such as collagen I and III by WJ-MSCs contributes to a supportive microenvironment that is crucial for sustaining long-term cell viability and function in regenerative therapies [124].

1.9 Three-Dimensional (3D) Culture Systems: A Superior Approach to Mimic *In Vivo* Conditions

In the field of stem cell research and regenerative medicine, the use of three-dimensional (3D) culture systems has emerged as a transformative approach to better replicate the physiological environment of cells (see Figure 7). Traditional two-dimensional (2D) cultures, in which cells are grown as a monolayer on flat surfaces, have long been the standard for *in vitro* studies. However, 2D cultures often fail to mimic the complex, three-dimensional architecture of tissues found *in vivo*, limiting the translational relevance of experimental results. One of the major limitations of 2D cultures is the restricted interaction of cells with their surrounding extracellular matrix (ECM) and other cells. *In vivo*, cells exist in a dynamic 3D microenvironment where they constantly interact with the ECM and neighboring cells, influencing crucial cellular behaviors such as proliferation, differentiation, migration, and apoptosis. The spatial constraints of 2D cultures prevent the full extent of these interactions, often leading to altered cell morphology, gene expression profiles, and reduced functionality. Moreover, 2D cultures do not effectively recreate gradients of nutrients, oxygen, or metabolites, which are essential for mimicking tissue homeostasis and pathophysiology [127,128].

In contrast, 3D culture systems allow cells to grow in all directions, more accurately simulating the *in vivo* environment. Cells cultured in 3D exhibit enhanced cell-cell and cell-ECM interactions, leading to more physiologically relevant behaviors [129]. For example, stem cells grown in 3D demonstrate improved differentiation potential and higher viability compared to 2D cultures [125]. The 3D architecture also promotes more natural tissue-like organization, facilitating more accurate studies of cellular processes, including differentiation pathways, drug metabolism, and immune responses [130]. Additionally, 3D cultures enable the creation of spheroids and organoids three-dimensional cell aggregates that closely mimic the structure and function of specific tissues [124]. These models are particularly valuable for studying stem cell differentiation, tissue regeneration, and disease modeling. For instance, in pancreatic research, 3D spheroids of insulin-producing cells (IPCs) have been shown to enhance insulin secretion and better respond to glucose stimulation, compared to cells grown in 2D [131]. This enhanced functionality is attributed to the fact that 3D cultures allow for more realistic cell polarity, intracellular signaling,

and ECM remodeling, which are critical for the maturation and function of differentiated cells. Another critical advantage of 3D culture is its ability to more accurately reflect the *in vivo* environment when studying cell therapies and tissue engineering. When stem cells are grown in 3D, they exhibit increased paracrine signaling, producing higher levels of cytokines and growth factors that are essential for tissue repair and immune modulation [132,133]. Moreover, 3D culture systems can be tailored to mimic disease states more effectively, providing valuable insights into how cells behave under pathological conditions, such as in cancer or autoimmune diseases [133–135].

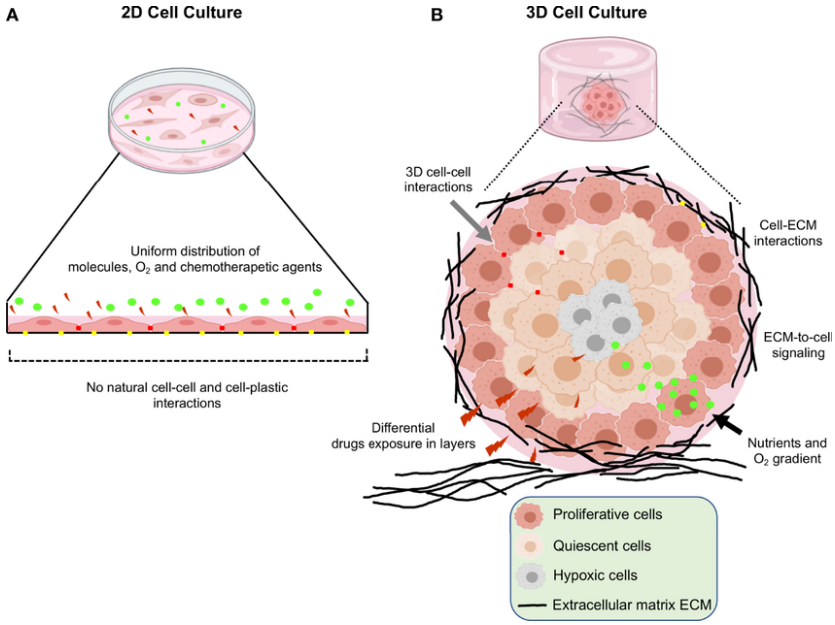

Figure 7 Schematic representation of the main differences between 2D and 3D cell cultures. (A) Traditional 2D cell culture in which flattened cells grown in a monolayer at the bottom of plastic plates. Reduced cell-cell interactions, unlimited exposure to nutrients, oxygen and drugs are limitations of this type of cultures. (B) 3D cell culture systems; in which increased cell-cell and cell-extracellular matrix interactions, limited access to nutrients, oxygen, and heterogeneity in the drugs interactions leads to better recapitulation of the tumor microenvironment occurring *in vivo* [136].

Aim of the Thesis

Type 1 Diabetes Mellitus (T1DM) is a chronic autoimmune disorder marked by the targeted destruction of pancreatic beta cells, resulting in a deficiency of insulin production and persistent hyperglycemia. The aim of this project is to develop an innovative therapeutic strategy based on perinatal stem cells, exploiting their dual potential for differentiation and immunomodulation.

The primary objective is to generate functional insulin-producing cells *in vitro* and to recreate pancreatic islet-like structures using a three-dimensional (3D) culture system. The 3D culture model offers a more physiologically relevant environment, promoting the maturation and enhanced functionality of beta-like cells. Additionally, it preserves the immunomodulatory properties of perinatal stem cells, which are critical for modulating immune responses and safeguarding the newly differentiated cells from autoimmune attack.

A central focus of this project is the ability of perinatal stem cells to simultaneously address both insulin deficiency and the autoimmune dysfunction underlying T1DM. By recreating islet-like structures and harnessing the immunomodulatory capacity of these cells, the project seeks to develop a comprehensive therapeutic approach. This strategy aims to mitigate or eliminate the need for chronic immunosuppression, a significant limitation of current cell replacement therapies.

While this approach is promising, several challenges remain, particularly regarding the long-term stability of the differentiated insulin-producing cells and the sustained efficacy of immune modulation. Addressing these challenges will lay the groundwork for future preclinical studies, with the ultimate goal of translating these findings into a viable therapeutic option for patients with T1DM.

Materials and Methods

2.1 Ethics Statement

This study was approved by the Local Ethical Committee (IRCCS St. Orsola-Malpighi University Hospital Ethical Committee, protocol n° 2481/2017, ref n° 68/2017/U/Tess/AOUBo). Placentas were obtained from healthy donor mothers undergoing elective caesarean section at term (37–40 weeks) after written informed consent. Perinatal tissues were maintained under sterile conditions until specific cell isolation was performed. For this study, perinatal tissues were obtained from nine donors for the isolation of amniotic epithelial cells (AECs) and nine donors for Wharton's jelly mesenchymal stromal cells (WJ-MSCs).

2.2. Isolation of Human Amniotic Epithelial Cells (AECs)

Fetal membranes were washed with ice-cold phosphate-buffered saline (PBS, Corning, NY, USA) with 1% penicillin–streptomycin solution (10,000 U/mL penicillin, 10,000 U/mL streptomycin, Corning, Steuben County, NY, USA). The amniotic membrane was mechanically peeled off the underlying chorion layer to remove any blood clots. Then the tissues were incubated for 10 min at room temperature with PBS/ethylenediaminetetraacetic acid (EDTA) 0.5 mM. The amniotic membrane was then minced into small pieces (4 cm^2 approximately) and digested twice for 30 min at 37 °C using trypsin-EDTA 0.25% (Corning, Steuben County, NY, USA) with gentle shaking. For both digestion steps, trypsin was inactivated with fetal bovine serum (FBS, Gibco, Life Technologies, Carlsbad, CA, USA) and the cell suspension was centrifuged for 10 min at 390× *g*. The cell pellet was resuspended in basal culture medium, Dulbecco's Modified Eagle's Medium–high glucose (DMEM H., Corning, Steuben County, NY, USA) containing 10% FBS, 1% penicillin-streptomycin solution, and 10 ng/mL of epithelial growth factor (EGF, Sigma-Aldrich, St. Louis, MO, USA). The single-cell suspension was counted and tested for viability using erythrosin B (Sigma-Aldrich, St. Louis, MO, USA). Only samples with >90% viability were used for further assays.

2.3. Isolation of Wharton's Jelly Mesenchymal Stromal Cells (WJ-MSCs)

First, the umbilical cord (UC) was removed from the placenta. UC was minced into pieces of approximately 2–3 cm lengths and rinsed 3–4 times with phosphate-buffered saline (PBS, Corning, NY, USA) containing 1% penicillin–streptomycin (10,000 U/mL penicillin, 10,000 U/mL streptomycin, Corning, Steuben County, NY, USA). After the removal of two arteries and a vein, Wharton's jelly (WJ) was chopped into pieces of 3–5 mm with a scalpel. These small pieces were transferred onto the culture dishes and covered with a drop of Dulbecco's Modified Eagle's Medium (DMEM) with 10% FBS (fetal bovine serum) to prevent the pieces of WJ from drying out. The dishes were placed in the incubator with 5% CO_2 for at least two hours and then 10 mL of medium was added to the dishes. The culture dishes were maintained and left untouched for 5 days in the incubator. On day 5 of culture, 3 mL of media was added. After approximately 7–14 days, WJ-MSCs were isolated. The explanted tissues were gently removed and the isolated cells were detached by the surface using Accutase® (P10-21500, Pan Biotech, Bayern, Germany) and centrifuged at 300× *g* for 5 min. After centrifugation, cells were recovered and the single-cell suspension was counted and tested for viability using erythrosin B (Sigma-Aldrich, St. Louis, MO, USA).

2.4. Immunophenotype of AECs and WJ-MSCs

Immunophenotypic characterization of isolated AECs and WJ-MSCs was performed using flow cytometry. Cells were fixed for 10 min at room temperature using Intraprep Kit (Beckman–Coulter Inc., Brea, CA, USA) and washed twice with PBS. Cells were incubated for 30 min at 4 °C with conjugated primary antibodies (1 µg/mL) specific for epithelial (anti-pan Cytokeratin (Pan-Ck)-PE, Santa Cruz Biotechnology, Santa Cruz, CA, USA), mesenchymal (anti-CD44-PE, anti-CD73-PECY7, anti-CD90-FITC, anti-CD105-PECY7, Beckman-Coulter Inc., Brea, CA, USA), hematopoietic (anti-CD14-PE, anti-CD34-PerCP, anti-CD45-FITC, Beckman-Coulter Inc., Brea, CA, USA), and stem cell (anti-state-specific embryonic antigen-4 (SSEA4) APC, Miltenyi Biotech, Germany) markers. For the analysis of Pan-Ck, we used the Pan-Ck Type I/II Antibody Cocktail (MA5-13156, Thermo Scientific, Waltham, MA, USA) and anti-mouse–Alexa Fluor 488 (A11001, Thermo Scientific, Waltham, MA, USA) as a secondary antibody. After

incubation, cells were washed with PBS and analyzed using the FACS Navio FC (Beckman-Coulter Inc., Brea, CA, USA) cytometer and the Kaluza FC C 1.2 Analysis software (Beckman-Coulter Inc., Brea, CA, USA).

2.5. Scaffold-free 3D perinatal cell culture

Spheroids were generated starting from isolated WJ-MSCs seeded as mono-culture or by combining WJ-MSCs with AECs using 96-well round-bottom cell-repellant plates (Greiner Bio-One, Kremsmünster, Austria). Briefly, 200 µL of DMEM with 10% FBS containing a total of 5000 cells/well were seeded in each well in both mono- and co-culture spheroids. In the co-culture setting, 2500 cells/well of each cellular subtype and EGF (10 ng/mL) were added. Immediately after seeding, the plates were centrifuged at 50× *g* for 3 min and placed in an incubator at 37 °C with 5% CO_2. The culture media was changed every day thereafter.

2.6. Time-lapse imaging of Spheroid Formation

Co-culture spheroids were generated starting from isolated WJ-MSCs stained using Vybrant™ DiD Cell-Labeling Solutions (Molecular Probes, Eugene, OR, USA) and AECs stained using Vybrant™ DiO Cell-Labeling Solutions (Molecular Probes, Eugene, OR, USA). Biefly, 1 × 10^6 cells/mL in serum-free DMEM were incubated for 20 min at 37 °C with the corresponding labelling solution (5 µL/mL). Cells were washed twice in PBS and seeded in 96-well round-bottom cell-repellant plates. Immediately after seeding, the plates were centrifuged at 50× *g* for 3 min and placed in the IncuCyte® S3 live imaging system (Sartorius) for 96 h at 37 °C in 5% CO_2. Bright-field and immunofluorescence images were acquired using 10× magnification every 3 h from the seeding to the complete spheroid formation after 96 h.

2.7. Prestoblue® Assay for Spheroid Viability

To determine the presence of metabolically active cells in our spheroids the resazurin reduction assay was performed[137]. The assay is based on the principle that resorufin, which is the reduced form of resazurin, can be measured using a fluorescent method, thus indirectly determining the viability rate of incubated spheroids. Following 4 and 14 days

of 3D culture, the spheroids were transferred to a non-ULA 96 well plate and incubated for 24 h to allow the spheroids to adhere. After 24 h 100 µL of 10% Prestoblue® stock solution was added and incubated for a maximum of 24 h at 37 °C under 5% CO_2 humidified conditions. The reduction of the reagent was measured at 595 nm at 2, 4, 6, 8, and 24 h using a multiplate reader (Victor II Perkin Elmer, Waltham, MA, USA).

2.8. Live and Dead Staining

Cell viability within the spheroids was tested using the Live/Dead Cell Assay Kit (Life Technologies). This assay was used to visually determine the group of cells within spheroids maintaining viability after clusterization indispensable for spheroid formation. Spheroids of mono- and co-culture at 4 and 14 days were incubated with a solution containing 1 µM calcein AM and 2 µM ethidium homodimer-1 at 37 °C for 45 min. After washing with PBS, spheroids were imaged with laser excitation of the sample at 488 nm and 561 nm using a Nikon Inverted Microscope (Nikon Instruments, Tokyo, Japan), and images were acquired with a Digital Sight camera DS-03 using the imaging software NIS-Elements 4.1 (Nikon Corporation, Tokyo, Japan).

2.9. Slide Preparation and Histology

The spheroids were washed in PBS and transferred to 1.5 mL Eppendorf tubes to encapsulate them with Epredia™ HistoGel™ Specimen Processing Gel (Fisher-Scientific, Loughborough, UK). Each gel specimen was moved to a cassette and loaded inside a tissue processor (Histo-line laboratories, Pantigliate, Italy). The samples were embedded in paraffin blocks using an automated inclusor (Medite Medical, Burgdorf, Germany). Microtome (Microme, Bio-Optica, Milano, Italy) sections of 10 µm were placed on Super Frost glass slides (DiaPath, Menzel, Martinengo, Italy) and allowed to dry. The sections were deparaffinized with 2 changes of xylene for 5 min and rehydrated with 2 changes of 100% ethanol, followed by washes in 90% ethanol and 70% ethanol for 3 min. Finally, the slides were rinsed in distilled water.

2.10. Hematoxylin and Eosin Staining

The slides were deparaffinized, rehydrated, and stained with hematoxylin and eosin. The sections were stained with Gill 2 hematoxylin (Bio-Optica) for 5 min, washed in tap water for 3 min, rinsed with distilled water, and subsequently stained with 1% eosin G (Bio-Optica) for 10 min, dehydrated in ethanol of ascending concentration (70, 90, and 100%), clarified in pure xylene, and mounted with Bio Mount balm (Bio-Optica). Stained sections were observed using a Leica DM 750 equipped with a Leica ICC50 HD digital camera.

2.11. Biophysical Properties Analysis of Perinatal Spheroids (W8 Analysis)

The W8 instrument (CellDynamics SRL) is able to accurately measure the size, weight, and density of the spheroids. Single spheroids free-fall into a vertical flow channel dedicated to analyzing their terminal velocity. The physical approach of this analysis and the mathematical equations used for the calculation is extensively described by Cristaldi et al.[138]. Before the measurement, the spheroids were fixed with paraformaldehyde (PFA) 4% for 72 h at 4 °C, resuspended in 4 mL of phosphate-buffered saline (PBS, Corning, NY, USA), transferred in a centrifuge conical tube, and then analyzed. A minimum of 10 spheroids was analyzed for both mono- and co-culture at different time points.

2.12. Immunofluorescence Analysis

Antigen retrieval was performed by incubating slides of sectioned spheroids in sodium citrate pH 6 at 95 °C for 30 min. Sections were washed with PBS and permeabilized by adding PBS 0.3% Triton (Triton X-100, Sigma-Aldrich, Co., St. Louis, MO, USA) for 10 min. Slides were incubated for 30 min with a blocking solution containing PBS 4% bovine serum albumin (BSA, Sigma-Aldrich, St. Louis, MO, USA) and 0.3% Triton, then incubated overnight at 4 °C with the primary antibodies listed in table 1 diluted in blocking solution. Secondary anti-mouse Alexa Fluor 488 (1:500, #A11001, Thermo Scientific, Waltham, MA, USA) and Alexa Fluor 594 (1:500, #A32754, Thermo Fisher Scientific, Waltham, MA, USA) were used for 1 h incubation at room temperature. After three washes with PBS, coverslips were mounted using the Prolong Gold Antifade Mountant with DAPI (Thermo Fisher Scientific, Monza, Italy). Stained cells were observed using a

Nikon Inverted Microscope (Nikon Instruments, Tokyo, Japan), and images were acquired with a Digital Sight camera DS-03 using the imaging software NIS-Elements 4.1 (Nikon Corporation, Tokyo, Japan).

Primary Antibodies	Dilution	Catalog Number / Producer
Vimentin	1:200	#MA5-14564, Thermo Fisher Scientific, Waltham, MA, USA
Pan-cytokeratin	1:200	#MA5-13156, Thermo Fisher Scientific, Waltham, MA, USA
Laminin	1:100	#L9393, Sigma-Aldrich, Co., St. Louis, MO, USA
Fibronectin	1:200	#F3648, Sigma-Aldrich, Co., St. Louis, MO, USA
Pan-Cadherin	1:200	#71-7100, Thermo Fisher Scientific, Waltham, MA, USA
Collagen I	1:200	#BK72026S, Cell Signaling Technology, Danvers MA, USA
SOX-17	1:200	#MAB1924, R&D system, Minneapolis, MN, USA
PDX-1	1:500	#PA5-78024, Thermo Fisher Scientific, Waltham, MA, USA
Neurogenin3	1:200	#MAB3444 R&D system, Minneapolis, MN, USA
C-peptide	1:200	#4593S Cell Signaling Technology, Danvers MA, USA
Insulin	1:200	#I2018 Sigma-Aldrich, Co., St. Louis, MO, USA

Table 3 List of primary antibodies, dilution and Specification for immunofluorescence staining.

2.13. Hypoxia Staining

The hypoxia level of whole-mounted spheroids was evaluated using the hypoxia LOX-1 probe (Organogenix- MBL) according to the manufacturer's instructions. The probe was added to the culture medium at a final concentration of 2 μM 24 h before detection. Images visualizing the hypoxic area in mono- and co-culture spheroids were obtained using a Nikon Inverted Microscope (Nikon Instruments, Tokyo, Japan), and images were acquired with a Digital Sight camera DS-03 using the imaging software NIS-Elements 4.1(Nikon Corporation, Tokyo, Japan). The percentage of the hypoxic area within a total spheroid area was determined.

2.14. Isolation of PBMCs

Peripheral Blood Mononucleated Cells (PBMCs) were obtained from the blood of healthy donors according to the protocol approved by the Ethics Committee. To isolate PBMCs, a buffy coat was collected from the hospital and opened with sterile scissors, blood was then diluited 1:10 with phosphate buffered saline (PBS).

Later diluited blood was added in 15mL Falcon tubes already containing Ficoll-Histopaque, to perform a cell separation through density gradient, by mean of the centrifuge.

After the first centrifuge of 30 minutes for 1500 rpm without brake, a ring containing PBMCs was formed and was collected with the help of cotton-plugged Pasteur and transferred into another 15mL Falcon tube.

After this transfer, a second centrifuge was performed for 10 minutes at 1500 rpm. Once upon centrifuge ended, supernatant was removed, PBS was added to the pellet and another centrifuge was performed. Finally pellet was resuspended and PBMCs were counted with Methyl Violet, which stains with blue the nucleus, to discriminate them from red blood cells and their viability was assessed with Erythrosine B. Freshly isolated PBMCs could be seeded in suspension with RPMI Medium at 10% of FBS or directly frozen at -80°C.

2.15. Coculture of PBMCs and spheroids

After 24 hours of formation, both monocellular (WJ-MSCs) and co-culture (WJs-AECs) spheroids were well constituted and ready for the following part of the experiment. For the coculture of spheroids with PBMCs, it was established a 1:10 ratio between the spheroids and the PBMCs. PBMCs were thawed, tested for their viability and then activated with anti-CD3 antibody (CD3 Monoclonal Antibody HIT3a, Functional Grade, eBioscience™ Invitrogen, Waltham, MA, USA) at 2:100uL and anti-CD28 antibody (CD28 Monoclonal Antibody), Functional Grade, eBioscience™, Invitrogen, Waltham, MA, USA) at concentration of 1:100 uL. For each well of a 96-ULA plate there was a spheroid lying and 180 uL of his culture medium were removed in order to add 180 uL of RPMI Medium containg activated PBMCs. Activated and unactivated PBMCs were seeded without spheroids to use them as positive and negative controls respectively and then the plate was incubated for 72 hours and occasionally checked.

2.16. Flow cytometry and labelling

After 72 hours of coculture between PBMCs and spheroids, spheroids were filtrated with specific strainers of 40 μm to collect PBMCs into the tubes for flow cytometry staining, excluding spheroids. Once PBMCs had been collected, they were labelled with specific antibodies to perform their phenotypic characterization and to assess the presence and the quantity of specific markers of expression related to T cell subset. For the detection of surface markers, the staining was performed by incubating cells for 30 minutes in PBS 0.1% BSA with antibodies at 4°C and avoiding light. After incubation cells were washed and resuspended in PBS 0.1% BSA. The surface antibodies used for the analysis of T cell markers were: anti-CD4 APC (Biolegend, Cat. No 300514), anti-CD8 PECy7, antiCD8-PE, anti-CD25 FITC (Biolegend, 302604). The analysis of Treg subset ($CD4^+CD25^+$) was completed with the analysis of intracellular marker FoxP3. For intracellular staining PBMCs were fixed and permeabilized with eBioscience™ FoxP3/ Transcription Factor Staining Buffer Set (Invitrogen, Cat. No 00-5523-00) according to manufacturer instructions. Briefly, cells were fixed for 30 minutes at 4° with Fixation/Permeabilization solution, previously diluted 1:4 with Foxp3 Fixation/Permeabilization Diluent, and then permeabilized for 15 minutes at room temperature with 1X Foxp3 Permeabilization

Buffer. Cells were labelled with anti-FoxP3 PE antibody (3:100uL) (Biolegend, Cat. No 320108) for 30 minutes at 4° in permeabilization buffer, then washed twice and resuspended in PBS 0.1% BSA. For the analysis of $CD8^+$ cells producing Granzyme B, cells were first stainded for CD8 marker, then fixed and permeabilized with BD Cytofix/Cytoperm™ Fixation/Permeabilization Kit (BD Bioscience, 554714) and stained with intracellular markers used were anti-Granzime B APC700 for 30 minutes at 4°C in pemeabilization buffer. Flow Cytometry analysis was performed with CytoFLEX instrument (Beckman Coulter) and results were analysed with FlowJo software.

2.17. Annexin/7-AAD labelling

The apoptosis of PBMCs with or without coculture was assessed using Annexin V/7-AAD kit (Biolegend, San Diego, CA, USA). Cells were stained according to manufacturer instructions. Briefly, PBMCs were collected, washed with PBS, and then labelled for 15 min at room temperature with anti-Annexin V PE and 7-AAD in binding buffer; both used 2:100. After the staining, 400 μL of binding buffer was added to each tube and samples were analysed by flow cytometry. Unstained PBMCs were used as negative controls and results were represented as a percentage of Annexin V $PE^+/7\text{-}AAD^-$ (early apoptosis) and Annexin V $PE^+/7\text{-}AAD^+$ (late apoptosis) cells among PBMCs.

2.18. CFSE Proliferation Assay

PBMCs rate of proliferation was assesed through Carboxyfluorescein succinimidyl ester (CFSE), which is a cell staining fluorescent dye. After thawing, PBMCs were incubated with CFSE for 10 minutes at 37°C in dark conditions and then seeded according to the experiment workflow. After labelling, PBMCs were activated with anti-CD3 and anti-CD28, and seeded in a 1:10 ratio on spheroids composed of 3000 cells each. PBMCs alone were seeded as positive and negative controls and the plate was incubated for 72 hours. After incubation, PBMCs were collected and stained for anti-CD4 and anti-CD8 antibodies, as previously described. CFSE staining allows to trace multiple generations using dye dilution by flow cytometry, to detect the percentage of $CD4^+$ and $CD8^+$ proliferating cells. Flow Cytometry analysis was performed with CytoFLEX instrument (Beckman Coulter) and results were analysed with FlowJo software.

2.19. Differentiation of co-culture spheroids into insulin producing islet-like spheroids

The differentiation of co-culture spheroids was performed after 48 hours after the spheroid seeding when spheroids were completely formed. Differentiation was initiated following a four-stage process using the STEMdiff™ Pancreatic Progenitor Kit (Stemcell Technologies)(see Table 2). The differentiation process spanned a total of 14 days, beginning with the induction of definitive endoderm, followed by the formation of the primitive gut tube, the posterior foregut, and the final differentiation into pancreatic progenitors. Daily medium changes were performed using specialized media prepared for each stage (see Table 2). At the end of the differentiation protocol, spheroids were collected and processed for histological analysis.

Stage	Duration (Days)	Medium Composition	Key Events
Stage 1: Definitive Endoderm	2	Endoderm Basal Medium + Supplement MR + Supplement CJ (Day 1), Endoderm Basal Medium + Supplement CJ (Day 2)	Induction of definitive endoderm markers
Stage 2: Primitive Gut Tube	3	Stage 2-4 Basal Medium + Supplement 2A + 2B (Day 1), Stage 2-4 Basal Medium + Supplement 2B (Days 2-3)	Formation of the primitive gut tube
Stage 3: Posterior Foregut	3	Stage 2-4 Basal Medium + Supplement 3	Induction of posterior foregut markers
Stage 4: Pancreatic Progenitors	6	Stage 2-4 Basal Medium + Supplement 4	Differentiation into pancreatic progenitors ($PDX1^+$, $NKX6.1^+$)

Table 4 Summary od Differentiation Stages Using the STEMdiff™ Pancreatic Progenitor Kit.

2.20. Differentiation of Amniotic Epithelial Cells into insulin producing cells

The differentiation of epithelial cells isolated from the amniotic membrane was performed at passage 1. Cells were seeded at a density of 40,000 cells/cm^2 in 6-well plates,

pre-coated with laminin at a concentration of 1 ng/mL. When the cultures reached 80% confluence, differentiation was initiated following a four-stage process using the STEMdiff™ Pancreatic Progenitor Kit (Stemcell Technologies) as previously describes (see Table 2). At the end of the differentiation protocol, the cells were detached using trypsin-EDTA 0.25% (Corning, Steuben County, NY, USA). A subset of the differentiated cells was seeded onto chamber slides (BD Biosciences, San Jose, CA, USA) for immunofluorescence analysis to evaluate the state of differentiation, while others were used for the formation of spheroids for further experimentation.

2.21. Formation of Pseudo-Islet Spheroids from Differentiated AECs and WJ-MSCs

Following the 2D differentiation of amniotic epithelial cells (AECs), the differentiated cells were utilized in combination with Wharton's jelly mesenchymal stem cells (WJ-MSCs) to form spheroids.

Spheroids were generated using 96-well round-bottom cell-repellent plates (Greiner Bio-One, Austria). A total of 1500 cells per well were seeded, consisting of an equal ratio (1:1) of 750 differentiated AECs and 750 WJ-MSCs, suspended in 200 μL of DMEM supplemented with 10% FBS. Immediately after seeding, the plates were centrifuged at 50×g for 3 minutes to promote cell aggregation and placed in an incubator at 37°C with 5% CO_2. Daily media changes were performed to maintain cell viability and promote spheroid formation.

2.22. Statistical Analysis

All the experiments, except the one for which details were already described, were performed on at least three human samples in technical triplicate. Data are presented as mean ± standard deviation (SD) and were analyzed with two-way ANOVA or *t*-test using Graph Pad Prism 9.0 software (San Diego, CA, USA). The significance threshold was set at $p < 0.05$.

Results

3.1. Immunophenotypic Characterization of Isolated AECs and WJ-MSCs

The immuno-phenotypic profile of isolated AECs and WJ-MSCs was assessed through flow cytometry, focusing on epithelial, mesenchymal, and hematopoietic markers. As shown in Figure 8a, AECs displayed high levels of Pan-Ck [139], confirming their epithelial origin. In addition to this, AECs were positive for the surface markers CD73 and CD105, but negative for CD44 and CD90, which is consistent with recent findings and corroborates previous studies [95,140]. For the mesenchymal cells, WJ-MSCs expressed all mesenchymal surface markers (CD73, CD90, CD105, and CD44), while showing no expression of the epithelial marker Pan-Ck, as demonstrated in Figure 8b. Both AECs and WJ-MSCs also exhibited positivity for the stem cell marker SSEA4. Hematopoietic markers such as CD14, CD34, and CD45 were absent in both AECs (Figure 8a) and WJ-MSCs (Figure 8b).

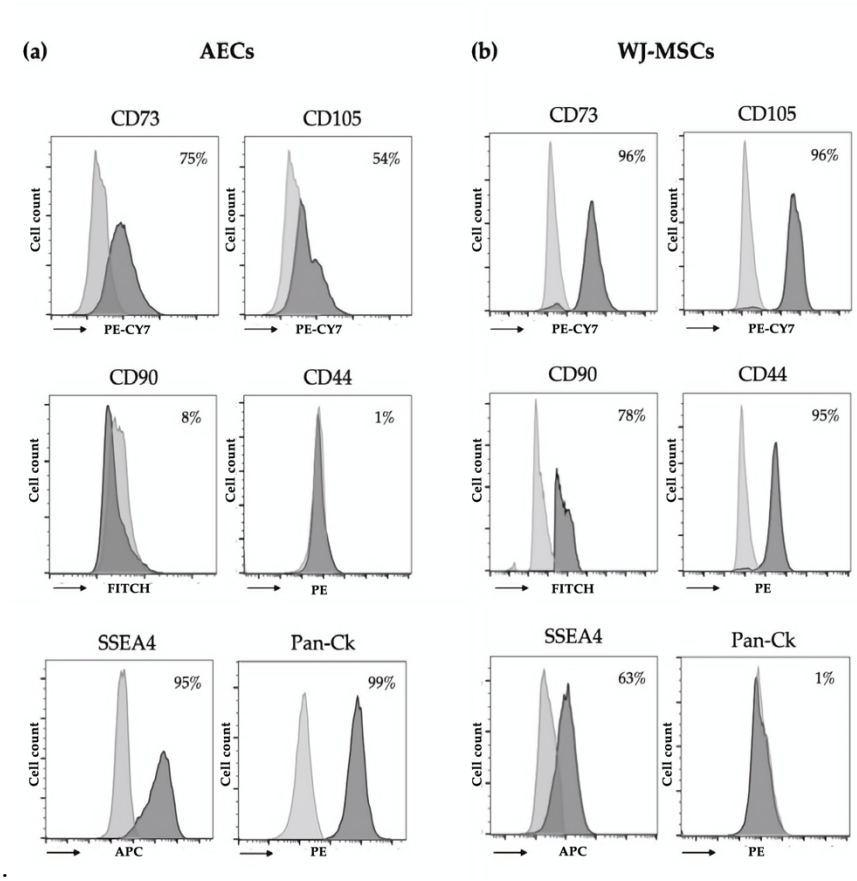

Figure 8 Immunophenotype of isolated AECs and WJ-MSCs. Data are representative of three independent experiments obtained from three human samples. Grey and black histograms represent the unstained controls and the specific cell markers, respectively. (**a**) Flow cytometry analysis of AECs: mesenchymal (CD44, CD73, CD90, CD105), stem cell (state-specific embryonic antigen-4, SSEA4), and epithelial (Pan-Cytokeratin, Pan-Ck) markers. (**b**) Flow cytometry analysis of WJ-MSCs: mesenchymal (CD44, CD73, CD90, CD105), epithelial (Pan-Ck), and stem cell (SSEA4) markers.

3.2. Spheroid Formation

To enhance cell–cell interactions, cells were seeded in cell-repellent plates, resulting in the formation of three-dimensional structures (spheroids, Figure 9a). In our study, two different cell types were tested for spheroid formation: AECs and WJ-MSCs. After seeding, the cells started to self-assemble in the well. After 4 days of incubation, WJ-MSC mono-cultures formed aggregates that were stable and easily handled, generating compact, rigid, spherically-shaped spheroids. Differently, AECs do not self-assemble in spheroids, but created a loose, compact sheet of cells that is easily dissociable. To set up a co-culture of AECs and WJ-MSCs that could display features of both cell types we tested three different ratios of AECs to WJ-MSCs: 2:1, 1:1, and 1:2. Spheroids with a 2:1 ratio were less compact and did not show spherical shapes. On the contrary, spheroids with a ratio

of 1:2 recapitulated the appearance of WJ-MSC mono-culture with compact, rigid, spherically-shaped spheroids. To maintain the highest number of AECs, we considered as appropriate the 1:1 ratio.

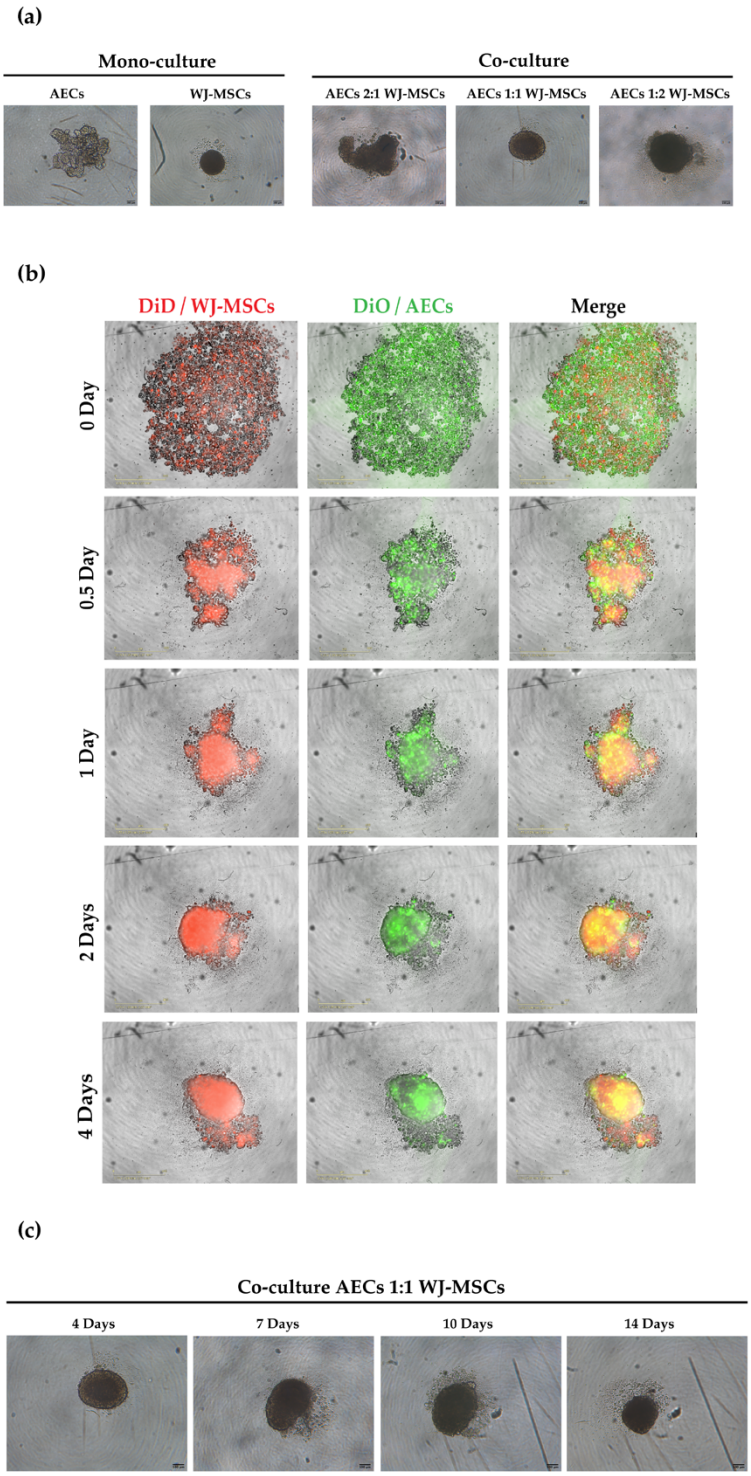

Figure 9 Representative images showing mono-culture spheroids of AECs and WJ-MSCs and co-culture spheroid formation at different ratios. (**a**) Mono-culture spheroid of AECs (5000 cells/spheroid) and WJ-MSCs (5000 cells/spheroid) and co-culture of AECs and WJ-MSCs with three different ratios of AECs:WJ-MSCs 2:1, 1:1, 1:2 (total 5000 cells/spheroid) after 4 days of culture. Images were acquired using a Leica

Labovert FS inverted microscope equipped with a Leica MC170 HD digital camera. Scale bars = 100 μm, magnification = 4×, N = 3 independent experiments. (**b**) Representative images of 1:1 co-culture spheroid formation at 0, 0.5, 1, 2, and 4 days using the IncuCyte® S3 live imaging system. WJ-MSCs were stained with DiD cell-labeling solution (red) and AECs were stained with DiO cell-labeling solution (green). Scale bars = 400 μm. Magnification = 10× (**c**) Long-term culture of 1:1 ratio spheroids. Images were acquired using a Leica Labovert FS inverted microscope equipped with a Leica MC170 HD digital camera. Scale bars = 100 μm, magnification = 4×, N = 3 independent experiments.

In order to visualize cell aggregation at an early time point we followed the cell culture from seeding to complete spheroid formation (4 days) using the IncuCyte® S3 live imaging system. As shown in Figure 9b, WJ-MSCs rapidly condensed in a cell mass, while AECs were distributed on the surface of the spheroid, increasing their compactness over time. Since the majority of the differentiation protocols in endo-pancreatic linages consist of 14 days of culture [95] we tested the stability of long-term culture. As shown in the representative images in Figure 9c, the co-culture spheroid maintained its shape and did not disaggregate during long-term culture.

3.3. Evaluation of Spheroid Viability

The viability of cells within the spheroids was evaluated using a Live/Dead Cell Assay Kit. The ethidium homodimer-1 staining indicates a compromised cell membrane (red fluorescence), and calcein fluorescence highlights viable cells (green fluorescence) (Figure10a). The WJ-MSC mono-culture appeared viable at 4 and 14 days. Co-culture spheroids appeared viable at 4 days, but the cell viability in the inner part was considerably compromised at 14 days. Metabolic activity of mono- and co-culture spheroids was also evaluated at 4 and 14 days using a Prestoblue® assay, as shown in Figure10b. At 4 days, co-culture spheroids expressed higher metabolic activity than the WJ-MSC mono-culture, while at 14 days a considerable decrease in the metabolic activity of both mono- and co-culture was detected. In accordance with the Live/Dead Cell Assay Kit, we assessed that WJ-MSC spheroids are viable and more metabolically active compared to co-culture.

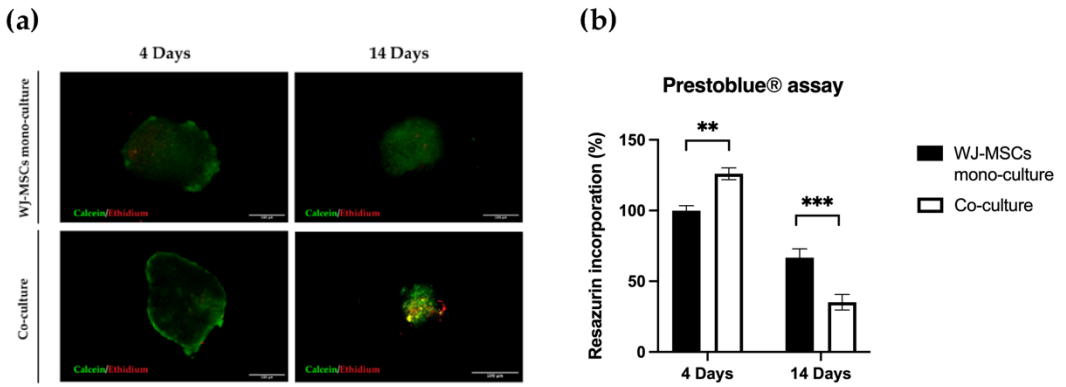

Figure 10 Viability of mono-culture WJ-MSC (black) spheroids and co-culture (white) spheroids. (**a**) Metabolic activity was measured with a Prestoblue® assay at 4 and 14 days in mono- and co-culture spheroids. N = 4 independent experiments. ** $p < 0.01$; *** $p < 0.001$; (**b**) Cell viability assay of spheroids in mono- and co-culture at 4 and 14 days, evaluated by staining with ethidium homodimer-1 and calcein-AM. Images are representative of three independent experiments. Green, viable cells; red, non-viable cells. Cells were observed using a Nikon Inverted Microscope (Nikon Instruments, Tokyo, Japan), and images were acquired with a Digital Sight camera DS-03 using the imaging software NIS-Elements 4.1 (Nikon Corporation, Tokyo, Japan). Scale bar = 100 μm. Magnification = 10×.

3.4. Histological Analysis

Hematoxylin and eosin staining was performed on spheroid sections at the early and late time points for both WJ-MSC mono-culture and co-culture. In Figure 11, WJ-MSC spheroids present a homogeneous structure and defined edges in both early- and late-time point spheroids. In contrast, at early time point, co-culture spheroids have a heterogeneous structure and irregular edges given by the presence of the two cell populations. At 14 days the co-culture displays an external ring of cells and a core characterized by a reduced number of nuclei and extensive ECM production.

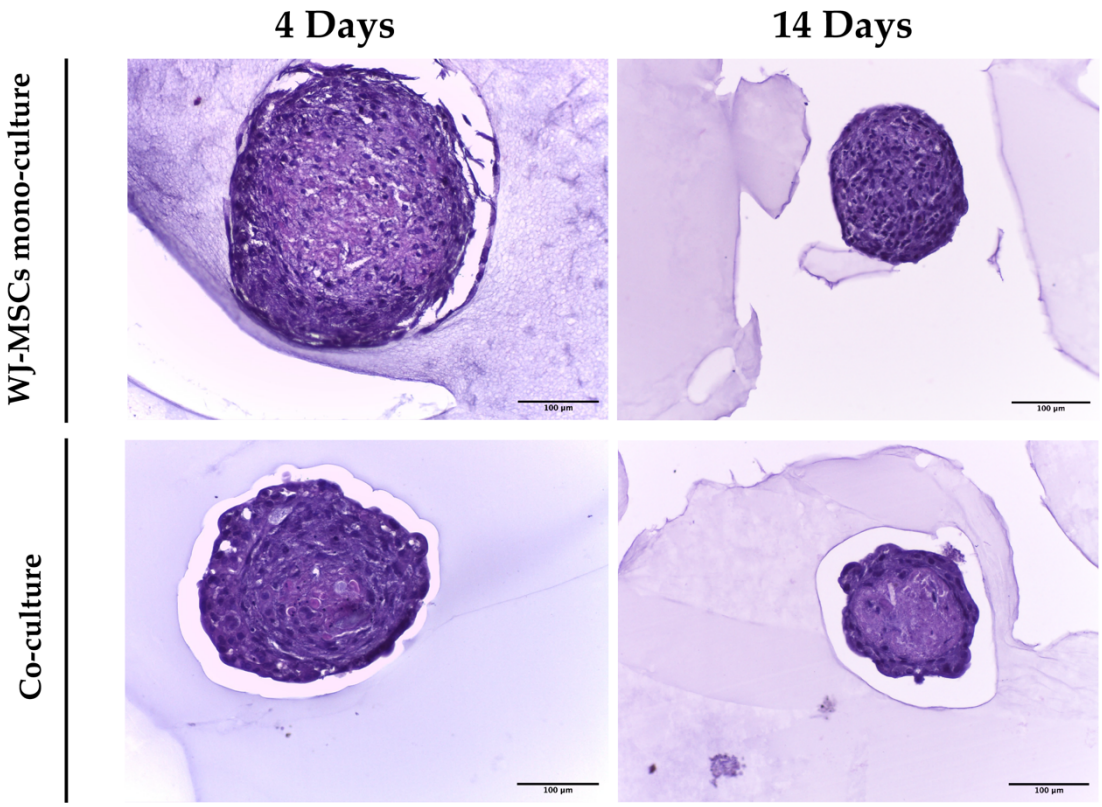

Figure 11 Hematoxylin and eosin staining on WJ-MSC mono-culture and co-culture spheroid sections after 4 and 14 days of culture. Spheroids were fixed in 4% PFA, then encapsulated with Epredia™ HistoGel™ Specimen Processing Gel (Fisher-Scientific, UK), sectioned, and then stained with hematoxylin and eosin. Images were acquired using a Leica DM 750 equipped with a Leica ICC50 HD digital camera. Scale bars = 100 µm. Magnification = 20×.

3.5. Characterization of the Physical Properties of Mono- and Co-Culture Spheroids

We analyzed mono-cultures of WJ-MSCs and co-cultures of WJ-MSCs and AEC spheroids obtained as described above. At least ten single spheroids for each condition were analyzed at four time points: 4, 7, 10, and 14 days of 3D culture. For each spheroid, the diameter and the mass density were analyzed. Experiments were performed on a homogeneous population of spheroids in terms of cell number (5000 cells/spheroid) to evaluate the contribution of each cell population in terms of density and diameter. Mono- and co-culture spheroid samples were fixed with 4% PFA and analyzed with the flow-based system. The diameter of WJ-MSC spheroids (µm), calculated automatically from the images acquired during the analysis, was stable during the four time points, as was the mass density (Figure 12). The average diameter of co-culture spheroids was progressively reduced over time, as shown in Figure 12a. The reduction in the diameter of the co-

cultures was associated with an increase in mass density (Figure 12b), suggesting not a loss in whole cell number but rather an increase in compactness and matrix production.

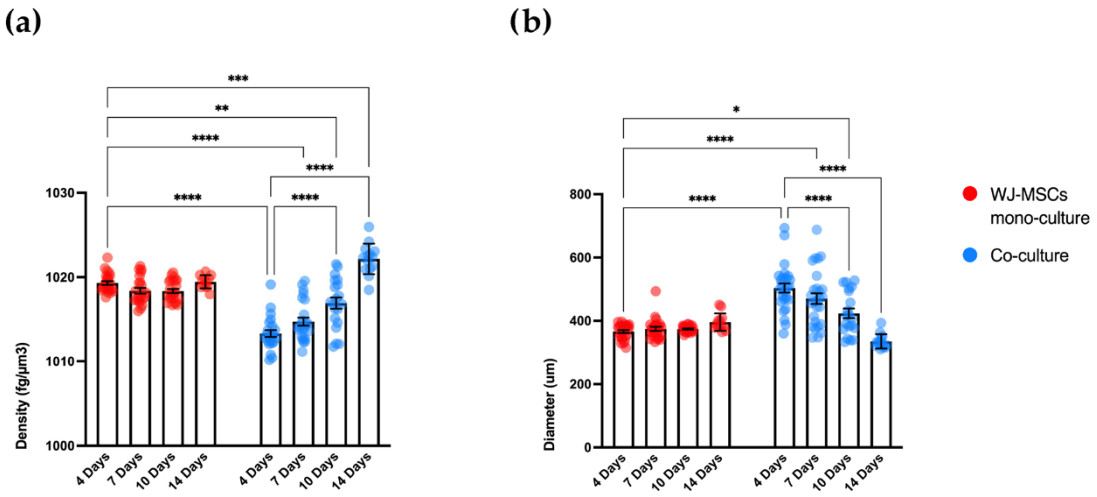

Figure 12 Measurement of mass density and diameter of mono-culture WJ-MSCs spheroids (red dots) and co-culture (WJ-MSCs + AECs) spheroids (blue dots). (**a**) Analysis of spheroid density (fg/µm³) at four time points: 4, 7, 10, and 14 days for both mono- and co-culture spheroids. The density of WJ-MSC spheroids remains stable over time while co-culture spheroids increase their density. (**b**) Analysis of spheroid diameter (µm) at four time points: 4, 7, 10, and 14 days for both mono- and co-culture spheroids. The diameter of WJ-MSC spheroids remains stable over time similarly to the density while co-culture diameter decreases with the increase in the density. N = 4 independent experiments. * $p < 0.05$; ** $p < 0.01$; *** $p < 0.001$; **** $p < 0.0001$.

3.6. Expression of Pan-Cadherins in Mono- and Co-Culture Spheroids

We investigated the presence of cadherin molecules in mono- and co-culture spheroids to evaluate cell–cell interactions. Cadherins are fundamental players in spheroid formation as they create homophilic cadherin–cadherin binding that contributes to spheroid compaction [137,141]. Cadherin's type and concentration are highly variable between different cell types; thus, we evaluated the presence of all cadherins with pan-cadherin antibody staining on the spheroid sections [137]. In Figure 13, cadherins accumulated after the first time point and their staining were maintained in long-term cultures, indicating a strong cell–cell interaction, in particular on the external surface of the spheroids.

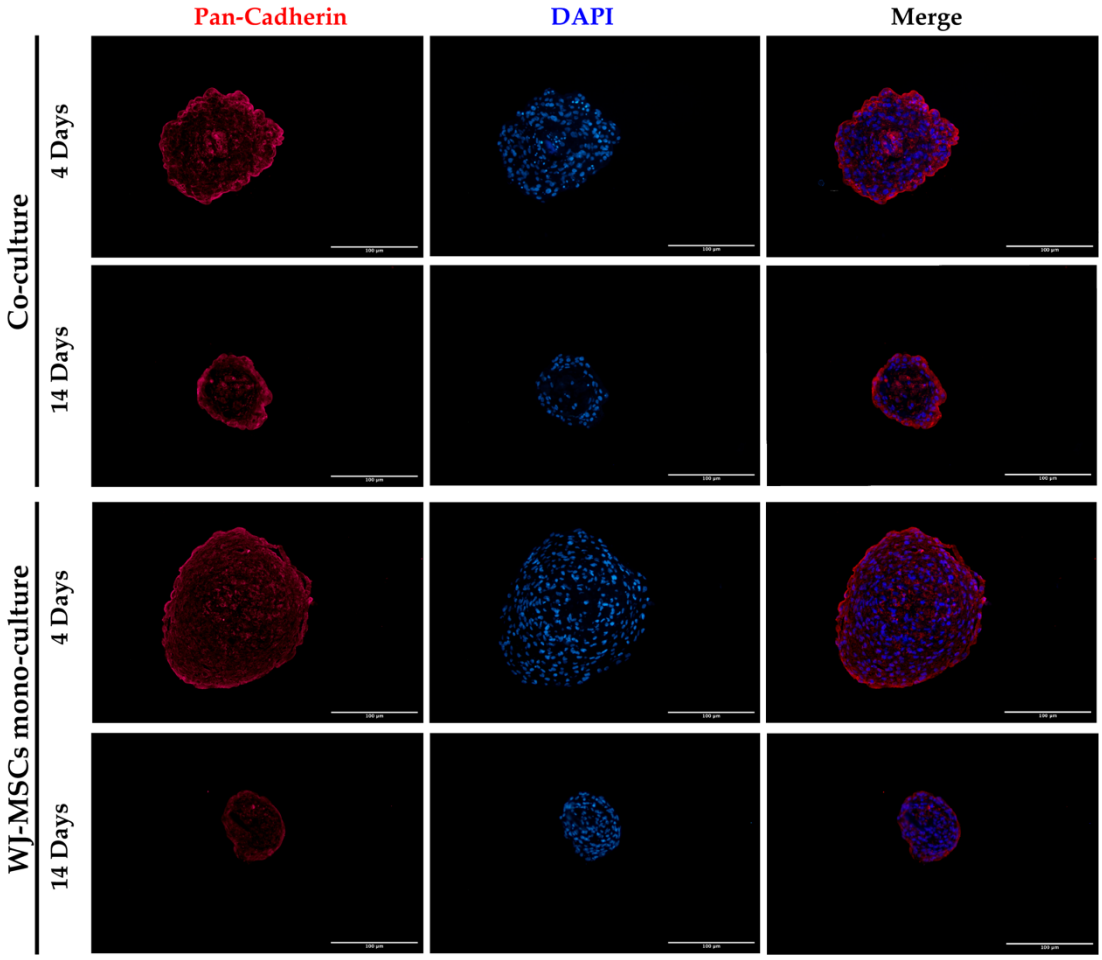

Figure 13 Representative images of WJ-MSC mono-culture and co-culture spheroids at early (4 days) and late (14 days) time points stained with Pan-Cadherin (red) and DAPI for nuclei staining (blue). Cells were observed using a Nikon Inverted Microscope (Nikon Instruments, Tokyo, Japan), and images were acquired with a Digital Sight camera DS-03 using the imaging software NIS-Elements 4.1 (Nikon Corporation, Tokyo, Japan). Scale bar = 100 μm. Magnification = 20×.

3.7. Pan-Cytokeratins and Vimentin Expression in Mono- and Co-Cultures

As the formation of the spheroids occurred through a self-organization process, we wanted to further characterize the structure of our 3D model co-culture to inspect the arrangement of the two cellular components within the spheroid and evaluate possible alterations during the long-term culture. Thanks to the immunofluorescence staining of the epithelial cell marker Pan-Ck (Figure 14), it was possible to appreciate that AECs covered the entire spheroid's surface, while only a few Pan-Ck positive cells were entrapped in the inner part of the 3D structure. On the contrary, no positivity for Pan-Ck staining was observed in WJ-MSC mono-cultures. WJ-MSCs were visualized as single-

positive for vimentin expression in co-cultures. In co-culture spheroids, at both 4 and 14 days, AECs co-expressed cytokeratin and vimentin, as already reported [142]. At 14 days co-culture spheroids reduced their diameter and in the core of the spheroid there was a reduced number of nuclei. Even though the expression of Pan-Ck did not change, degeneration during long term-culture were observable in WJ-MSCs.

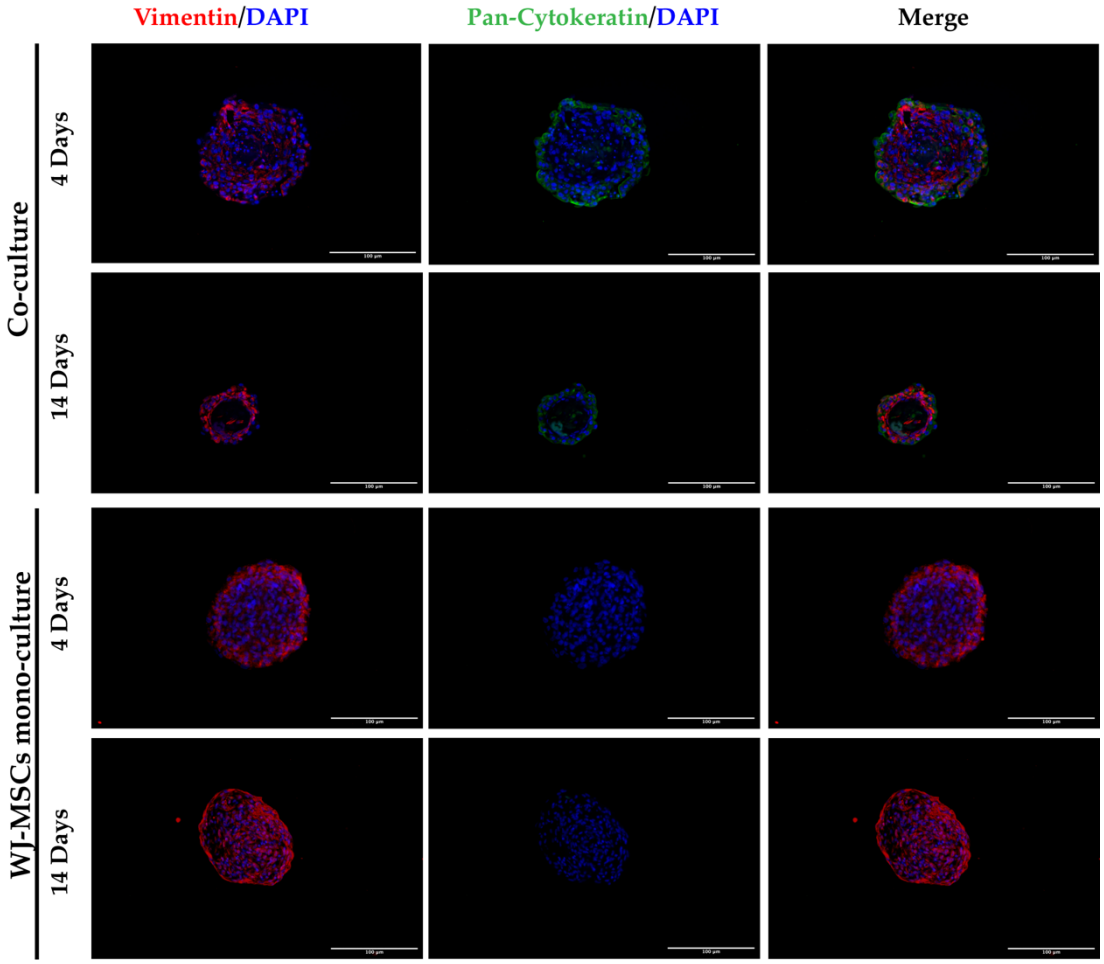

Figure 14 Representative images of WJ-MSC mono-culture and co-culture spheroids at early (4 days) and late (14 days) time points stained with Pan-Ck (green), vimentin (red), and DAPI for nuclei staining (blue). Cells were observed using a Nikon Inverted Microscope (Nikon Instruments, Tokyo, Japan), and images were acquired with a Digital Sight camera DS-03 using the imaging software NIS-Elements 4.1 (Nikon Corporation, Tokyo, Japan). Scale bar = 100 μm.

3.8. Extracellular Matrix Formation

We evaluated the presence of ECM proteins in our spheroids. ECM is widely known to provide structural support in tissues and also plays important roles in cell behavior, including cell adhesion, migration, and compartmentalization [129]. In particular, the presence of three different components was assessed. Figure 15 shows laminin,

fibronectin, and type I collagen immunofluorescence staining. As observed in Figure 15, laminin was not observed in WJ-MSC mono-cultures, but it was detected in co-cultures, particularly in correspondence with the epithelial cell layer. The production of laminin by epithelial cells in a 3D model of AECs has also been observed in our previous study [95] and recapitulated *in vivo* tissue organization. Type I collagen is the most prevalent ECM component providing structural support [143], while fibronectin is mainly responsible for cell adhesion and cellular migration. In both mono- and co-culture, fibronectin and type I collagen were expressed even at early time points, establishing a 3D ECM network. The presence of an ECM network, which is usually inconsistent in 2D culture, represents an important structural support for the artificial reconstruction of pancreatic tissue.

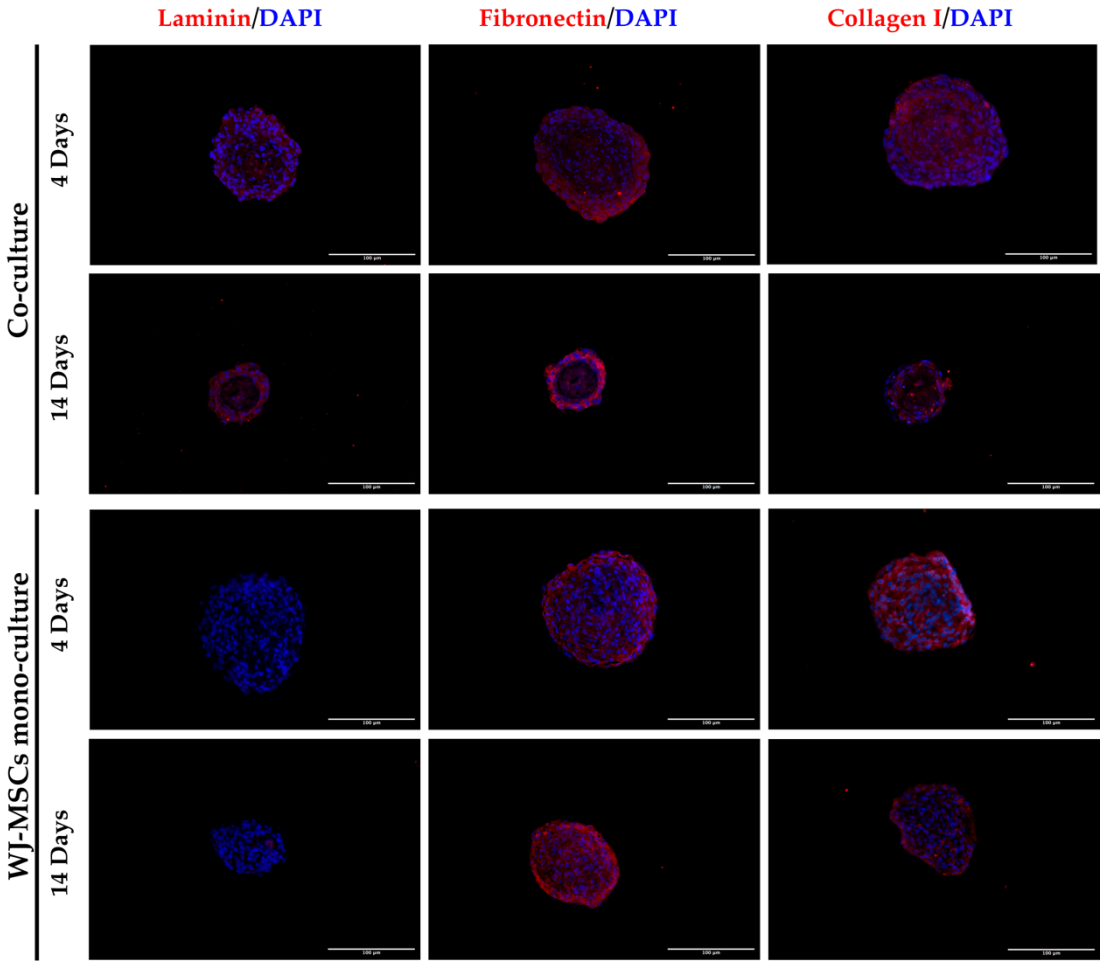

Figure 15 Representative images of WJ-MSC mono-culture and co-culture spheroids at early (4 days) and late (14 days) time points stained to evaluate the presence of ECM proteins with laminin, fibronectin, and collagen I (red) and DAPI for nuclei staining (blue). Cells were observed using a Nikon Inverted Microscope (Nikon Instruments, Tokyo, Japan), and images were acquired with a Digital Sight camera DS-03 using the imaging software NIS-Elements 4.1(Nikon Corporation, Tokyo, Japan). Scale bar = 100 μm. Magnification = 20×.

3.9. Evaluation of Hypoxia

To further characterize WJ-MSC mono-culture and co-culture spheroids we evaluated the hypoxic state at 4 and 14 days. A hypoxia LOX-1 probe (Figure 16) was used and its signal was acquired with the fluorescent microscope. Red fluorescence indicated a low oxygen level inside the multicellular spheroids. As shown in Figure 16a, a spread inner hypoxic signal was detected in a large area of both mono-culture and co-culture spheroids. The levels of hypoxia did not significantly change among spheroids after long-term culture (14 days) (Figure 16b).

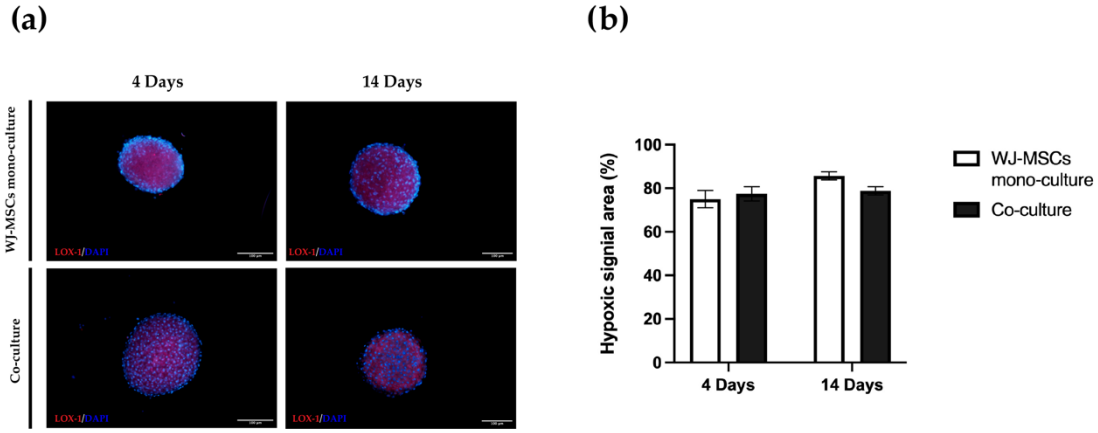

Figure 16 Hypoxia levels in mono-culture WJ-MSC spheroids and co-culture spheroids. (**a**) Images are representative of three independent experiments. Hypoxic signal in red (LOX-1); cell nuclei in blue (DAPI). Cells were observed using a Nikon Inverted Microscope (Nikon Instruments, Tokyo, Japan), and images were acquired with a Digital Sight camera DS-03 using the imaging software NIS-Elements 4.1 (Nikon Corporation, Tokyo, Japan). Scale bar = 100 µm. Magnification = 10×. (**b**) Hypoxia probe quantification was calculated as percentage of hypoxic area on the total spheroid area using ImageJ software v1.53k. WJ-MSC mono-culture (white); co-culture (black). N = 4 independent experiments.

3.10 Co-culture of Perinatal spheroids and PBMCs

Once spheroids were formed in ultra-low attachment (ULA) plates after 24 hours of culture, activated peripheral blood mononuclear cells (PBMCs) were added in co-culture with the spheroids at a consistent ratio of 1:10, corresponding to 30,000 PBMCs per well. PBMC activation was achieved using anti-CD3 and anti-CD28 antibodies, leading to their tendency to form several visible aggregates, as shown in Figure 17. Two control conditions were included: one with non-activated PBMCs and another with activated PBMCs cultured alone, without the presence of perinatal spheroids. The purpose of these

controls was to assess the baseline behavior of PBMCs, both in their quiescent and activated states, in the absence of any immunomodulatory influence from the perinatal spheroids.

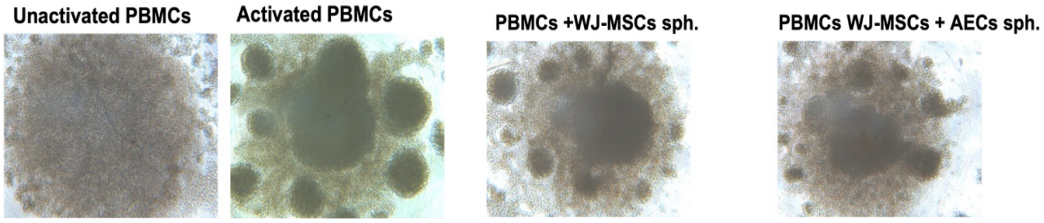

Figure 17 Immunomodulation Assay: Co-culture of perinatal spheroids and PBMCs. Unactivated PBMCs were used as the negative control, while activated PBMCs served as the positive control. Co-cultures included PBMCs with spheroids composed of either WJ-MSC monocultures or WJ-MSC and AEC co-cultures. Images were captured using a Leica Labovert FS inverted microscope equipped with a Leica MC170 HD digital camera. Magnification = 4×.

3.11 Analysis of apoptosis and proliferation rate of PBMCs

After 72 hours of co-culture, PBMCs were harvested and analyzed for apoptosis using Annexin V staining and proliferation rates using CFSE staining. The results were compared to the positive control, which consisted of activated PBMCs cultured alone. The apoptosis analysis revealed that across all three experimental conditions, PBMCs exhibited similar behavior, with no significant increase in apoptosis observed (Figure 18a). In terms of proliferation, assessed via CFSE dilution, a significant decrease in the proliferation rate was detected when PBMCs were co-cultured with either of the two spheroid models. This inhibitory effect on proliferation is illustrated in Figure 18b.

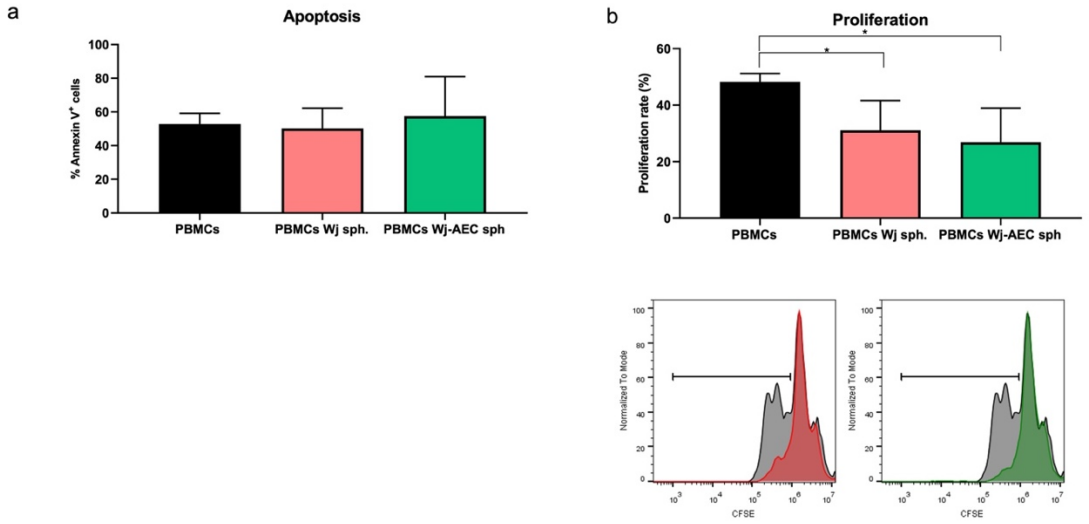

Figure 18 Apoptosis and proliferation rates of PBMCs under various experimental conditions. (a) Flow cytometry analysis of PBMC apoptosis rates across three conditions: activated PBMCs cultured alone (black), PBMCs co-cultured with WJ-MSC monoculture spheroids (red), and PBMCs co-cultured with WJ-MSC and AEC co-culture spheroids (green). (b) Flow cytometry analysis of PBMC proliferation rates, with histograms showing the proliferation of activated PBMCs as the reference (black), compared to PBMCs in contact with WJ-MSC spheroids (red) and WJ-MSC/AEC spheroids (green). Data are presented as mean ± SEM. * $p < 0.05$; ** $p < 0.01$; *** $p < 0.001$; **** $p < 0.0001$.

3.12. Analysis of proliferation rate of CD4⁺ and CD8⁺ T cells

In addition to examining the overall proliferation rate of the PBMC population, we specifically assessed the proliferation of $CD4^+$ and $CD8^+$ T cells using CFSE staining. The results showed a notable decrease in the proliferation rate of $CD4^+$ T cells, particularly in PBMCs co-cultured with WJ-AEC spheroids, when compared to the activated PBMC control.

Similarly, the analysis of $CD8^+$ T cells revealed a comparable trend, with the most pronounced reduction in proliferation occurring in the condition where PBMCs were co-cultured with WJ-AEC spheroids. However, WJ spheroids alone also significantly reduced the proliferation of both $CD4^+$ and $CD8^+$ T cells. The results are illustrated in Figure 19 (a, b).

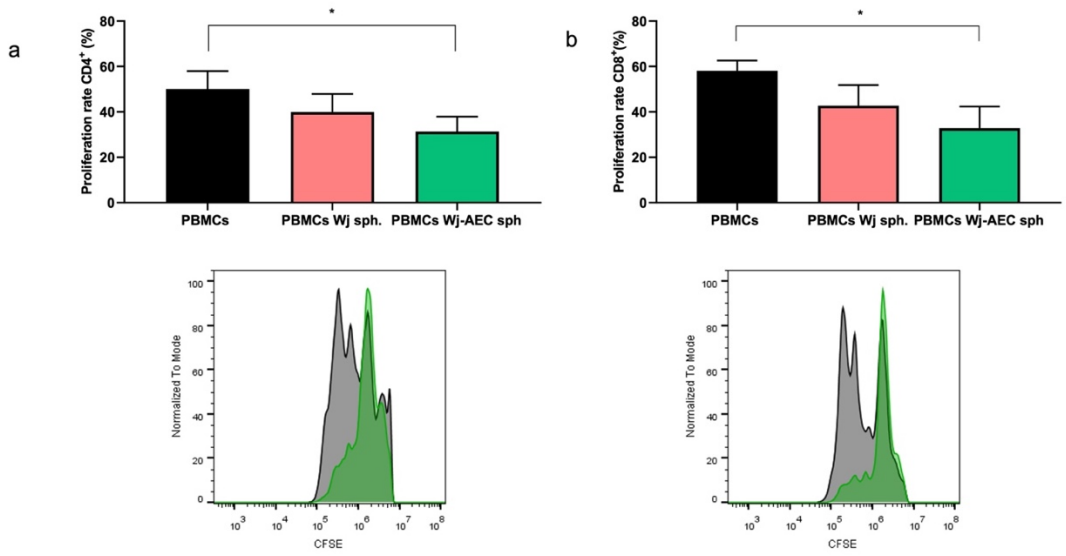

Figure 19 Proliferation rates of $CD4^+$ and $CD8^+$ T cells in the various experimental conditions. (a) Flow cytometry analysis of $CD4^+$ T cell proliferation rates across three conditions: activated PBMCs cultured alone (black), PBMCs co-cultured with WJ-MSC monoculture spheroids (red), and PBMCs co-cultured with WJ-AEC spheroids (green). The accompanying histogram shows the reference proliferation of $CD4^+$ T cells (black) compared with the other two conditions (red and green). (b) Flow cytometry analysis of $CD8^+$ T cell proliferation rates, with the same color coding: activated PBMCs cultured alone (black), PBMCs co-cultured with WJ spheroids (red), and PBMCs co-cultured with WJ-AEC spheroids (green). The histogram compares the $CD8^+$ T cell proliferation across the conditions. Data are presented as mean ± SEM. * $p < 0.05$; ** $p < 0.01$; *** $p < 0.001$; **** $p < 0.0001$.

3.13. Analysis of immune activation of CD4⁺ and CD8⁺ T cells

Next, we focused on two subpopulations within the T cell pool: $CD4^+$ and $CD8^+$ T cells. The first analysis we conducted was the expression of the immune activation marker CD69, assessed by flow cytometry.

The analysis revealed a slight decrease in CD69 expression in $CD4^+$ T cells in both experimental conditions, where PBMCs were co-cultured either with AEC spheroids or WJ-MSC spheroids. A similar trend was observed in $CD8^+$ T cells, with a slight reduction in CD69 expression across both conditions. Although WJ-MSC spheroids appeared slightly more effective than AEC spheroids in reducing CD69 expression in both $CD4^+$ and $CD8^+$ T cells, the differences between the experimental groups were not statistically significant. The results are presented in Figure 20 (a, b).

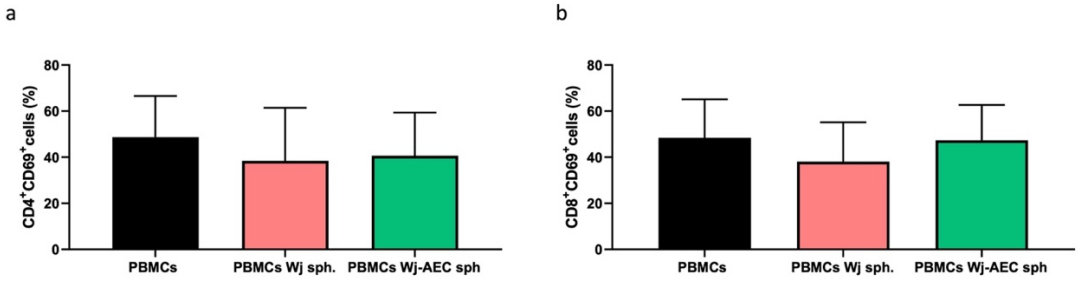

Figure 20 Flow cytometry analysis of CD69 expression in $CD4^+$ and $CD8^+$ T cells under the three experimental conditions. (a) CD69 expression in $CD4^+$ T cells: activated PBMCs cultured alone (black), PBMCs co-cultured with WJ-MSC spheroids (red), and PBMCs co-cultured with WJ-AEC spheroids (green). (b) CD69 expression in $CD8^+$ T cells under the same experimental conditions: activated PBMCs alone (black), PBMCs with WJ spheroids (red), and PBMCs with WJ-AEC spheroids (green). Data are presented as mean ± SEM. * $p < 0.05$; ** $p < 0.01$; *** $p < 0.001$; **** $p < 0.0001$.

3.14. Immunophenotypic analysis of regulatory T cells and GrzB-secreting T cells ($CD8^+$)

Within the lymphocyte population, we focused on the immunophenotypic analysis of two specific subpopulations: regulatory T cells (Tregs) and $CD8^+$ T cells that secrete granzyme B (GrzB). These analyses were conducted using flow cytometry.

First, we analyzed the population of $CD4^+$ regulatory T cells, which express the CD25 and FoxP3 markers. As shown in Figure 21a, the percentage of $CD4^+$ regulatory T cells significantly increased in both the "PBMCs WJ sph." and "PBMCs WJ-AEC sph." conditions compared to the control (activated PBMCs alone). Although both conditions induced an increase in Tregs, the co-culture with WJ-AEC spheroids appeared to be slightly more effective than the WJ spheroids alone.

Next, we examined a rare subset of regulatory T cells that express CD25, FoxP3, and CD8. As depicted in Figure 21b, this subset also showed an increase in both experimental conditions, with the WJ-AEC spheroids once again demonstrating a stronger effect compared to WJ spheroids alone.

Finally, we evaluated $CD8^+$ T cells producing granzyme B. The flow cytometry analysis (Figure 21c) revealed a decrease in GrzB-producing $CD8^+$ T cells in both conditions, with a more pronounced reduction in the "PBMCs WJ-AEC sph." condition. This suggests a potential immunomodulatory effect exerted by the spheroids on the cytotoxic activity of $CD8^+$ T cells.

These results highlight the differential effects of WJ and WJ-AEC spheroids on both regulatory and cytotoxic T cell populations, underscoring the potential immunoregulatory role of these perinatal cell-derived spheroids.

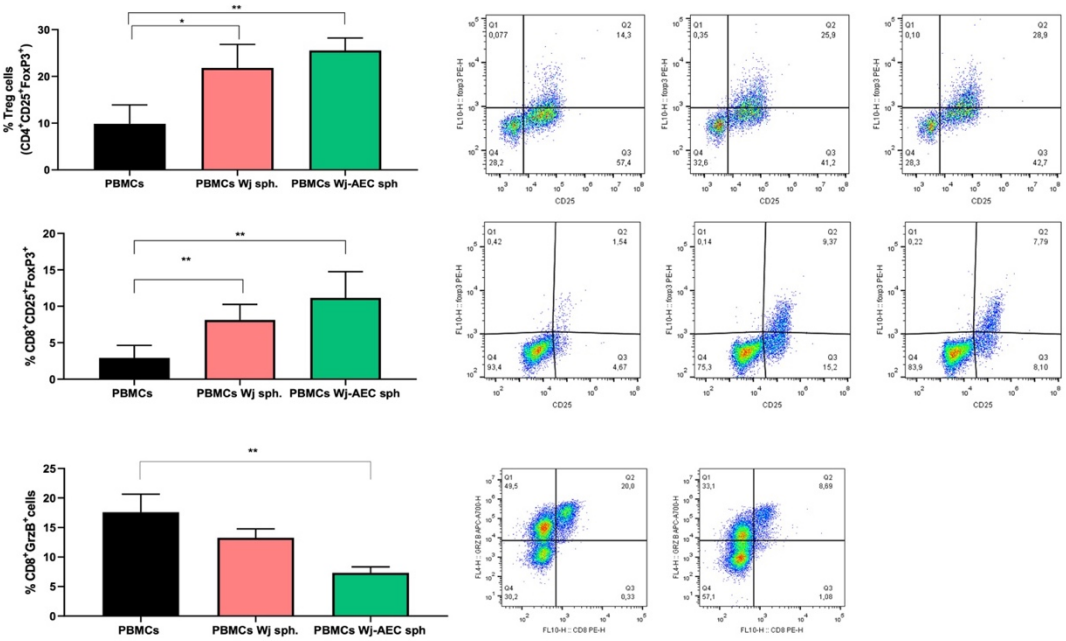

Figure 21 Immunophenotypic analysis of $CD4^+$ Treg, $CD8^+$ Treg and $CD8^+$ T cells producing granzyme B (GrB) (a) Immunophenotypic analysis of $CD4^+$ regulatory T cells ($CD4^+$, $CD25^+$, $FoxP3^+$) and corresponding flow cytometry gating plots in the conditions: "PBMCs" (black), "PBMCs WJ sph." (red), and "PBMCs WJ-AEC sph." (green). (b) Immunophenotypic analysis of $CD8^+$ regulatory T cells ($CD8^+$, $CD25^+$, $FoxP3^+$) and corresponding flow cytometry gating plots in the same experimental conditions. (c) Immunophenotypic analysis of $CD8^+$ T cells producing granzyme B (GrB), along with flow cytometry gating plots for the "PBMCs", "PBMCs WJ sph.", and "PBMCs WJ-AEC sph." conditions. Data are presented as mean ± SEM. * $p < 0.05$; ** $p < 0.01$; *** $p < 0.001$; **** $p < 0.0001$.

3.15. Differentiation of co-culture spheroids into insulin producing islet-like spheroids

The differentiation potential of WJ-AEC co-culture spheroids towards the β-pancreatic lineage was evaluated using the STEMdiff™ Pancreatic Progenitor Kit (Stemcell Technologies) (see Table 2). The differentiation process lasted 14 days, progressing through four defined stages: induction of definitive endoderm, formation of the primitive gut tube, differentiation into the posterior foregut, and finally the generation of pancreatic progenitors. Each stage required a tailored composition of factors in the differentiation

medium. As a control, WJ-AEC spheroids that were not exposed to the differentiation medium and received only standard culture medium were used.

Immunofluorescence analysis was subsequently performed to assess the expression of differentiation markers indicative of pancreatic lineage commitment. However, the analysis did not reveal the expression of insulin (data not shown). Among the tested markers, only neurogenin3 (NGN3), a key transcription factor involved in pancreatic development, was positively detected (Figure 22). Additionally, a significant reduction in nuclei count was observed in the differentiated spheroids, which may be attributed to the extended culture period.

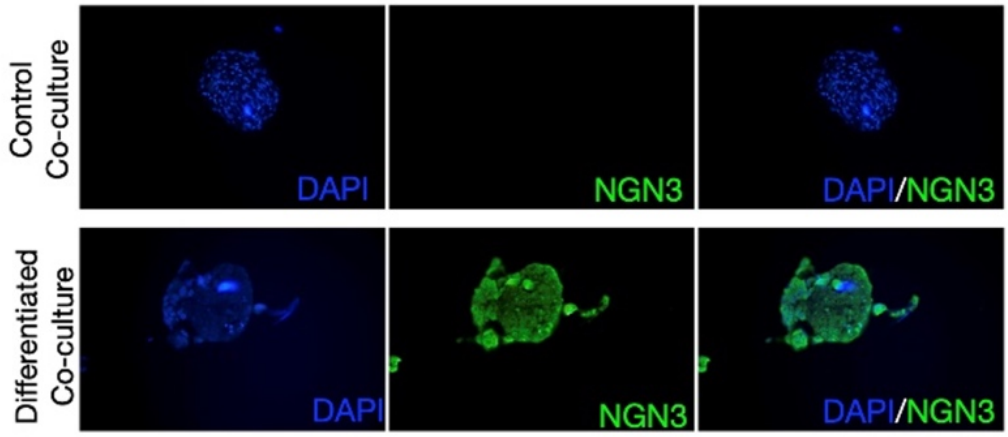

Figure 22 Immunofluorescence analysis of WJ-AEC co-culture spheroids after 14 days of differentiation towards the beta-pancreatic lineage. Spheroids subjected to the differentiation protocol did not express insulin, but a positive staining for neurogenin3 (NGN3) was observed (green). Control spheroids, which were not exposed to differentiation medium, showed no expression of NGN3 or insulin. A significant reduction in the number of nuclei (stained with DAPI, blue) was observed in the differentiated spheroids compared to controls. Cells were observed using a Nikon Inverted Microscope (Nikon Instruments, Tokyo, Japan), and images were acquired with a Digital Sight camera DS-03 using the imaging software NIS-Elements 4.1 (Nikon Corporation, Tokyo, Japan).

3.16 Differentiation of AEC into insulin producing cells

To address the limitations associated with direct differentiation on 3D spheroids, AECs were differentiated into insulin-producing cells in a 2D culture system on a laminin-coated surface. The differentiation was carried out using the STEMdiff™ Pancreatic Progenitor Kit (Stemcell Technologies) (see Table 2), following a 14-day protocol.

At the end of the differentiation process, the AECs were evaluated using immunofluorescence staining to assess the expression of key markers associated with

pancreatic endocrine differentiation. Cells were cultured under three conditions: pre-differentiation (pre-diff), non-induced control (CTR), and post-differentiation (diff). The following markers were used for the immunofluorescence analysis: SOX17 (definitive endoderm marker), vimentin (mesenchymal marker), Neurogenin3 (endocrine progenitor marker), PDX-1 (pancreatic progenitor marker), insulin, and C-peptide (markers of functional beta-cells).

The expression of SOX17, a definitive endoderm marker, and vimentin, a mesenchymal marker, was assessed (Figure 23). In the pre-diff condition, cells displayed low expression of SOX17 and moderate levels of vimentin, consistent with their initial epithelial phenotype. In the control condition (CTR), there was a slight increase in vimentin expression, while SOX17 expression remained unchanged. After differentiation, cells showed strong expression of SOX17, indicating successful commitment to a definitive endodermal lineage. However, the concurrent expression of vimentin suggests the persistence of mesenchymal characteristics in the differentiated cells.

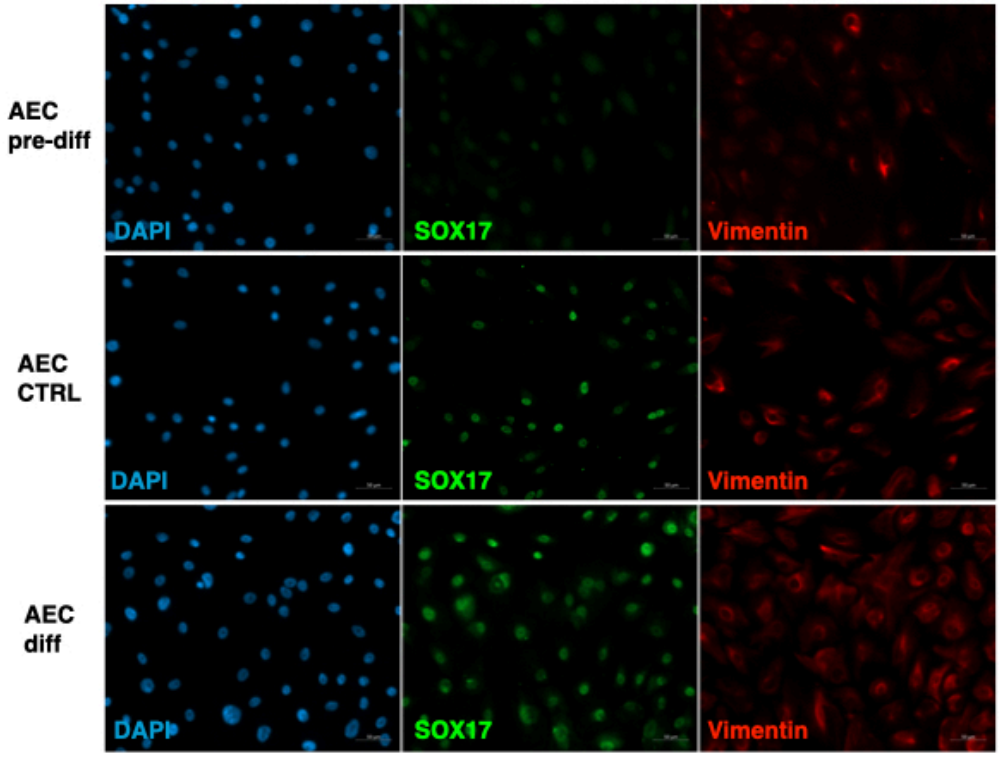

Figure 23 Immunofluorescence staining for DAPI (blue, nucleus), Sox17 (Sox17, green), and Vimentin (red) in AEC cells. (Top) Pre-differentiation condition shows low detectable Sox17 and Vimentin expression. (Middle) Control cells (CTR) in non-inductive increased expression of nuclear Sox17 and Vimentin. (Bottom) Differentiated cells exhibit higher expression of Sox17 and Vimentin. Scale bar: 20 μm. Images were acquired with Zeiss Axio Observer 7 microscopy.

Neurog3 and PDX-1, critical markers of pancreatic endocrine progenitors, were analyzed (Figure 24). In the pre-diff condition, AECs showed no detectable expression of Neurog3 or PDX-1, confirming the absence of initial endocrine differentiation. Similarly, control cells (CTR) maintained low levels of these markers, showing no significant change. However, after differentiation, cells exhibited robust co-expression of Neurog3 and PDX-1, indicating the activation of pancreatic endocrine differentiation and progression towards an endocrine progenitor phenotype.

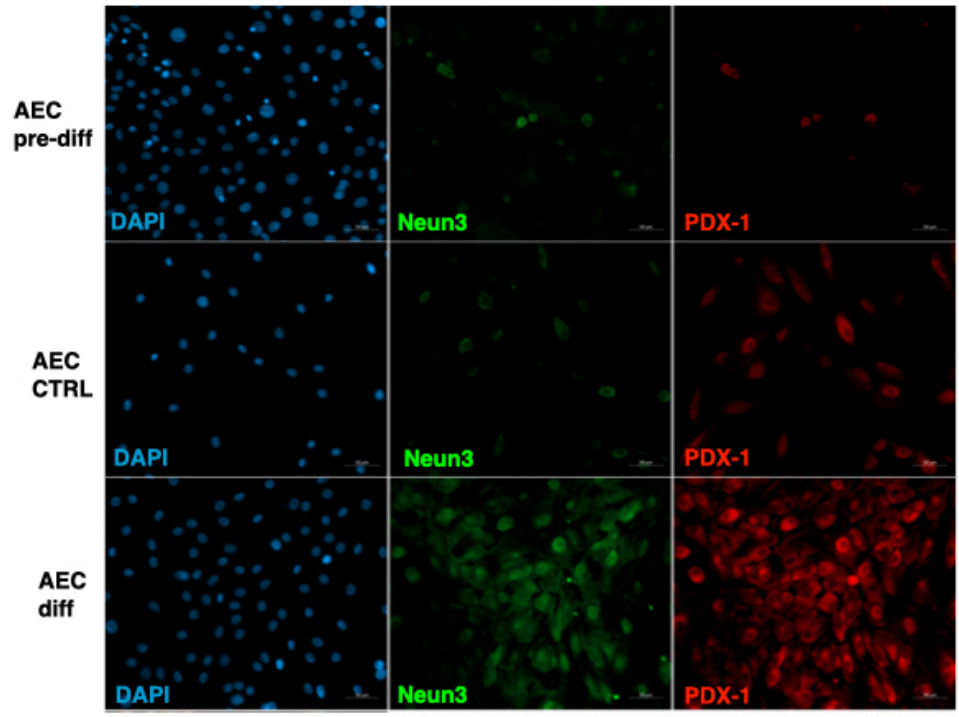

Figure 24 Immunofluorescence staining for DAPI (blue, nucleus), Neurog3 (Neun3, green), and PDX-1 (red) in AEC cells. (Top) Pre-differentiation condition shows no detectable Neun3 or PDX-1 expression. (Middle) Control cells (CTR) in non-inductive medium also show negligible expression. (Bottom) Differentiated cells exhibit strong co-expression of Neun3 and PDX-1, indicative of pancreatic endocrine progenitor differentiation. Scale bar: 20 μm. Images were acquired with Zeiss Axio Observer 7 microscopy.

Finally, insulin (INS) and C-peptide (C-PEP) expression was evaluated (Figure 25). Pre-differentiation cells showed no significant expression of INS or C-PEP, reflecting their undifferentiated state. In the control condition (CTR), where the cells were not exposed to pancreatic inductive factors, the expression of INS and C-PEP remained absent. In contrast, after differentiation, the cells showed strong co-expression of INS and C-PEP, indicating successful differentiation towards insulin-producing, beta-like cells.

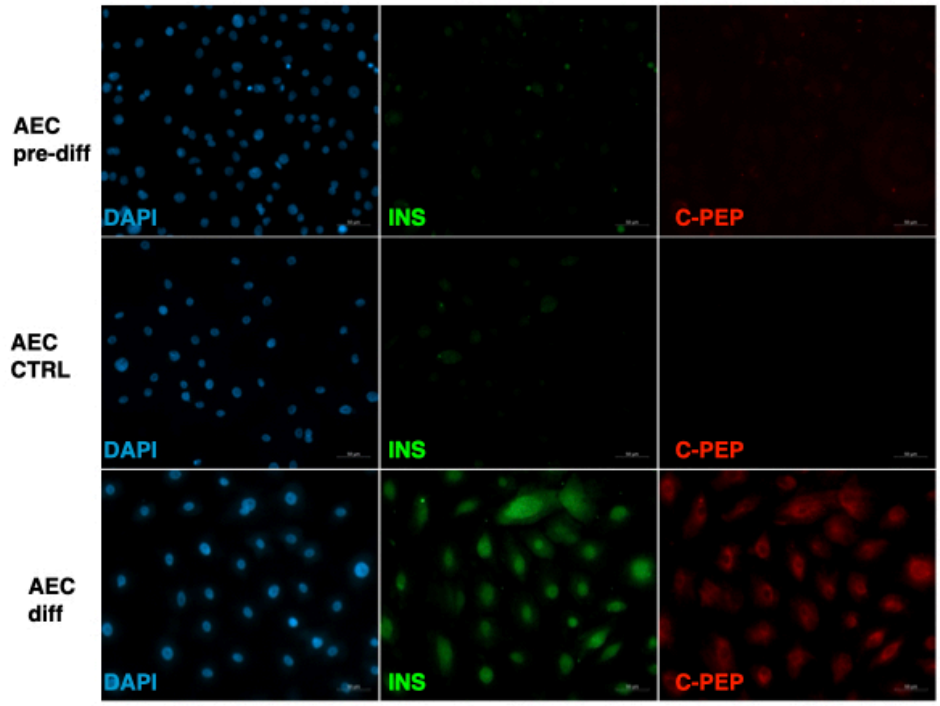

Figure 25 Immunofluorescence of AEC cells stained for DAPI (blue, nucleus), insulin (INS, green), and C-peptide (C-PEP, red). (Top) Pre-differentiation condition shows no significant expression of INS or C-PEP. (Middle) Control cells with non-inductive medium (CTR) exhibit no detectable expression. (Bottom) Differentiated cells show co-expression of INS and C-PEP, confirming successful differentiation toward an insulin-producing phenotype. Scale bar: 20 µm. Images were acquired with Zeiss Axio Observer 7 microscopy.

3.17 Formation of Pseudo-Islet Spheroids from Differentiated AECs and WJ-MSCs

Following the 2D differentiation of amniotic epithelial cells (AECs), the differentiated cells were utilized in combination with Wharton's jelly mesenchymal stem cells (WJ-MSCs) to form a pseudo-islet spheroid.

The Figure 26 presents the analysis of three physical parameters of the spheroids: diameter, density, and weight. The spheroids were compared in two experimental conditions: in blue, spheroids composed of non-differentiated AEC and WJ cells, while in green, spheroids composed of AEC cells differentiated in 2D and subsequently assembled with WJ cells. For each spheroid, measurements of diameter, weight and mass density were performed. The experiments utilized a homogeneous population of

spheroids with a standardized initial cell number of 1500 per spheroid to accurately assess the contribution of each cell type in terms of spheroid diameter and density.

Spheroid samples from both conditions were fixed with 4% paraformaldehyde (PFA) and analyzed using a flow-based system

The analysis did not reveal statistically significant differences between the two conditions for any of the parameters measured. Both the diameter and the density and mass showed comparable values between the two groups, suggesting that the preliminary differentiation of AEC cells did not markedly affect the physical properties of the spheroids under these experimental conditions.

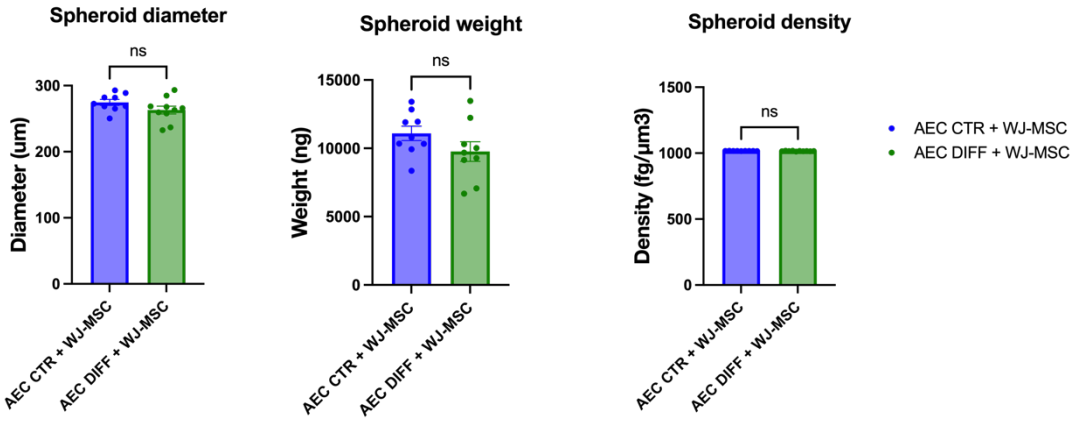

Figure 26 Comparison of the physical parameters diameter (µm), density (fg/µm3), and mass (ng) of spheroids composed of non-differentiated AEC and WJ cells (blue) and spheroids assembled with AEC cells differentiated in 2D and WJ cells (green). No statistically significant differences were observed between the two conditions (ns). Data are presented as mean ± SEM, with individual points representing biological replicates.

3.18 Pan-Cytokeratin and Vimentin Expression in Pseudo-Islet Spheroids

To further investigate the structural organization of the pseudo-islet spheroids, immunofluorescence staining was performed to evaluate the spatial distribution of the two cellular components, AEC and WJ-MSC, in the spheroids under different conditions (Figure 27). Specifically, spheroids composed of non-differentiated AEC and WJ-MSC (control condition) were compared to spheroids assembled with 2D-differentiated AEC and WJ-MSC (pseudo-islet spheroids).

Immunofluorescence staining for the epithelial marker Pan-Ck confirmed the localization of AECs primarily on the spheroid in control conditions, with minimal Pan-Ck expression

observed in the core of the structures. While in pseudo-islets spheroids Pan-Ck expression appear in the core of the spheroid. Vimentin, a mesenchymal marker, was used to visualize WJ-MSCs, which appeared interspersed throughout the spheroid in both conditions, with no evident alterations in spatial organization between the differentiated and non-differentiated AEC co-cultures.

Interestingly, in the merged images, AECs in both conditions co-expressed Pan-Ck and vimentin, suggesting that, regardless of differentiation status, a subset of AECs retained a mesenchymal phenotype, as observed in previous studies [144,145].

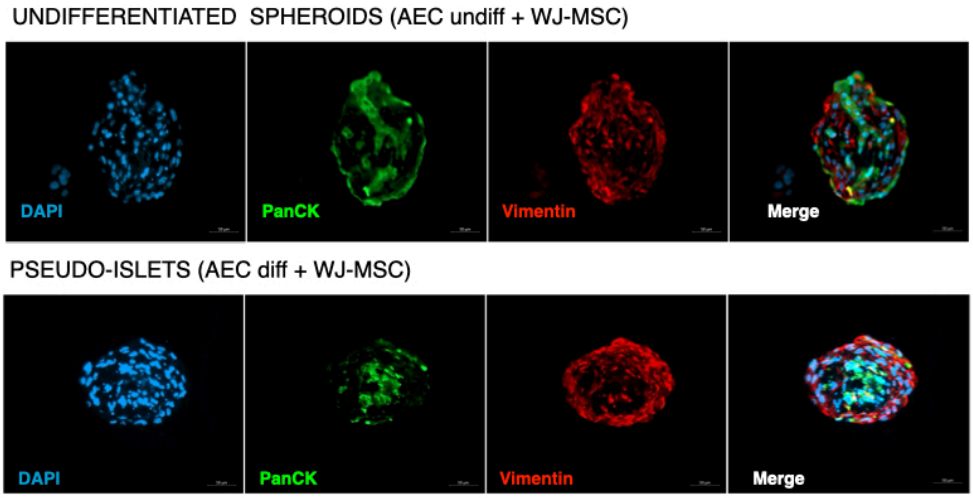

Figure 27 Representative images of co-culture spheroids and pseudo-islet spheroids stained with Pan-Ck (green), vimentin (red), and DAPI for nuclei staining (blue). Scale bar: 20 μm. Images were acquired with Zeiss Axio Observer 7 microscopy.

3.19 Pancreatic differentiation marker in Pseudo-Islet Spheroids

Immunofluorescence analysis was performed to evaluate the expression of key differentiation markers in the spheroids under different conditions. Specifically, spheroids composed of non-differentiated AEC and WJ-MSC (control condition) were compared to spheroids assembled with 2D-differentiated AEC and WJ-MSC (pseudo-islet spheroids).

The following markers were used for the immunofluorescence analysis: SOX17 (definitive endoderm marker), Neurogenin3 (endocrine progenitor marker), PDX-1 (pancreatic progenitor marker), insulin, and C-peptide (markers of functional beta-cells).

SOX17 expression, indicative of definitive endoderm differentiation, was assessed across both conditions (Figure 28). In the control spheroids (non-differentiated AEC and WJ-MSC), there was a similar expression of SOX17 compared to the 2D undifferentiated control AECs (see section 3.16). In the differentiated condition (pseudo-islet spheroids), SOX17 expression remained comparable to that observed in 2D differentiation, suggesting limited progression beyond the endodermal stage in either condition.

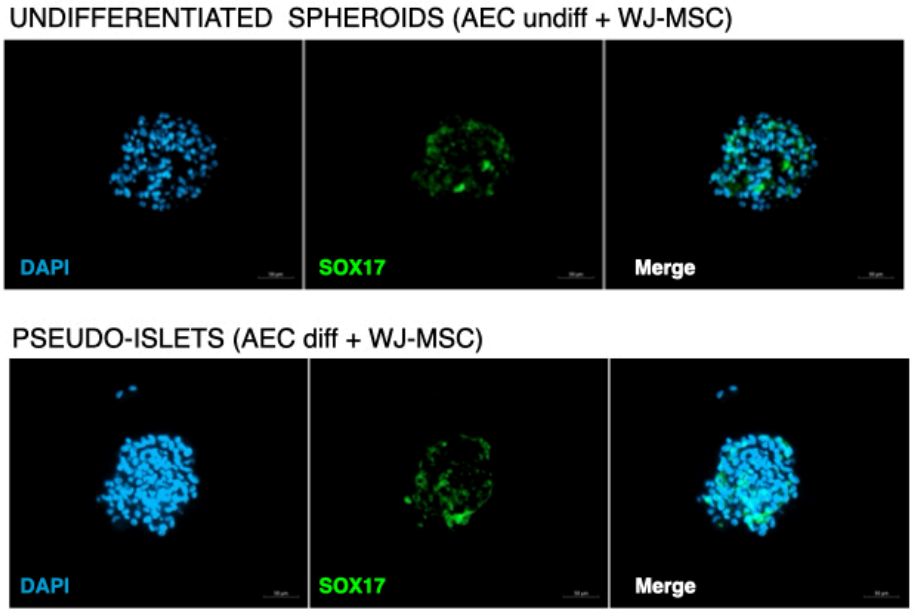

Figure 28 Immunofluorescence analysis of SOX17 expression in spheroids composed of non-differentiated AEC and WJ-MSC (control condition) and spheroids assembled with 2D-differentiated AEC and WJ-MSC (pseudo-islet spheroids). SOX17, a marker of definitive endoderm, is highly expressed in the control spheroids compared to the pseudo-islet spheroids. The expression of SOX17 remained consistent across both conditions, indicating limited progression beyond the endodermal stage.

Next, the expression of Neurog3 and PDX-1, two critical markers of pancreatic endocrine progenitors, was examined (Figure 29). Both markers were detected in spheroids from both the control and differentiated conditions. Importantly, Neurog3 co-localized with PDX-1 in these spheroids, suggesting that the 3D culture environment may promote the differentiation of AECs towards a pancreatic endocrine progenitor phenotype, even in the absence of prior 2D differentiation. This result indicates that both undifferentiated and differentiated AECs have the capacity to progress toward an endocrine progenitor state when cultured in 3D.

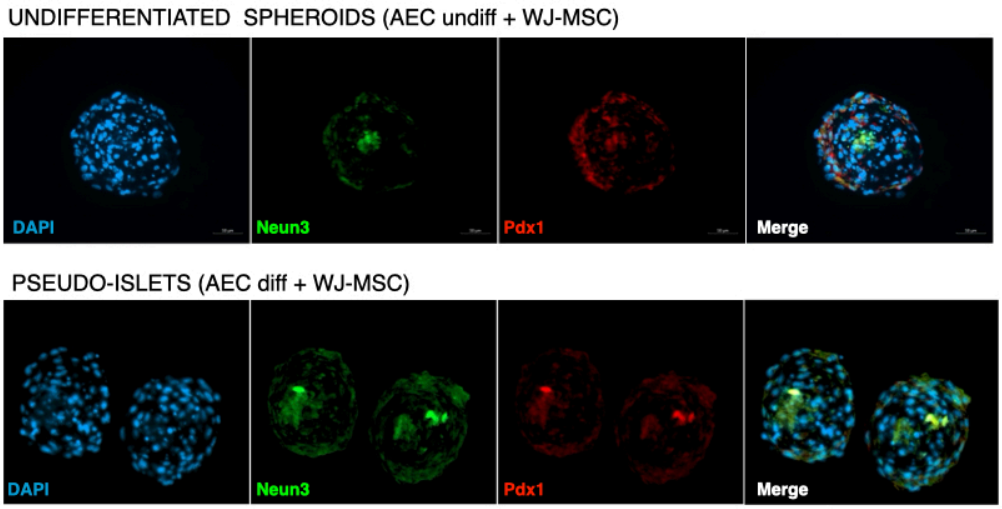

Figure 29 Immunofluorescence analysis of Neurogenin3 (Neurog3) and PDX-1 expression in control and pseudo-islet spheroids. Both markers are detectable in spheroids from both conditions. The co-localization of Neurog3 and PDX-1 suggests that the 3D culture environment promotes differentiation toward a pancreatic endocrine progenitor phenotype, even in undifferentiated AECs.

Finally, insulin (INS) and C-peptide (C-PEP) expression was evaluated to determine the extent of β-cell-like differentiation (Figure 30). In the control spheroids (non-differentiated AEC and WJ-MSC), only low levels of INS and C-PEP expression were observed, indicating minimal differentiation into functional beta-cells. In contrast, the pseudo-islet spheroids (assembled with 2D-differentiated AEC and WJ-MSC) showed a stronger co-expression of INS and C-PEP. This co-expression suggests that the 2D differentiation prior to spheroid assembly enhanced the cells' progression towards an insulin-producing, beta-like cell phenotype.

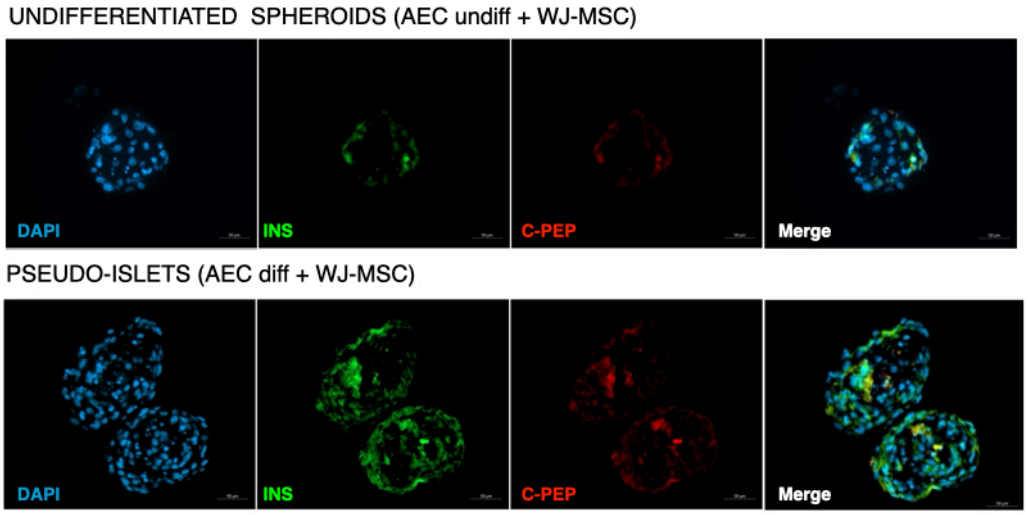

Figure 30 Immunofluorescence analysis of insulin (INS) and C-peptide (C-PEP) expression in control and pseudo-islet spheroids. The control spheroids show minimal expression of INS and C-PEP. In contrast, the pseudo-islet spheroids demonstrate stronger co-expression of INS and C-PEP, indicating enhanced differentiation towards insulin-producing β-like cells in the differentiated condition.

Discussion

Type 1 Diabetes Mellitus (T1DM) is an autoimmune disease characterized by the destruction of insulin-producing beta-cells in the pancreas. Despite advancements in insulin therapies, current treatments remain primarily palliative, requiring continuous monitoring of blood glucose and administration of exogenous insulin to prevent life-threatening complications. This approach does little to address the underlying autoimmune cause of the disease, which continues to attack remaining beta-cells, leading to progressive loss of function. Hence, novel strategies, such as cell-based therapies, are urgently needed to replace the destroyed beta-cells and potentially modulate the autoimmune response that drives T1DM.

Perinatal stem cells, specifically Amniotic Epithelial Cells (AECs) and Wharton's Jelly Mesenchymal Stromal Cells (WJ-MSCs), have emerged as promising candidates for such therapies due to their immunomodulatory and regenerative properties. AECs possess the potential to differentiate into insulin-producing cells, while WJ-MSCs offer robust structural support and immunomodulatory effects that could protect the newly differentiated beta-cells from immune-mediated destruction. The aim of this study was to investigate the potential of combining these two cell types in a 3D co-culture model to enhance the efficiency of pancreatic differentiation and explore the immunomodulatory capacity of the spheroids generated.

The first step in our study involved optimizing the co-culture ratio of AECs and WJ-MSCs to form stable spheroids. Our results showed that spheroids composed of only AECs were structurally unstable, forming irregular aggregates that lacked the compactness and uniformity required for further differentiation studies. This instability likely depends on the epithelial nature of AECs, which, unlike mesenchymal cells, are not naturally predisposed to forming spheroidal structures due to their lack of extracellular matrix (ECM)-secreting ability. In contrast, WJ-MSCs, extensively characterized for their ability to secrete ECM proteins and form compact spheroids, produced more stable spheroids when cultured alone.

Through a series of experiments testing various ratios, we determined that a 1:1 ratio of AECs to WJ-MSCs produced the most consistent and stable spheroids. This ratio provided a balance where WJ-MSCs could act as a scaffold, producing ECM components

such as collagen I and fibronectin, while AECs, which spontaneously localized to the periphery of the spheroid, were positioned to undergo differentiation into pancreatic endocrine cells. The average diameter of the co-culture spheroids was approximately 400 μm after four days, a size within the physiological range of human pancreatic islets, which are typically around 500 μm in diameter. This finding is crucial, as spheroids of this size are easy to manipulate during media changes and downstream applications, and their compact nature may provide an optimal environment for efficient cell-cell and cell-ECM interactions, essential for differentiation.

The physical characteristics of the spheroids were further analyzed using the W8 Physical Cytometer, which provides label-free measurements of spheroid weight, diameter, and mass density. The W8 analysis revealed that while WJ-MSC spheroids maintained a relatively stable diameter over time, the co-culture spheroids exhibited a reduction in diameter and an increase in mass density as the culture progressed. This compaction process can be attributed to the increased deposition of ECM components, which promote tighter cell-cell junctions and spheroid stability. The increased density observed in the co-culture spheroids may indicate enhanced structural integrity, a critical factor in ensuring the long-term viability of the spheroids and their ability to withstand the differentiation process.

The deposition of ECM proteins, particularly fibronectin and collagen I, was observed through immunofluorescence staining, confirming the mesenchymal contribution of WJ-MSCs to the structural composition of the spheroids. Fibronectin plays a key role in cell adhesion and motility, both essential processes during pancreatic islet development, and its presence suggests that the co-culture spheroids may more closely mimic the native pancreatic microenvironment than either cell type alone. The presence of laminin, localized primarily near the AECs, suggests that these epithelial cells are actively secreting this basement membrane protein, further supporting their role in mimicking the natural epithelial-stromal interactions found in pancreatic islets.

Interestingly, although the co-culture spheroids showed increased density over time, we observed a loss of cellular nuclei in the core of the spheroids at later time points, suggesting the onset of hypoxic conditions. This is a common challenge in 3D spheroid cultures, where limited nutrient and oxygen diffusion can lead to the formation of necrotic cores. While the WJ-MSCs contributed to the structural integrity of the spheroids, they

may not be as resistent as AECs in long-term cultures, which is evidenced by the fact that AECs showed better viability at 14 days, probably due to their surface localization. This highlights the importance of optimizing culture conditions, such as reducing the diameter of the spheroids and incorporating dynamic culture systems like bioreactors, to ensure adequate nutrient and oxygen supply during extended culture periods.

One of the most promising aspects of using perinatal cells in cell therapy for T1DM is their immunomodulatory potential. Both AECs and WJ-MSCs have been shown to suppress immune responses, an essential feature for preventing the autoimmune destruction of beta-cells. To assess the immunomodulatory properties of the spheroids, we co-cultured them with activated peripheral blood mononuclear cells (PBMCs) and measured the proliferation and activation status of $CD4^+$ and $CD8^+$ T cells.
Our results showed a significant reduction in the proliferation of both $CD4^+$and $CD8^+$ T cells in the presence of perinatal spheroids, with the co-culture spheroids exhibiting a more pronounced immunosuppressive effect compared to WJ-MSC monocultures. This suggests that the combination of AECs and WJ-MSCs creates a more immunosuppressive microenvironment than epithelial or stromal cell alone. The reduction in proliferation rate observed in both $CD4^+$ and $CD8^+$ cells was not associated with increased levels of apoptosis or necrosis in PBMCs. Importantly this result is a crucial, as the objective is to modulate the immune system rather than induce immunosuppression.
The analysis of the immune activation marker CD69 on $CD4^+$ and $CD8^+$ T cells, reported only a slight, not statistically significant, reduction in CD69 expression when PBMCs were co-cultured with perinatal spheroids. CD69 is classically known as an early activation marker, rapidly expressed on T cells after stimulation [146]. However, CD69 plays dual roles, not only as an activation marker but also in promoting immunosuppressive functions, particularly in regulatory cell populations [147,148]. This duality could obscure a clear reduction in its expression, as a subset of activated T cells might include regulatory phenotypes maintaining CD69 expression despite immune modulation activity. Moreover, CD69 is a transient early activation marker, downregulated over time [149,150]. The timing of the analysis could therefore influence the observed levels, and it is possible that CD69 expression may have already peaked by the time of measurement, resulting in the subtle changes we observed.

Importantly, the co-culture spheroids also induced an increase in regulatory T cells (Tregs), which are essential for maintaining immune tolerance and preventing autoimmune responses. The ability of the spheroids to enhance Treg populations is particularly relevant for T1DM, as the disease is characterized by a breakdown in immune tolerance towards beta-cells and in the context of T1DM, Tregs are often dysfunctional. Interestingly, we also observed an increase in $CD8^+$ regulatory T cells ($CD8^+$ Tregs), a population that, while not yet fully characterized, is gaining recognition for its potential immunoregulatory roles. $CD8^+$ Tregs are thought to contribute to immune tolerance by suppressing effector T cells through various mechanisms, including the secretion of inhibitory cytokines like IL-10 and TGF-β, and the expression of molecules such as CTLA-4 and FasL [151–153]. In the context of T1DM, their involvement could be crucial, as evidence suggests that $CD8^+$ Tregs may help mitigate autoimmune responses by directly suppressing autoreactive $CD4^+$ and $CD8^+$ T cells [154].

Furthermore, the co-culture spheroids reduced the population of $CD8^+$ T cells producing granzyme B, a key cytotoxic molecule involved in the destruction of beta-cells [155,156]. This finding suggests that the spheroids not only suppress T cell proliferation but also modulate the functional activity of cytotoxic T cells, potentially reducing their capacity to mediate beta-cell destruction.

In parallel to their immunomodulatory properties, we focused on the differentiation potential of AECs and WJ-MSCs to form pseudo-islet spheroids capable of producing insulin. Our primary goal was to induce the differentiation of AECs toward a beta-pancreatic lineage while maintaining the structural and immunomodulatory properties of WJ cells. However, the differentiation process within 3D spheroids proved challenging. Cells located in the core of the spheroids exhibited significant cell death, likely due to hypoxia or insufficient access to essential nutrients and growth factors required for proper differentiation. This internal cell death might have released factors that negatively impacted the surrounding cells, thus preventing the completion of the differentiation process.

Given these challenges, we decided to adopt a different strategy, shifting from attempting direct differentiation of the entire 3D spheroid to a more targeted approach: we first differentiated AECs in a 2D system and subsequently combined these differentiated cells with undifferentiated WJ-MSCs to form spheroids. This adjustment proved crucial to the success of our experiment. In the 2D system, AECs responded well to the differentiation

protocol, expressing insulin, a clear marker of their conversion towards a beta-cell-like phenotype. Once insulin expression was confirmed in 2D, we combined these cells with undifferentiated WJ-MSCs to create new spheroids, which we termed "pseudo-islets," given their resemblance to pancreatic islets.

The combination of differentiated AECs and undifferentiated WJ cells enabled the formation of spheroids that retained key characteristics: the AECs continued to express insulin, while the WJ-MSCs provided structural support and maintained immunomodulatory properties, potentially protecting the differentiated AECs from immune responses. The presence of WJ-MSCs within the spheroid may act as a protective "shield" for the insulin-producing beta-like cells, potentially reducing the risk of immune rejection or destruction.

During the characterization of these newly formed spheroids, we initially evaluated physical parameters such as weight, diameter, and density. The results showed no significant differences between spheroids composed of undifferentiated AECs and WJ cells and those formed from 2D-differentiated AECs and WJ cells. This suggests that the physical organization of the spheroids is not significantly influenced by the differentiation state of the AECs, at least in terms of dimensional parameters. However, these physical characteristics may not fully capture the functional properties of the pseudo-islets. Moving forward, it will be crucial to assess their long-term viability and their ability to respond to external stimuli, such as glucose levels, to determine their functional relevance in the context of diabetes treatment.

Another notable finding during the spheroid characterization was the persistence of co-expression of epithelial marker Pan-Ck and mesenchymal marker vimentin in AECs, even after differentiation. This co-expression suggests the retention of a mixed epithelial-mesenchymal phenotype. This persistence could indicate that the AECs had not fully transitioned into a mature beta-cell state, thereby hindering their complete differentiation into functional beta cells. However, the presence of mesenchymal phenotype may confer certain advantages to the cells, particularly regarding their immunomodulatory capacity [95]. The potential benefits of this mixed phenotype, such as maintaining greater functional flexibility and immune protection, will be explored in future analyses.

Furthermore, the expression of markers such as Neurogenin3 (NGN3) and PDX-1, both indicators of pancreatic endocrine progenitors, was observed in both differentiated and non-differentiated spheroids. This suggests that the 3D environment itself may promote

the progression of AECs toward an endocrine progenitor phenotype, even without prior 2D differentiation. However, the absence of strong insulin expression in the non-differentiated spheroids indicates that, while the 3D environment facilitates the initiation of differentiation, it is insufficient to fully induce maturation into functional beta cells.

Our final analysis focused on the expression of insulin and C-peptide (C-PEP), both markers of functional beta cells. In spheroids composed of undifferentiated AECs and WJ-MSCs, insulin and C-PEP expression was minimal, confirming that without prior differentiation, AECs do not achieve a beta-cell-like phenotype. In contrast, spheroids formed with AECs pre-differentiated in 2D and combined with WJ-MSCs exhibited robust co-expression of insulin and C-PEP, indicating that 2D differentiation is crucial for the successful acquisition of insulin-producing capabilities. Despite the encouraging results, this study lacks the direct quantification of insulin levels and functional validation, such as glucose-stimulated insulin secretion, to confirm the functional maturity of the differentiated cells. Explicitly addressing these aspects in future studies will be essential to strengthen the translational potential of these findings. Additionally, it will be crucial to evaluate whether the insulin produced within the spheroids is secreted in a glucose-dependent manner, as this is a key characteristic of functional beta cells. To enhance pancreatic differentiation efficiency, future studies could incorporate additional growth factors or small molecules into the differentiation protocol. Moreover, exploring dynamic culture systems could improve nutrient and oxygen delivery to the pseudo-islets during differentiation, potentially overcoming the limitations observed in static culture systems.

Finally, a more detailed analysis of the immune interactions within the spheroids will be necessary to fully understand their immunomodulatory capacity and potential for long-term functionality. However, it is important to acknowledge that the complexity of immune responses, particularly in autoimmune diseases like T1DM, cannot be fully captured in in vitro models. The absence of long-term or *in vivo* data is a significant limitation of this study, underlining the need for future research to address these gaps. These data will be critical to evaluate the safety, efficacy, and immunological interactions of the spheroids in clinically relevant settings, enabling their translation into potential therapeutic applications.

Conclusions

This study highlights the potential of combining Amniotic Epithelial Cells (AECs) and Wharton's Jelly Mesenchymal Stromal Cells (WJ-MSCs) to create insulin-producing pseudo-islet spheroids for Type 1 Diabetes Mellitus (T1DM). Through a combination of 2D differentiation of AECs followed by their assembly with WJ-MSCs into 3D spheroids, we successfully induced insulin and C-peptide expression. The structural support provided by WJ-MSCs, along with their immunomodulatory properties, enhanced the stability of the spheroids and contributed to the suppression of T cell proliferation, while promoting the expansion of regulatory T cells.

However, challenges such as incomplete differentiation and lower insulin levels compared to natural islets indicate that further optimization of the differentiation protocol is needed. Future work should focus on refining the differentiation protocol, evaluating glucose-stimulated insulin secretion and exploring dynamic culture systems to improve nutrient and oxygen delivery. Despite these challenges, the combination of AECs and WJ-MSCs already holds significant promise for cell-based therapies aimed at treating T1DM, by replacing destroyed beta-cells and modulating the immune response.

Bibliography

1. Martinez-Sanchez, A. *et al.* Pancreatic Beta Cell Identity in Humans and the Role of Type 2 Diabetes. *Frontiers in Cell and Developmental Biology | www.frontiersin.org* **5**, 55 (2017).
2. Diagnosis and Classification of Diabetes Mellitus. *Diabetes Care* **37**, S81–S90 (2014).
3. Atkinson, M. A., Eisenbarth, G. S. & Michels, A. W. Type 1 diabetes. *The Lancet* **383**, 69–82 (2014).
4. Lende, M. & Rijhsinghani, A. Gestational Diabetes: Overview with Emphasis on Medical Management. doi:10.3390/ijerph17249573.
5. Daneman, D. Type 1 diabetes. *The Lancet* **367**, 847–858 (2006).
6. Vanderniet, J. A., Jenkins, A. J., Kim, · & Donaghue, C. Epidemiology of Type 1 Diabetes. **1**, 3 (2022).
7. Eisenbarth, G. S. Banting Lecture 2009: An Unfinished Journey: Molecular Pathogenesis to Prevention of Type 1A Diabetes. (2010) doi:10.2337/db09-1855.
8. Noble, J. A. & Erlich, H. A. Genetics of Type 1 Diabetes. doi:10.1101/cshperspect.a007732.
9. Xie, Z., Chang, C. & Zhou, Z. Molecular Mechanisms in Autoimmune Type 1 Diabetes: a Critical Review. doi:10.1007/s12016-014-8422-2.
10. Wållberg, M. & Cooke, A. Immune mechanisms in type 1 diabetes. *Trends Immunol* **34**, 583–591 (2013).
11. Powers, A. C. Type 1 diabetes mellitus: Much progress, many opportunities. *Journal of Clinical Investigation* **131**, (2021).
12. Rewers, M. & Ludvigsson, J. Environmental risk factors for type 1 diabetes. *The Lancet* **387**, 2340–2348 (2016).
13. Bluestone, J. A., Herold, K. & Eisenbarth, G. Genetics, pathogenesis and clinical interventions in type 1 diabetes. *Nature* **464**, 1293 (2010).
14. Skowera, A. *et al.* CTLs are targeted to kill β cells in patients with type 1 diabetes through recognition of a glucose-regulated preproinsulin epitope. *J Clin Invest* **118**, 3390–3402 (2008).
15. Knight, R. R. *et al.* Human β-Cell Killing by Autoreactive Preproinsulin-Specific CD8 T Cells Is Predominantly Granule-Mediated With the Potency Dependent Upon T-Cell Receptor Avidity. *Diabetes* **62**, 205–213 (2013).
16. Hawiger, D., Moser, M., Kretschmer, K., Price, J. D. & Tarbell, K. V. The role of dendritic cell subsets and innate immunity in the pathogenesis of type 1 diabetes and other autoimmune diseases. (2015) doi:10.3389/fimmu.2015.00288.
17. Poligone, B., Weaver, D. J., Sen, P., Baldwin, A. S. & Tisch, R. Elevated NF-κB Activation in Nonobese Diabetic Mouse Dendritic Cells Results in Enhanced APC Function. *The Journal of Immunology* **168**, 188–196 (2002).

18. Ghaemi Oskouie, F. *et al.* High Levels of Adenosine Deaminase on Dendritic Cells Promote Autoreactive T Cell Activation and Diabetes in Nonobese Diabetic Mice. *The Journal of Immunology* **186**, 6798–6806 (2011).
19. Pugliese, A. Autoreactive T cells in type 1 diabetes. *J Clin Invest* **127**, 2881–2891 (2017).
20. Debray-Sachs, M. *et al.* Prevention of diabetes in NOD mice treated with antibody to murine IFNγ. *J Autoimmun* **4**, 237–248 (1991).
21. Savinov, A. Y., Wong, F. S. & Chervonsky, A. V. IFN-γ Affects Homing of Diabetogenic T Cells. *The Journal of Immunology* **167**, 6637–6643 (2001).
22. Walker, L. S. K. & von Herrath, M. CD4 T cell differentiation in type 1 diabetes. *Clin Exp Immunol* **183**, 16–29 (2015).
23. Serreze, D., Fleming, S., … H. C.-T. J. of & 1998, undefined. B lymphocytes are critical antigen-presenting cells for the initiation of T cell-mediated autoimmune diabetes in nonobese diabetic mice. *journals.aai.orgDV Serreze, SA Fleming, HD Chapman, SD Richard, EH Leiter, RM TischThe Journal of Immunology, 1998•journals.aai.org.*
24. Noorchashm, H., Lieu, Y., … N. N.-T. J. of & 1999, undefined. I-Ag7-mediated antigen presentation by B lymphocytes is critical in overcoming a checkpoint in T cell tolerance to islet β cells of nonobese diabetic mice. *journals.aai.orgH Noorchashm, YK Lieu, N Noorchashm, SY Rostami, SAS Greeley, A SchlachtermanThe Journal of Immunology, 1999•journals.aai.org.*
25. Silveira, P. A. & Grey, S. T. B cells in the spotlight: innocent bystanders or major players in the pathogenesis of type 1 diabetes. *Trends in Endocrinology & Metabolism* **17**, 128–135 (2006).
26. Hu, C.-Y. *et al.* Treatment with CD20-specific antibody prevents and reverses autoimmune diabetes in mice. *Am Soc Clin InvestigC Hu, D Rodriguez-Pinto, W Du, A Ahuja, O Henegariu, FS Wong, MJ Shlomchik, L WenThe Journal of clinical investigation, 2007•Am Soc Clin Investig* **117**, 3857–3867 (2007).
27. Xiu, Y. *et al.* B Lymphocyte Depletion by CD20 Monoclonal Antibody Prevents Diabetes in Nonobese Diabetic Mice despite Isotype-Specific Differences in FcγR Effector Functions. *The Journal of Immunology* **180**, 2863–2875 (2008).
28. Sakaguchi, S., Yamaguchi, T., Nomura, T. & Ono, M. Regulatory T Cells and Immune Tolerance. *Cell* **133**, 775–787 (2008).
29. Sakaguchi, S., Sakaguchi, N., Asano, M., Itoh, M. & Toda, M. Immunologic self-tolerance maintained by activated T cells expressing IL-2 receptor alpha-chains (CD25). Breakdown of a single mechanism of self-tolerance causes various autoimmune diseases. *The Journal of Immunology* **155**, 1151–1164 (1995).
30. Maynard, C., Harrington, L., … K. J.-N. & 2007, undefined. Regulatory T cells expressing interleukin 10 develop from Foxp3+ and Foxp3− precursor cells in the absence of interleukin 10. *nature.comCL Maynard, LE Harrington, KM Janowski, JR Oliver, CL Zindl, AY Rudensky, CT WeaverNature immunology, 2007•nature.com.*
31. Misra, N., Bayry, J., … S. L.-D.-T. J. of & 2004, undefined. Cutting edge: human CD4+ CD25+ T cells restrain the maturation and antigen-presenting function of

dendritic cells. *journals.aai.orgN Misra, J Bayry, S Lacroix-Desmazes, MD Kazatchkine, SV KaveriThe Journal of Immunology, 2004•journals.aai.org.*

32. Read, S., Greenwald, R., Izcue, A., … N. R.-T. J. of & 2006, undefined. Blockade of CTLA-4 on CD4+ CD25+ regulatory T cells abrogates their function in vivo. *journals.aai.orgS Read, R Greenwald, A Izcue, N Robinson, D Mandelbrot, L Francisco, AH SharpeThe Journal of Immunology, 2006•journals.aai.org.*
33. Pandiyan, P., Zheng, L., Ishihara, S., … J. R.-N. & 2007, undefined. CD4+CD25+Foxp3+ regulatory T cells induce cytokine deprivation–mediated apoptosis of effector CD4+ T cells. *nature.comP Pandiyan, L Zheng, S Ishihara, J Reed, MJ LenardoNature immunology, 2007•nature.com.*
34. Shevach, E. M. Mechanisms of Foxp3+ T Regulatory Cell-Mediated Suppression. *Immunity* **30**, 636–645 (2009).
35. Ben-Skowronek, I. *et al.* Potential Therapeutic Application of Regulatory T Cells in Diabetes Mellitus Type 1. *International Journal of Molecular Sciences 2022, Vol. 23, Page 390* **23**, 390 (2021).
36. Brusko, T. M., Wasserfall, C. H., Clare-Salzler, M. J., Schatz, D. A. & Atkinson, M. A. Functional Defects and the Influence of Age on the Frequency of CD4+CD25+ T-Cells in Type 1 Diabetes. *Diabetes* **54**, 1407–1414 (2005).
37. Hull, C. M., Peakman, M. & Tree, T. I. M. Regulatory T cell dysfunction in type 1 diabetes: what's broken and how can we fix it? *Diabetologia* **60**, 1839–1850 (2017).
38. Rosenzwajg, M. *et al.* Low-dose interleukin-2 fosters a dose-dependent regulatory T cell tuned milieu in T1D patients. *J Autoimmun* **58**, 48–58 (2015).
39. Marek-Trzonkowska, N. *et al.* Therapy of type 1 diabetes with CD4(+)CD25(high)CD127-regulatory T cells prolongs survival of pancreatic islets - results of one year follow-up. *Clin Immunol* **153**, 23–30 (2014).
40. Paris, F. *et al.* Perinatal Stem Cell Therapy to Treat Type 1 Diabetes Mellitus: A Never-Say-Die Story of Differentiation and Immunomodulation. *Int J Mol Sci* **23**, 14597 (2022).
41. Grattoni, A. *et al.* Harnessing cellular therapeutics for type 1 diabetes mellitus: progress, challenges, and the road ahead. *Nature Reviews Endocrinology 2024* 1–17 (2024) doi:10.1038/s41574-024-01029-0.
42. Boscari, F. & Avogaro, A. Current treatment options and challenges in patients with Type 1 diabetes: Pharmacological, technical advances and future perspectives. *Reviews in Endocrine and Metabolic Disorders 2021 22:2* **22**, 217–240 (2021).
43. Grunberger, G. The need for better insulin therapy. *Diabetes Obes Metab* **15**, 1–5 (2013).
44. Shapiro, A. M. J., Pokrywczynska, M. & Ricordi, C. Clinical pancreatic islet transplantation. *Nat Rev Endocrinol* **13**, 268–277 (2017).
45. James Shapiro, A. M. Islet Transplantation in Type 1 Diabetes: Ongoing Challenges, Refined Procedures, and Long-Term Outcome. *Rev Diabet Stud* **9**, 385 (2012).

46. Perri, V. *et al.* Expression of PD-1 Molecule on Regulatory T Lymphocytes in Patients with Insulin-Dependent Diabetes Mellitus. *Int J Mol Sci* **16**, 22584 (2015).
47. Evans-Molina, C. & Oram, R. A. Teplizumab approval for type 1 diabetes in the USA. *Lancet Diabetes Endocrinol* **11**, 76–77 (2023).
48. Teplizumab and β-Cell Function in Newly Diagnosed Type 1 Diabetes | Enhanced Reader.
49. Matthews, J. B., Staeva, T. P., Bernstein, P. L., Peakman, M. & Von Herrath, M. Developing combination immunotherapies for type 1 diabetes: recommendations from the ITN-JDRF Type 1 Diabetes Combination Therapy Assessment Group. *Clin Exp Immunol* **160**, 176–184 (2010).
50. Chellappan, D. K. *et al.* Gene therapy and type 1 diabetes mellitus. *Biomedicine & Pharmacotherapy* **108**, 1188–1200 (2018).
51. Lee, H. C., Kim, S. J., Kim, K. S., Shin, H. C. & Yoon, J. W. Remission in models of type 1 diabetes by gene therapy using a single-chain insulin analogue. *Nature 2000 408:6811* **408**, 483–488 (2000).
52. Srinivasan, M., Thangaraj, S. R. & Arzoun, H. Gene Therapy - Can it Cure Type 1 Diabetes? *Cureus* **13**, (2021).
53. Wang, S. *et al.* Transplantation of chemically induced pluripotent stem-cell-derived islets under abdominal anterior rectus sheath in a type 1 diabetes patient. *Cell* **0**, (2024).
54. Mallapaty, S. Stem cells reverse woman's diabetes - a world first. *Nature* (2024) doi:10.1038/D41586-024-03129-3.
55. Ghoneim, M. A., Gabr, M. M., El-Halawani, S. M. & Refaie, A. F. Current status of stem cell therapy for type 1 diabetes: a critique and a prospective consideration. *Stem Cell Research & Therapy 2024 15:1* **15**, 1–13 (2024).
56. Torre, P. de la & Flores, A. I. Current Status and Future Prospects of Perinatal Stem Cells. *Genes (Basel)* **12**, 6 (2020).
57. Silini, A. R., Masserdotti, A., Papait, A. & Parolini, O. Shaping the Future of Perinatal Cells: Lessons From the Past and Interpretations of the Present. *Front Bioeng Biotechnol* **7**, (2019).
58. Maltepe, E. & Fisher, S. J. Placenta: the forgotten organ. *Annu Rev Cell Dev Biol* **31**, 523–552 (2015).
59. Silini, A. R. *et al.* Perinatal Derivatives: Where Do We Stand? A Roadmap of the Human Placenta and Consensus for Tissue and Cell Nomenclature. *Front Bioeng Biotechnol* **8**, (2020).
60. Knöfler, M. *et al.* Human placenta and trophoblast development: key molecular mechanisms and model systems. *Cell Mol Life Sci* **76**, 3479–3496 (2019).
61. Gian Paolo Bagnara. *Stem Cell* . (Società Editrice Escuplapio, 2020).
62. Burton, G. J. & Fowden, A. L. The placenta: a multifaceted, transient organ. *Philos Trans R Soc Lond B Biol Sci* **370**, (2015).
63. Gude, N. M., Roberts, C. T., Kalionis, B. & King, R. G. Growth and function of the normal human placenta. *Thromb Res* **114**, 397–407 (2004).

64. Silini, A. R. *et al.* Perinatal Derivatives: Where Do We Stand? A Roadmap of the Human Placenta and Consensus for Tissue and Cell Nomenclature. *Front Bioeng Biotechnol* **8**, (2020).
65. Dockery, P., Bermingham, J. & Jenkins, D. Structure-function relations in the human placenta. *Biochem Soc Trans* **28**, 202–208 (2000).
66. Cindrova-Davies, T. & Sferruzzi-Perri, A. N. Human placental development and function. *Semin Cell Dev Biol* **131**, 66–77 (2022).
67. Ferreira, L. M. R., Meissner, T. B., Tilburgs, T. & Strominger, J. L. HLA-G: At the Interface of Maternal-Fetal Tolerance. *Trends Immunol* **38**, 272–286 (2017).
68. Agrawal, S. & Pandey, M. K. The Potential Role of HLA-G Polymorphism in Maternal Tolerance to the Developing Fetus. *J Hematother Stem Cell Res* **12**, 749–756 (2003).
69. Costa, M. A. The endocrine function of human placenta: an overview. *Reprod Biomed Online* **32**, 14–43 (2016).
70. Megli, C. J. & Coyne, C. B. Infections at the maternal–fetal interface: an overview of pathogenesis and defence. *Nature Reviews Microbiology 2021 20:2* **20**, 67–82 (2021).
71. Deus, I. A., Mano, J. F. & Custódio, C. A. Perinatal tissues and cells in tissue engineering and regenerative medicine. *Acta Biomater* **110**, 1–14 (2020).
72. Bhonde, R. R., Sheshadri, P., Sharma, S. & Kumar, A. Making surrogate β-cells from mesenchymal stromal cells: Perspectives and future endeavors. *Int J Biochem Cell Biol* **46**, 90–102 (2014).
73. Murray, H. E. *et al.* The potential role of multifunctional human amniotic epithelial cells in pancreatic islet transplantation. *J Tissue Eng Regen Med* **15**, 599–611 (2021).
74. Parolini, O. *et al.* Concise review: isolation and characterization of cells from human term placenta: outcome of the first international Workshop on Placenta Derived Stem Cells. *Stem Cells* **26**, 300–311 (2008).
75. Paris, F. *et al.* Perinatal Stem Cell Therapy to Treat Type 1 Diabetes Mellitus: A Never-Say-Die Story of Differentiation and Immunomodulation. *Int J Mol Sci* **23**, 14597 (2022).
76. Bourne, G. L. The microscopic anatomy of the human amnion and chorion. *Am J Obstet Gynecol* **79**, 1070–1073 (1960).
77. Cross, J. C. Formation of the Placenta and Extraembryonic Membranes. *Ann N Y Acad Sci* **857**, 23–32 (1998).
78. Alviano, F. *et al.* Term amniotic membrane is a high throughput source for multipotent mesenchymal stem cells with the ability to differentiate into endothelial cells in vitro. *BMC Dev Biol* **7**, 1–14 (2007).
79. Trosan, P. *et al.* The enzymatic de-epithelialization technique determines denuded amniotic membrane integrity and viability of harvested epithelial cells. *PLoS One* **13**, e0194820 (2018).
80. Motedayyen, H. *et al.* Method and key points for isolation of human amniotic epithelial cells with high yield, viability and purity. *BMC Res Notes* **10**, 1–8 (2017).

81. Centurione, L. *et al.* Mapping of the Human Placenta: Experimental Evidence of Amniotic Epithelial Cell Heterogeneity. *Cell Transplant* **27**, 12–22 (2018).
82. Fatimah, S. S., Tan, G. C., Chua, K. H., Tan, A. E. & Hayati, A. R. Effects of epidermal growth factor on the proliferation and cell cycle regulation of cultured human amnion epithelial cells. *J Biosci Bioeng* **114**, 220–227 (2012).
83. Pratama, G. *et al.* Changes in Culture Expanded Human Amniotic Epithelial Cells: Implications for Potential Therapeutic Applications. *PLoS One* **6**, e26136 (2011).
84. Miki, T., Lehmann, T., Cai, H., Stolz, D. B. & Strom, S. C. Stem Cell Characteristics of Amniotic Epithelial Cells. *Stem Cells* **23**, 1549–1559 (2005).
85. Koike, N. *et al.* Distribution of amniotic stem cells in human term amnion membrane. *Microscopy* **71**, 66–76 (2022).
86. Tabatabaei, M. *et al.* Isolation and Partial Characterization of Human Amniotic Epithelial Cells: The Effect of Trypsin. *Avicenna J Med Biotechnol* **6**, 10 (2014).
87. Zhang, Q. & Lai, D. Application of human amniotic epithelial cells in regenerative medicine: a systematic review. *Stem Cell Research & Therapy 2020 11:1* **11**, 1–16 (2020).
88. Marongiu, F. *et al.* Hepatic differentiation of amniotic epithelial cells. *Hepatology* **53**, 1719–1729 (2011).
89. Niknejad, H., Peirovi, H., Ahmadiani, A., Ghanavi, J. & Jorjani, M. Differentiation factors that influence neuronal markers expression in vitro from human amniotic epithelial cells. *Eur Cell Mater* **19**, 22–29 (2010).
90. Yao, M. *et al.* Differentiation of human amniotic epithelial cells into corneal epithelial-like cells in vitro. *Int J Ophthalmol* **6**, 564–572 (2013).
91. Hou, Y., Huang, Q., Liu, T. & Guo, L. Human amnion epithelial cells can be induced to differentiate into functional insulin-producing cells. *Acta Biochim Biophys Sin (Shanghai)* **40**, 830–839 (2008).
92. Wei, J. P. *et al.* Human amnion-isolated cells normalize blood glucose in streptozotocin-induced diabetic mice. *Cell Transplant* **12**, 545–552 (2003).
93. Bhandari, D. R. *et al.* The simplest method for in vitro β-cell production from human adult stem cells. *Differentiation* **82**, 144–152 (2011).
94. Liu, X. *et al.* Enhanced differentiation of human pluripotent stem cells into pancreatic endocrine cells in 3D culture by inhibition of focal adhesion kinase. *Stem Cell Res Ther* **11**, (2020).
95. Okere, B. *et al.* In vitro differentiation of human amniotic epithelial cells into insulinproducing 3D spheroids. *Int J Immunopathol Pharmacol* **28**, 390–402 (2015).
96. Parolini, O. & Caruso, M. Review: Preclinical studies on placenta-derived cells and amniotic membrane: An update. *Placenta* **32**, (2011).
97. Rizzo, R. *et al.* A functional role for soluble HLA-G antigens in immune modulation mediated by mesenchymal stromal cells. *Cytotherapy* **10**, 364–375 (2008).
98. Braud, V. M., Allan, D. S. & McMichael, A. J. Functions of nonclassical MHC and non-MHC-encoded class I molecules. *Curr Opin Immunol* **11**, 100–108 (1999).

99. Morandi, F. *et al.* Human amnion epithelial cells impair T cell proliferation: The role of HLA-G and HLA-E molecules. *Cells* **9**, 1–15 (2020).
100. Tan, J. L. *et al.* Amnion cell-mediated immune modulation following bleomycin challenge: Controlling the regulatory T cell response. *Stem Cell Res Ther* **6**, (2015).
101. Li, H. *et al.* Immunosuppressive factors secreted by human amniotic epithelial cells. *Invest Ophthalmol Vis Sci* **46**, 900–907 (2005).
102. Zhu, D. *et al.* Human amnion cells reverse acute and chronic pulmonary damage in experimental neonatal lung injury. *Stem Cell Res Ther* **8**, (2017).
103. Cargnoni, A. *et al.* Effect of human amniotic epithelial cells on pro-fibrogenic resident hepatic cells in a rat model of liver fibrosis. *Wiley Online LibraryA Cargnoni, S Farigu, E Cotti Piccinelli, P Bonassi Signoroni, P Romele, G Vanosi, I ToschiJournal of Cellular and Molecular Medicine, 2018•Wiley Online Library* **22**, 1202–1213 (2018).
104. Tan, J. L. *et al.* Amnion Epithelial Cell-Derived Exosomes Restrict Lung Injury and Enhance Endogenous Lung Repair. *Stem Cells Transl Med* **7**, 180–196 (2018).
105. Lebreton, F. *et al.* Insulin-producing organoids engineered from islet and amniotic epithelial cells to treat diabetes. *Nat Commun* **10**, (2019).
106. Song, Y. S. *et al.* Transplanted human amniotic epithelial cells secrete paracrine proangiogenic cytokines in rat model of myocardial infarction. *Cell Transplant* **24**, 2055–2064 (2015).
107. Podestà, M. A., Remuzzi, G. & Casiraghi, F. Mesenchymal stromal cells for transplant tolerance. *Front Immunol* **10**, (2019).
108. Jun, Y. *et al.* Microchip-based engineering of super-pancreatic islets supported by adipose-derived stem cells. *Biomaterials* **35**, 4815–4826 (2014).
109. Qureshi, K. M. *et al.* Human amniotic epithelial cells induce localized cell-mediated immune privilege in vitro: Implications for pancreatic islet transplantation. *Cell Transplant* **20**, 523–534 (2011).
110. Zafar, A. *et al.* Rotational culture and integration with amniotic stem cells reduce porcine islet immunoreactivity in vitro and slow xeno-rejection in a murine model of islet. *Wiley Online LibraryA Zafar, J Lee, S Yesmin, MB Paget, CJ Bailey, HE Murray, R DowningXenotransplantation, 2019•Wiley Online Library* **26**, (2019).
111. Cui, W., Khan, K. M., Ma, X., Chen, G. & Desai, C. S. Human Amniotic Epithelial Cells and Human Amniotic Membrane as a Vehicle for Islet Cell Transplantation. *Transplant Proc* **52**, 982–986 (2020).
112. McELREAVEY, K., IRVINE, A., ENNIS, K. & McLean, W. Isolation, culture and characterisation of fibroblast-like cells derived from the Wharton's jelly portion of human umbilical cord. *Biochem Soc Trans* **19**, (1991).
113. Musiał-Wysocka, A., Kot, M., Sułkowski, M., Badyra, B. & Majka, M. Molecular and Functional Verification of Wharton's Jelly Mesenchymal Stem Cells (WJ-MSCs) Pluripotency. *International Journal of Molecular Sciences 2019, Vol. 20, Page 1807* **20**, 1807 (2019).
114. Ali, H., Al-Yatama, M. K., Abu-Farha, M., Behbehani, K. & Madhoun, A. Al. Multi-Lineage Differentiation of Human Umbilical Cord Wharton's Jelly

Mesenchymal Stromal Cells Mediates Changes in the Expression Profile of Stemness Markers. *PLoS One* **10**, e0122465 (2015).
115. Nekoei, S. M., Azarpira, N., Sadeghi, L. & Kamalifar, S. In vitro differentiation of human umbilical cord Wharton's jelly mesenchymal stromal cells to insulin producing clusters. *World Journal of Clinical Cases : WJCC* **3**, 640 (2015).
116. Ranjbaran, H. *et al.* Differentiation of Wharton's Jelly Derived Mesenchymal Stem Cells into Insulin Producing Cells. *Int J Hematol Oncol Stem Cell Res* **12**, 220 (2018).
117. Bhonde, R. R., Sheshadri, P., Sharma, S. & Kumar, A. Making surrogate β-cells from mesenchymal stromal cells: Perspectives and future endeavors. *International Journal of Biochemistry and Cell Biology* Preprint at https://doi.org/10.1016/j.biocel.2013.11.006 (2014).
118. Tsai, P. J. *et al.* Undifferentiated Wharton's jelly mesenchymal stem cell transplantation induces insulin-producing cell differentiation and suppression of T-cell-mediated autoimmunity in nonobese diabetic mice. *Cell Transplant* **24**, 1555–1570 (2015).
119. Shi, Y. *et al.* Immunoregulatory mechanisms of mesenchymal stem and stromal cells in inflammatory diseases. *Nat Rev Nephrol* **14**, 493–507 (2018).
120. Prasanna, S. J., Gopalakrishnan, D., Shankar, S. R. & Vasandan, A. B. Pro-Inflammatory Cytokines, IFNγ and TNFα, Influence Immune Properties of Human Bone Marrow and Wharton Jelly Mesenchymal Stem Cells Differentially. *PLoS One* **5**, e9016 (2010).
121. Lanzoni, G. *et al.* Umbilical cord mesenchymal stem cells for COVID-19 acute respiratory distress syndrome: A double-blind, phase 1/2a, randomized controlled trial. *Stem Cells Transl Med* **10**, 660–673 (2021).
122. Waterman, R. S., Tomchuck, S. L., Henkle, S. L. & Betancourt, A. M. A New Mesenchymal Stem Cell (MSC) Paradigm: Polarization into a Pro-Inflammatory MSC1 or an Immunosuppressive MSC2 Phenotype. *PLoS One* **5**, e10088 (2010).
123. Lech, W., Zychowicz, M., Figiel-Dabrowska, A., Domanska-Janik, K. & Buzanska, L. Immunomodulatory capacity of Wharton's Jelly mesenchymal stem cells after stimulation in vitro: cytokines and growth factors transcriptional response analysis. *Acta Neurobiol Exp (Wars)* **77**, (2017).
124. Paris, F. *et al.* Characterization of Perinatal Stem Cell Spheroids for the Development of Cell Therapy Strategy. *Bioengineering* **10**, 189 (2023).
125. Thakur, G. *et al.* Scaffold-free 3D culturing enhance pluripotency, immunomodulatory factors, and differentiation potential of Wharton's jelly-mesenchymal stem cells. *Eur J Cell Biol* **101**, 151245 (2022).
126. Ghezelayagh, Z. *et al.* Improved Differentiation of hESC-Derived Pancreatic Progenitors by Using Human Fetal Pancreatic Mesenchymal Cells in a Micro-scalable Three-Dimensional Co-culture System. *Stem Cell Rev Rep* **18**, 360–377 (2022).
127. Jensen, C. & Teng, Y. Is It Time to Start Transitioning From 2D to 3D Cell Culture? *Front Mol Biosci* **7**, 513823 (2020).

128. Joseph, J. S. *et al.* Two-Dimensional (2D) and Three-Dimensional (3D) Cell Culturing in Drug Discovery. *Cell Culture* (2018) doi:10.5772/INTECHOPEN.81552.
129. Valdoz, J. C. *et al.* The ECM: To Scaffold, or Not to Scaffold, That Is the Question. *Int J Mol Sci* **22**, 12690 (2021).
130. Smith, L. R., Cho, S. & Discher, D. E. Stem Cell Differentiation is Regulated by Extracellular Matrix Mechanics. *Physiology* **33**, 16–25 (2018).
131. Okere, B. *et al. In vitro* differentiation of human amniotic epithelial cells into insulin-producing 3D spheroids. *Int J Immunopathol Pharmacol* **28**, 390–402 (2015).
132. Miceli, V. *et al.* Comparison of Immunosuppressive and Angiogenic Properties of Human Amnion-Derived Mesenchymal Stem Cells between 2D and 3D Culture Systems. *Stem Cells Int* **2019**, 1–16 (2019).
133. Bartosh, T. J. *et al.* Aggregation of human mesenchymal stromal cells (MSCs) into 3D spheroids enhances their antiinflammatory properties. *Proc Natl Acad Sci U S A* **107**, 13724–13729 (2010).
134. Jauković, A. *et al.* Specificity of 3D MSC Spheroids Microenvironment: Impact on MSC Behavior and Properties. *Stem Cell Rev Rep* **16**, 853–875 (2020).
135. Gallo, A. *et al.* Changes in the Transcriptome Profiles of Human Amnion-Derived Mesenchymal Stromal/Stem Cells Induced by Three-Dimensional Culture: A Potential Priming Strategy to Improve Their Properties. *Int J Mol Sci* **23**, 863 (2022).
136. Salinas-Vera, Y. M. *et al.* Three-Dimensional 3D Culture Models in Gynecological and Breast Cancer Research. *Front Oncol* **12**, 826113 (2022).
137. Cui, X., Hartanto, Y. & Zhang, H. Advances in multicellular spheroids formation. *J R Soc Interface* **14**, 20160877 (2017).
138. Cristaldi, D. A. *et al.* A Reliable Flow-Based Method for the Accurate Measure of Mass Density, Size and Weight of Live 3D Tumor Spheroids. *Micromachines (Basel)* **11**, 465 (2020).
139. Yang, P. *et al.* Biological characterization of human amniotic epithelial cells in a serum-free system and their safety evaluation. *Acta Pharmacol Sin* **39**, 1305–1316 (2018).
140. Silini, A. R. *et al.* Perinatal Derivatives: Where Do We Stand? A Roadmap of the Human Placenta and Consensus for Tissue and Cell Nomenclature. *Front Bioeng Biotechnol* **8**, (2020).
141. Lin, R.-Z., Chou, L.-F., Chien, C.-C. M. & Chang, H.-Y. Dynamic analysis of hepatoma spheroid formation: roles of E-cadherin and β1-integrin. *Cell Tissue Res* **324**, 411–422 (2006).
142. Regauer, S., Franke, W. W. & Virtanen, I. Intermediate filament cytoskeleton of amnion epithelium and cultured amnion epithelial cells: expression of epidermal cytokeratins in cells of a simple epithelium. *J Cell Biol* **100**, 997–1009 (1985).
143. Egeblad, M., Rasch, M. G. & Weaver, V. M. Dynamic interplay between the collagen scaffold and tumor evolution. *Curr Opin Cell Biol* **22**, 697–706 (2010).

144. Richardson, L. & Menon, R. Proliferative, Migratory, and Transition Properties Reveal Metastate of Human Amnion Cells. *American Journal of Pathology* **188**, 2004–2015 (2018).
145. Alcaraz, A. *et al.* Autocrine TGF-β induces epithelial to mesenchymal transition in human amniotic epithelial cells. *Cell Transplant* **22**, 1351–1367 (2013).
146. Ziegler, S. F., Ramsdell, F. & Alderson, M. R. The activation antigen CD69. *Stem Cells* **12**, 456–465 (1994).
147. Yu, L. *et al.* CD69 enhances immunosuppressive function of regulatory T-cells and attenuates colitis by prompting IL-10 production. *Cell Death Dis* **9**, 905 (2018).
148. Blanco-Domínguez, R. *et al.* CD69 expression on regulatory T cells protects from immune damage after myocardial infarction. *Journal of Clinical Investigation* **132**, (2022).
149. Marzio, R., Jirillo, E., Ransijn, A., Mauël, J. & Corradin, S. B. Expression and function of the early activation antigen CD69 in murine macrophages. *J Leukoc Biol* **62**, 349–355 (1997).
150. Radulovic, K. *et al.* The Early Activation Marker CD69 Regulates the Expression of Chemokines and CD4 T Cell Accumulation in Intestine. *PLoS One* **8**, e65413 (2013).
151. Niederlova, V., Tsyklauri, O., Chadimova, T. & Stepanek, O. CD8 $^{+}$ Tregs revisited: A heterogeneous population with different phenotypes and properties. *Eur J Immunol* **51**, 512–530 (2021).
152. Mishra, S., Srinivasan, S., Ma, C. & Zhang, N. CD8+ Regulatory T Cell – A Mystery to Be Revealed. *Front Immunol* **12**, (2021).
153. Vieyra-Lobato, M. R., Vela-Ojeda, J., Montiel-Cervantes, L., López-Santiago, R. & Moreno-Lafont, M. C. Description of CD8 $^{+}$ Regulatory T Lymphocytes and Their Specific Intervention in Graft-versus-Host and Infectious Diseases, Autoimmunity, and Cancer. *J Immunol Res* **2018**, 1–16 (2018).
154. Shimokawa, C. *et al.* CD8+ regulatory T cells are critical in prevention of autoimmune-mediated diabetes. *Nat Commun* **11**, 1922 (2020).
155. Mollah, Z. U. *et al.* Granzyme B Is Dispensable in the Development of Diabetes in Non-Obese Diabetic Mice. *PLoS One* **7**, e40357 (2012).
156. Thomas, H. E., Trapani, J. A. & Kay, T. W. H. The role of perforin and granzymes in diabetes. *Cell Death Differ* **17**, 577–585 (2010).